Summary of the Bulletin of the International Seismological Centre

2020

July – December

Volume 57 Issue II

www.isc.ac.uk

ISSN 2309-236X

2023

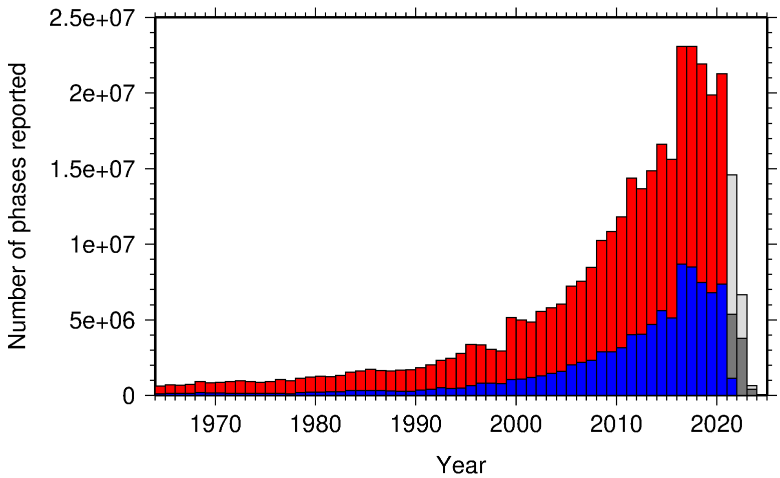

The number of phases (red) and number of amplitudes (blue) collected by the ISC for events each year since 1964. The data in grey covers the current period where data are still being collected before the ISC review takes place and are accurate at the time of publication. See Section 7.3.

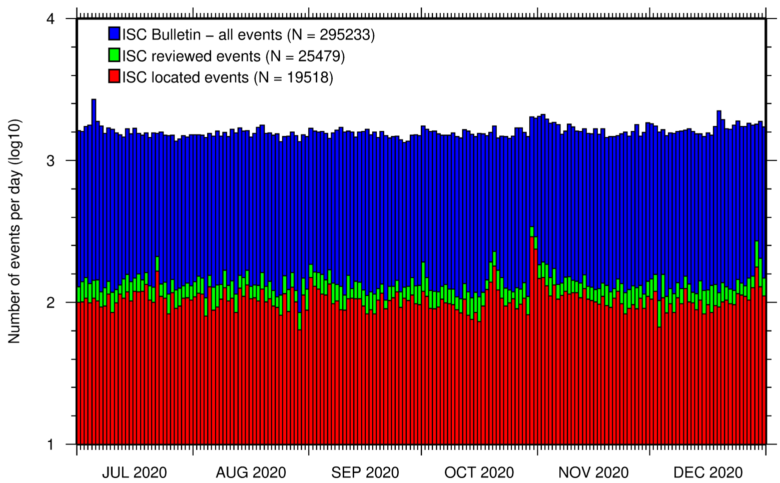

The number of events within the Bulletin for the current summary period. The vertical scale is logarithmic. See Section 8.1.

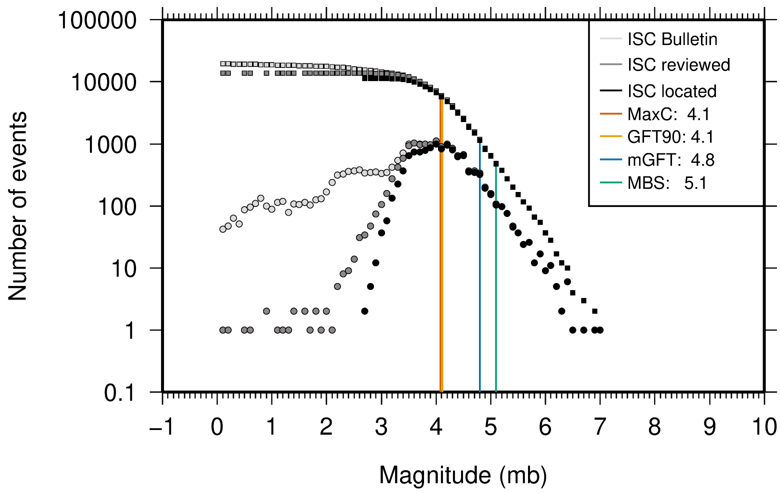

Frequency and cumulative frequency magnitude distribution for all events in the ISC Bulletin, ISC reviewed events and events located by the ISC. The magnitude of completeness (M_C) is shown for the ISC Bulletin. Note: only events with values of m_b are represented in the figure. See Section 8.4.

Summary of the Bulletin of the International Seismological Centre

2020

July - December

Volume 57 Issue II

Produced and edited by:
Kathrin Lieser, James Harris, Natalia Poiata and Dmitry Storchak

International Seismological Centre

Published by
International Seismological Centre

The International Seismological Centre (ISC) is a Charitable Incorporated Organization (CIO) registered with The Charity Commission for England and Wales. Registered charity number: 1188971.

ISC Data Products

http://www.isc.ac.uk/products/

ISC Bulletin:
  http://www.isc.ac.uk/iscbulletin/search

ISC Bulletin and Catalogue monthly files, to the last reviewed month in FFB or ISF1 format:
  http://download.isc.ac.uk/[isf|ffb]/[bulletin|catalogue]/*yyyy*/*yyyymm*.gz
  ftp://www.isc.ac.uk/pub/[isf|ffb]/[bulletin|catalogue]/*yyyy*/*yyyymm*.gz

Datafiles for the ISC data before the rebuild:
  http://download.isc.ac.uk//prerebuild/[isf|ffb]/[bulletin|catalogue]/*yyyy*/*yyyymm*.gz
  ftp://www.isc.ac.uk/pub/prerebuild/[isf|ffb]/[bulletin|catalogue]/*yyyy*/*yyyymm*.gz

ISC-EHB Bulletin:
  http://www.isc.ac.uk/isc-ehb/search/

IASPEI Reference Event List (GT bulletin):
  http://www.isc.ac.uk/gtevents/search/

ISC-GEM Global Instrumental Earthquake Catalogue:
  http://www.isc.ac.uk/iscgem/download.php

ISC Event Bibliography:
  http://www.isc.ac.uk/event_bibliography/bibsearch.php

International Seismograph Station Registry:
  http://www.isc.ac.uk/registries/search/

Seismological Contacts:
  http://www.isc.ac.uk/projects/seismocontacts/

International Seismological Centre
Pipers Lane
Thatcham
RG19 4NS
United Kingdom
www.isc.ac.uk

The International Seismological Centre (ISC) is a Charitable Incorporated Organization (CIO) registered with The Charity Commission for England and Wales. Registered charity number: 1188971.

ISSN 2309-236X

Printed and bound in Wales by Cambrian Printers.

Contents

1

Preface

Dear Colleague,

This is the second 2020 issue of the Summary of the ISC Bulletin, which remains the most fundamental reason for continued operations at the ISC. This issue covers earthquakes and other seismic events that occurred during the period from July to December 2020. Users can search the ISC Bulletin on the ISC website. The monthly Bulletin files are available from the ISC ftp site. For instructions, please see the www.isc.ac.uk/iscbulletin/.

This publication contains information on the ISC, its staff, Members, Sponsors and Data providers. It offers analysis of the data contributed to the ISC by many seismological agencies worldwide as well as analysis of the data in the ISC Bulletin itself. This somewhat smaller issue misses some of the standard information on routine procedures usually published in the first issue of each year.

I would like to reiterate here that all ISC hypocenter solutions (1964-present) are now based on the ak135 velocity model and all ISC magnitudes (1964-present) are based on the latest robust procedures.

We usually publish invited articles on notable seismic events as well as articles describing the history, status and operational procedures at networks that contribute parametric data to the ISC. This time, the topic of an invited article is somewhat different – history of the broadband seismometry.

We hope that you find this publication useful in your work. If your home-institution or company is unable, for one reason or another, to support the long-term international operations of the ISC in full by becoming a Member or a Sponsor, then, please, consider subscribing to this publication by contacting us at admin@isc.ac.uk.

With kind regards to our Data Contributors, Members, Sponsors and users,

Dr Dmitry A. Storchak
Director
International Seismological Centre (ISC)

2

The International Seismological Centre

2.1 The ISC Mandate

The International Seismological Centre (ISC) was set up in 1964 with the assistance of UNESCO as a successor to the International Seismological Summary (ISS) to carry forward the pioneering work of Prof. John Milne, Sir Harold Jeffreys and other British scientists in collecting, archiving and processing seismic station and network bulletins and preparing and distributing the definitive summary of world seismicity.

Under the umbrella of the International Association of Seismology and Physics of the Earth Interior (IASPEI/IUGG), the ISC has played an important role in setting international standards such as the International Seismic Bulletin Format (ISF), the IASPEI Standard Seismic Phase List (SSPL) and both the old and New IASPEI Manual of the Seismological Observatory Practice (NMSOP-2) (www.iaspei.org/projects/NMSOP.html).

The ISC has contributed to scientific research and prominent scientists such as John Hodgson, Eugine Herrin, Hal Thirlaway, Jack Oliver, Anton Hales, Ola Dahlman, Shigeji Suehiro, Nadia Kondorskaya, Vit Karnik, Stephan Müller, David Denham, Bob Engdahl, Adam Dziewonski, John Woodhouse and Guy Masters all considered it an important duty to serve on the ISC Executive Committee and the Governing Council.

The current mission of the ISC is to maintain:

- the ISC **Bulletin** – the longest continuous definitive summary of World seismicity (collaborating with 130 seismic networks and data centres around the world). (www.isc.ac.uk/iscbulletin/)
- the International Seismographic Station Registry (**IR**, jointly with the World Data Center for Seismology, Denver). (www.isc.ac.uk/registries/)
- the IASPEI Reference Event List (Ground Truth, **GT**, jointly with IASPEI). (www.isc.ac.uk/gtevents/)

These are fundamentally important tasks. Bulletin data produced, archived and distributed by the ISC for almost 50 years are the definitive source of such information and are used by thousands of seismologists worldwide for seismic hazard estimation, for tectonic studies and for regional and global imaging of the Earth's structure. Key information in global tomographic imaging is derived from the analysis of ISC data. The ISC Bulletin served as a major source of data for such well known products as the ak135 global 1-D velocity model and the EHB (*Engdahl et al.*, 1998) and Centennial (*Engdahl and Villaseñor*, 2002) catalogues. It presents an important quality-control benchmark for the Comprehensive Nuclear-Test-Ban Treaty Organization (CTBTO). Hypocentre parameters from the ISC Bulletin are used by the Data Management Center of the Incorporated Research Institutions for Seismology (IRIS DMC) to serve event-oriented user-requests for waveform data. The ISC-GEM Bulletin is a cornerstone of the ISC-GEM Global Instrumental Reference Earthquake Catalogue for Global Earthquake risk Model (GEM).

The ISC Bulletin contains over 8 million seismic events: earthquakes, chemical and nuclear explosions, mine blasts and mining induced events. Almost 2 million of them are regional and teleseismically recorded events that have been reviewed by the ISC analysts. The ISC Bulletin contains approximately 255 million individual seismic station readings of arrival times, amplitudes, periods, SNR, slowness and azimuth, reported by approximately 19,000 seismic stations currently registered in the IR. Over 9,000 stations have contributed to the ISC Bulletin in recent years. This number includes the numerous sites of the USArray. The IASPEI GT List currently contains 10187 events for which latitude, longitude and depth of origin are known with high confidence (to 5 km or better) and seismic signals were recorded at regional and/or teleseismic distances.

2.2 Brief History of the ISC

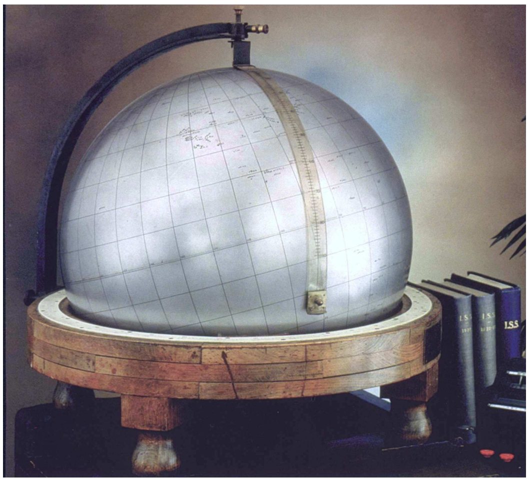

Figure 2.1: *The steel globe bearing positions of early seismic stations was used for locating positions of earthquakes for the International Seismological Summaries.*

Earthquake effects have been noted and documented from the earliest times, but it is only since the development of earthquake recording instruments in the latter half of the 19th century that a proper study of their occurrence has been possible. After the first teleseismic observation of an earthquake in 1889, the need for international exchange of readings was recognised in 1895 by Prof. John Milne and by Ernst von Rebeur Paschwitz together with Georg Gerland, resulting in the publication of the first international seismic bulletins. Milne's "Shide Circulars" were issued under the auspices of the Seismological Committee of the British Association for the Advancement of Science (BAAS), while co-workers of Gerland at the Central Bureau of the International Association of Seismology worked independently in Strasbourg (BCIS).

Following Milne's death in 1913, Seismological Bulletins of the BAAS were continued under Prof. H.H. Turner, later based at Oxford University. Upon formal post-war dissolution of the International Association of Seismology in 1922 the newly founded Seismological Section of the International Union of Geodesy and Geophysics (IUGG) set up the International Seismological Summary (ISS) to continue at Oxford under Turner, to produce the definitive global catalogues from the 1918 data-year onwards, under the auspices of IUGG and with the support of the BAAS.

ISS production, led by several professors at Oxford University, and Sir Harold Jeffreys at Cambridge

University, continued until it was superseded by the ISC Bulletin, after the ISC was formed in Edinburgh in 1964 with Dr P.L. Willmore as its first director.

During the period 1964 to 1970, with the help of UNESCO and other international scientific bodies, the ISC was reconstituted as an international non-governmental body, funded by interested institutions from various countries. Initially there were supporting members from seven countries, now there are almost 60, and member institutions include national academies, research foundations, government departments and research institutes, national observatories and universities. Each member, contributing a minimum unit of subscription or more, appoints a representative to the ISC's Governing Council, which meets every two years to decide the ISC's policy and operational programme. Representatives from the International Association of Seismology and Physics of the Earth's Interior also attend these meetings. The Governing Council appoints the Director and a small Executive Committee to oversee the ISC's operations.

Figure 2.2: *ISC building in Thatcham, Berkshire, UK.*

In 1975, the ISC moved to Newbury in southern England to make use of better computing facilities there. The ISC subsequently acquired its own computer and in 1986 moved to its own building at Pipers Lane, Thatcham, near Newbury. The internal layout of the new premises was designed for the ISC and includes not only office space but provision for the storage of extensive stocks of ISS and ISC publications and a library of seismological observatory bulletins, journals and books collected over many tens of years.

In 1997 the first set of the ISC Bulletin CD-ROMs was produced (not counting an earlier effort at USGS). The first ISC website appeared in 1998 and the first ISC database was put in day-to-day operations from 2001.

Throughout 2009-2011 a major internal reconstruction of the ISC building was undertaken to allow for more members of staff working in mainstream ISC operations as well as major development projects such as the CTBTO Link, ISC-GEM Catalogue and the ISC Bulletin Rebuild.

2.3 Former Directors of the ISC and its U.K. Predecessors

John Milne
Publisher of the Shide Cicular Reports on Earthquakes
1899-1913

Herbert Hall Turner

Seismological Bulletins of the BAAS

1913-1922
Director of the ISS
1922-1930

Harry Hemley Plaskett
Director of the ISS
1931-1946

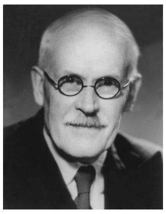

Harold Jeffreys
Director of the ISS
1946-1957

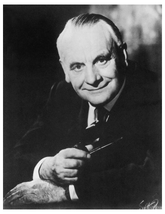

Robert Stoneley
Director of the ISS
1957-1963

P.L. (Pat) Willmore
Director of the ISS
1963-1970
Director of the ISC
1964-1970

Edouard P. Arnold
Director of the ISC
1970-1977

Anthony A. Hughes
Director of the ISC
1977-1997

Raymond J. Willemann
Director of the ISC
1998-2003

Avi Shapira
Director of the ISC
2004-2007

2.4 Member Institutions of the ISC

Article IV(a-b) of the ISC Working Statutes stipulates that any national academy, agency, scientific institution or other non-profit organisation may become a Member of the ISC on payment to the ISC of a sum equal to at least one unit of subscription and the nomination of a voting representative to serve on the ISC's governing body. Membership shall be effective for one year from the date of receipt at the ISC of the annual contribution of the Member and is thereafter renewable for periods of one year.

The ISC is currently supported with funding from its 62 Member Institutions and a four-year Grant Award EAR-1811737 from the US National Science Foundation.

Figures 2.3 and 2.4 show major sectors to which the ISC Member Institutions belong and proportional financial contributions that each of these sectors make towards the ISC's annual budget.

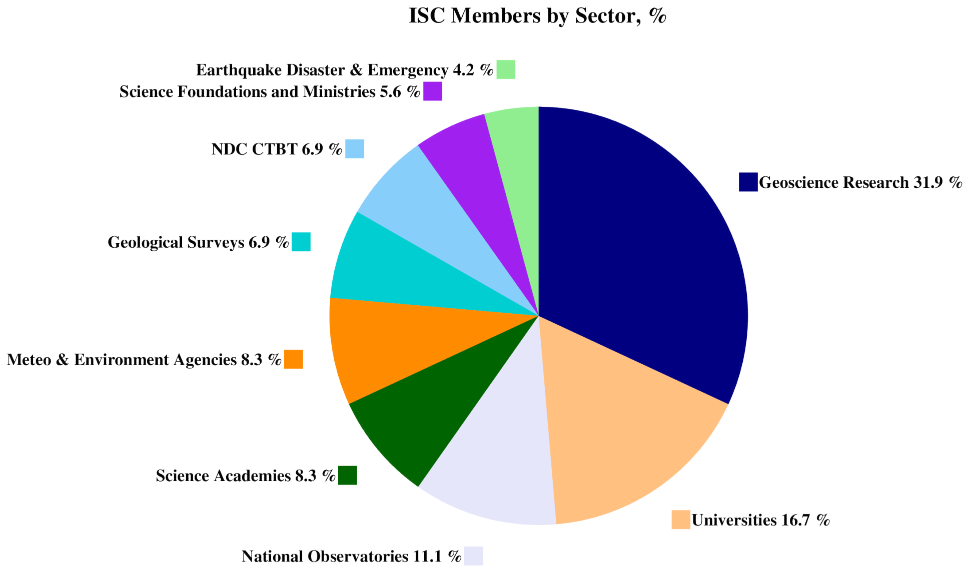

Figure 2.3: *Distribution of the ISC Member Institutions by sector during the review of data in this Summary as a percentage of total number of Members.*

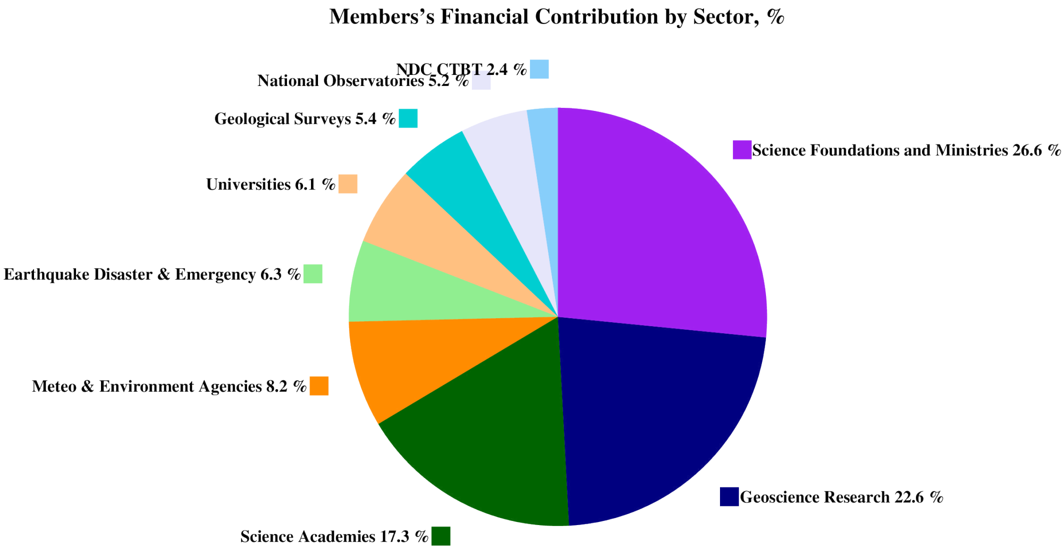

Figure 2.4: *Distribution of Member's financial contributions to the ISC by sector during the review of data in this Summary as a percentage of total annual Member contributions.*

There follows a list of all current Member Institutions with a category (1 through 9) assigned according to the ISC Working Statutes. Each category relates to the number of membership units contributed.

Centre de Recherche en Astronomie, Astrophysique et Géophysique (CRAAG)
Algeria
www.craag.dz
Category: 1

Geoscience Australia
Australia
www.ga.gov.au
Category: 4

Federal Ministry for Education, Science and Research
Austria

Category: 2

Centre of Geophysical Monitoring (CGM) of the National Academy of Sciences of Belarus
Belarus
www.cgm.org.by
Category: 1

Belgian Science Policy Office (BELSPO)
Belgium

Category: 1

Observatorio Nacional
Brazil
www.on.br
Category: 1

Universidade de São Paulo, Centro de Sismologia
Brazil
www.sismo.iag.usp.br
Category: 1

Seismological Observatory, Institute of Geosciences, University of Brasilia
Brazil
www.obsis.unb.br
Category: 1

National Institute of Geophysics, Geodesy and Geography (NIGGG), Bulgarian Academy of Sciences
Bulgaria
www.niggg.bas.bg
Category: 1

The Geological Survey of Canada
Canada
gsc.nrcan.gc.ca
Category: 4

Centro Sismologico Nacional, Universidad de Chile
Chile

Category: 1

China Earthquake Administration
China
www.cea.gov.cn
Category: 4

Institute of Earth Sciences, Academia Sinica
Chinese Taipei
www.earth.sinica.edu.tw
Category: 1

Geological Survey Department
Cyprus
www.moa.gov.cy
Category: 1

Institute of Geophysics, Czech Academy of Sciences
Czech Republic

Category: 1

Geological Survey of Denmark and Greenland (GEUS)
Denmark
www.geus.dk
Category: 2

National Research Institute for Astronomy and Geophysics (NRIAG), Cairo
Egypt
www.nriag.sci.eg
Category: 1

The University of Helsinki
Finland
www.helsinki.fi
Category: 2

Laboratoire de Détection et de Géophysique/CEA
France
www-dase.cea.fr
Category: 2

Institute of Radiological and Nuclear Safety (IRSN), joint authority of the Ministries of Defense, the Environment, Industry, Research, and Health
France

Category: 1

Institute National des Sciences de l'Univers
France
www.insu.cnrs.fr
Category: 4

GeoForschungsZentrum Potsdam
Germany
www.gfz-potsdam.de
Category: 2

Bundesanstalt für Geowissenschaften und Rohstoffe
Germany
www.bgr.bund.de
Category: 4

The Seismological Institute, National Observatory of Athens
Greece
www.noa.gr
Category: 1

Institute of Earth Physics and Space Science (EPSS), Hungarian Research Network (ELKH)
Hungary

Category: 1

The Icelandic Meteorological Office
Iceland
www.vedur.is
Category: 1

National Geophysical Research Institute (NGRI), Council of Scientific and Industrial Research (CSIR)
India

Category: 2

National Centre for Seismology, Ministry of Earth Sciences of India
India
www.moes.gov.in
Category: 4

Iraqi Meteorological Organization and Seismology
Iraq
www.imos-tm.com
Category: 1

Dublin Institute for Advanced Studies
Ireland
www.dias.ie
Category: 1

Geological Survey of Israel
Israel

Category: 1

Soreq Nuclear Research Centre (SNRC)
Israel
www.soreq.gov.il
Category: 1

Istituto Nazionale di Oceanografia e di Geofisica Sperimentale
Italy
www.ogs.trieste.it
Category: 1

Istituto Nazionale di Geofisica e Vulcanologia
Italy
www.ingv.it
Category: 3

University of the West Indies at Mona
Jamaica
www.mona.uwi.edu
Category: 1

The Japan Meteorological Agency (JMA)
Japan
www.jma.go.jp
Category: 5

Japan Agency for Marine-Earth Science and Technology (JAMSTEC)
Japan
www.jamstec.go.jp
Category: 2

Earthquake Research Institute, University of Tokyo
Japan
www.eri.u-tokyo.ac.jp
Category: 3

National Institute of Polar Research (NIPR)
Japan
www.nipr.ac.jp
Category: 1

Institute of Geophysics, National University of Mexico
Mexico
www.igeofcu.unam.mx
Category: 1

Centro de Investigación Científica y de Educación Superior de Ensenada (CICESE)
Mexico
resnom.cicese.mx
Category: 1

The Royal Netherlands Meteorological Institute (KNMI)
Netherlands
www.knmi.nl
Category: 2

GNS Science
New Zealand
www.gns.cri.nz
Category: 3

The Centre for Earth Evolution and Dynamics (CEED), the University of Oslo
Norway

Category: 1

The University of Bergen
Norway
www.uib.no
Category: 2

Stiftelsen NORSAR
Norway
www.norsar.no
Category: 2

Institute of Geophysics, Polish Academy of Sciences
Poland
www.igf.edu.pl
Category: 1

Instituto Português do Mar e da Atmosfera
Portugal
www.ipma.pt
Category: 2

Red Sísmica de Puerto Rico
Puerto Rico
redsismica.uprm.edu
Category: 1

Korean Meterological Administration
Republic of Korea
www.kma.go.kr
Category: 1

National Institute for Earth Physics
Romania
www.infp.ro
Category: 1

Russian Academy of Sciences
Russia
www.ras.ru
Category: 5

Earth Observatory of Singapore (EOS), an autonomous Institute of Nanyang Technological University
Singapore
www.earthobservatory.sg
Category: 1

Environmental Agency of Slovenia
Slovenia
www.arso.gov.si
Category: 1

Council for Geoscience
South Africa
www.geoscience.org.za
Category: 1

Instituto Geografico Nacional
Spain

Category: 3

Institut Cartogràfic i Geològic de Catalunya (ICGC)
Spain
www.icgc.cat
Category: 1

Institute of Marine Sciences (ICM-CSIC) Spain Category: 1	National Defence Research Establishment (FOI) Sweden www.foi.se Category: 1	Uppsala Universitet Sweden www.uu.se Category: 2
The Swiss Academy of Sciences Switzerland www.scnat.ch Category: 2	Disaster and Emergency Management Authority (AFAD) Turkey www.deprem.gov.tr Category: 2	Kandilli Observatory and Earthquake Research Institute Turkey www.koeri.boun.edu.tr Category: 1
AWE Blacknest United Kingdom www.blacknest.gov.uk Category: 1	British Geological Survey United Kingdom www.bgs.ac.uk Category: 2	The Royal Society United Kingdom www.royalsociety.org Category: 6
National Earthquake Information Center, U.S. Geological Survey U.S.A. www.neic.usgs.gov Category: 1	Alaska Earthquake Center (AEC), University of Alaska Fairbanks U.S.A. Category: 1	University of Utah Seismograph Stations (UUSS) U.S.A. Category: 1
The National Science Foundation of the United States. (Grant No. EAR-1811737) U.S.A. www.nsf.gov Category: 9	Texas Seismological Network (TexNet), Bureau of Economic Geology, J.A. and K.G. Jackson School of Geosciences, University of Texas at Austin U.S.A. www.beg.utexas.edu Category: 1	Incorporated Research Institutions for Seismology U.S.A. www.iris.edu Category: 1

In addition the ISC is currently in receipt of grants from the International Data Centre (IDC) of the Preparatory Commission of the Comprehensive Nuclear-Test-Ban Treaty Organization (CTBTO), FM Global, Lighthill Risk Network, and AXA XL.

2.5 Sponsoring Organisations

Article IV(c) of the ISC Working Statutes stipulates any commercial organisation with an interest in the objectives and/or output of the ISC may become an Associate Member of the ISC on payment of an Associate membership fee, but without entitlement to representation with a vote on the ISC's governing body.

GeoSIG swiss made to measure http://www.geosig.com/

GeoSIG provides earthquake, seismic, structural, dynamic and static monitoring and measuring solutions As an ISO Certified company, GeoSIG is a world leader in design and manufacture of a diverse range of high quality, precision instruments for vibration and earthquake monitoring. GeoSIG instruments are at work today in more than 100 countries around the world with well-known projects such as the NetQuakes installation with USGS and Oresund Bridge in Denmark. GeoSIG offers off-the-shelf solutions as well as highly customised solutions to fulfil the challenging requirements in many vertical markets including the following:

- Earthquake Early Warning and Rapid Response (EEWRR)
- Seismic and Earthquake Monitoring and Measuring
- Industrial Facility Seismic Monitoring and Shutdown
- Structural Analysis and Ambient Vibration Testing
- Induced Vibration Monitoring
- Research and Scientific Applications

sara electronic instruments http://www.sara.pg.it

SARA designs and manufactures seismometers, accelerometers and portable multichannel seismographs for both seismology and applied geophysics. Since 2002 we provided over 5,000 seismic units, 15,000 acceleration transducers and 15,000 geophysical exploration channels, to thousands of professionals and researchers who are using our equipment with success. Providing low-cost instrumentation for developing countries is our main goal. We developed our seismological software SEISMOWIN which provides full support for all international file formats and communication standards like miniSEED, GSE, SeedLink and a number of tools for earthquake location and site assessment. The GEOEXPLORER software suite offers a number of modules for geological surveys.

In 2023 we introduced our new compact broadband seismometer to the market, suitable for surface, posthole and borehole installation, and new versions of our popular SL06 recorder with rack mount housing and ADC with PGA offering 24 or 32 bit streaming.

Visit our web site and download the free tools available at: www.sara.pg.it

MS&AD InterRisk Research & Consulting

http://www.irric.co.jp/en/corporate/

MS&AD InterRisk Research & Consulting, Inc. is responsible for the core of risk-related service businesses in the MS&AD group. We provide services which meet various expectations of the clients, including consulting, research and investigation, seminars and publications for risk management in addition to the think-tank functions.

https://www.gaiacode.com/

Gaiacode is a science based, forward looking, innovative company designing and building the next generation of seismic instrumentation.

2.6 Data Contributing Agencies

In addition to its Members and Sponsors, the ISC owes its existence and successful long-term operations to its 150 seismic bulletin data contributors. These include government agencies responsible for national seismic networks, geoscience research institutions, geological surveys, meteorological agencies, universities, national data centres for monitoring the CTBT and individual observatories. There would be no ISC Bulletin available without the regular stream of data that are unselfishly and generously contributed to the ISC on a free basis.

Institute of Geosciences, Polytechnic University of Tirana Albania TIR	Centre de Recherche en Astronomie, Astrophysique et Géophysique Algeria CRAAG	Universidad Nacional de La Plata Argentina LPA
Instituto Nacional de Prevención Sísmica Argentina SJA	National Survey of Seismic Protection Armenia NSSP	Geoscience Australia Australia AUST

Curtin University
Australia
CUPWA

Zentralanstalt für Meteorologie und Geodynamik (ZAMG)
Austria
VIE

International Data Centre, CTBTO
Austria
IDC

Republican Seismic Survey Center of Azerbaijan National Academy of Sciences
Azerbaijan
AZER

Royal Observatory of Belgium
Belgium
UCC

Observatorio San Calixto
Bolivia
SCB

Republic Hydrometeorological Service, Seismological Observatory, Banja Luka
Bosnia and Herzegovina
RHSSO

Botswana Geoscience Institute
Botswana
BGSI

Observatory Seismological of the University of Brasilia
Brazil
OSUNB

Instituto Astronomico e Geofísico
Brazil
VAO

National Institute of Geophysics, Geology and Geography
Bulgaria
SOF

Canadian Hazards Information Service, Natural Resources Canada
Canada
OTT

Centro Sismológico Nacional, Universidad de Chile
Chile
GUC

China Earthquake Networks Center
China
BJI

Institute of Earth Sciences, Academia Sinica
Chinese Taipei
ASIES

Central Weather Bureau (CWB)
Chinese Taipei
TAP

Red Sismológica Nacional de Colombia
Colombia
RSNC

Sección de Sismología, Vulcanología y Exploración Geofísica
Costa Rica
UCR

Seismological Survey of the Republic of Croatia
Croatia
ZAG

Servicio Sismológico Nacional Cubano
Cuba
SSNC

Cyprus Geological Survey Department
Cyprus
NIC

The Institute of Physics of the Earth (IPEC)
Czech Republic
IPEC

Institute of Geophysics, Czech Academy of Sciences
Czech Republic
PRU

Institute of Geophysics, Czech Academy of Sciences
Czech Republic
WBNET

Korea Earthquake Administration
Democratic People's Republic of Korea
KEA

Geological Survey of Denmark and Greenland
Denmark
DNK

Universidad Autonoma de Santo Domingo
Dominican Republic
SDD

Observatorio Sismologico Politecnico Loyola
Dominican Republic
OSPL

Servicio Nacional de Sismología y Vulcanología
Ecuador
IGQ

National Research Institute of Astronomy and Geophysics
Egypt
HLW

Servicio Nacional de Estudios Territoriales
El Salvador
SNET

Institute of Seismology, University of Helsinki
Finland
HEL

Institut de Physique du Globe de Paris
France
IPGP

EOST / RéNaSS
France
STR

Laboratoire de Détection et de Géophysique/CEA
France
LDG

Laboratoire de Géophysique/CEA
French Polynesia
PPT

Institute of Earth Sciences/ National Seismic Monitoring Center
Georgia
TIF

Alfred Wegener Institute for Polar and Marine Research
Germany
AWI

Geophysikalisches Observatorium Collm
Germany
CLL

Bundesanstalt für Geowissenschaften und Rohstoffe
Germany
BGR

Seismological Observatory Berggießhübel, TU Bergakademie Freiberg
Germany
BRG

Helmholtz Centre Potsdam GFZ German Research Centre For Geosciences
Germany
GFZ

National Observatory of Athens
Greece
ATH

Department of Geophysics, Aristotle University of Thessaloniki
Greece
THE

University of Patras, Department of Geology
Greece
UPSL

INSIVUMEH
Guatemala
GCG

Hong Kong Observatory
Hong Kong
HKC

Geodetic and Geophysical Reasearch Institute, Hungarian Academy of Sciences
Hungary
KRSZO

Icelandic Meteorological Office
Iceland
REY

National Centre for Seismology of the Ministry of Earth Sciences of India
India
NDI

National Geophysical Research Institute
India
HYB

Badan Meteorologi, Klimatologi dan Geofisika
Indonesia
DJA

Tehran University
Iran
TEH

International Institute of Earthquake Engineering and Seismology (IIEES)
Iran
THR

Iraqi Meteorological and Seismology Organisation
Iraq
ISN

Dublin Institute for Advanced Studies
Ireland
DIAS

The Geophysical Institute of Israel
Israel
GII

Laboratory of Research on Experimental and Computational Seimology
Italy
RISSC

Istituto Nazionale di Geofisica e Vulcanologia
Italy
ROM

SARA Electronic Instrument s.r.l.
Italy
SARA

MedNet Regional Centroid - Moment Tensors
Italy
MED_RCMT

Dipartimento per lo Studio del Territorio e delle sue Risorse (RSNI)
Italy
GEN

Istituto Nazionale di Oceanografia e di Geofisica Sperimentale (OGS)
Italy
TRI

Jamaica Seismic Network
Jamaica
JSN

National Institute of Polar Research
Japan
SYO

National Research Institute for Earth Science and Disaster Resilience
Japan
NIED

Japan Meteorological Agency
Japan
JMA

Jordan Seismological Observatory
Jordan
JSO

Seismological Experimental Methodological Expedition
Kazakhstan
SOME

National Nuclear Center
Kazakhstan
NNC

Institute of Seismology, Academy of Sciences of Kyrgyz Republic
Kyrgyzstan
KRNET

Kyrgyz Seismic Network
Kyrgyzstan
KNET

Latvian Seismic Network
Latvia
LVSN

National Council for Scientific Research
Lebanon
GRAL

Geological Survey of Lithuania
Lithuania
LIT

Macao Meteorological and Geophysical Bureau
Macao, China
MCO

Antananarivo
Madagascar
TAN

Instituto de Geofísica de la UNAM
Mexico
MEX

Centro de Investigación Científica y de Educación Superior de Ensenada
Mexico
ECX

Institute of Hydrometeorology and Seismology of Montenegro
Montenegro
PDG

Centre National de Recherche
Morocco
CNRM

The Geological Survey of Namibia
Namibia
NAM

National Seismological Centre, Nepal
Nepal
DMN

IRD Centre de Nouméa
New Caledonia
NOU

Institute of Geological and Nuclear Sciences
New Zealand
WEL

Central American Tsunami Advisory Center
Nicaragua
CATAC

Seismological Observatory Skopje
North Macedonia
SKO

University of Bergen
Norway
BER

Stiftelsen NORSAR
Norway
NAO

Sultan Qaboos University
Oman
OMAN

Universidad de Panama
Panama
UPA

Manila Observatory
Philippines
QCP

Philippine Institute of Volcanology and Seismology
Philippines
MAN

Private Observatory of Pawel Jacek Wiejacz, D.Sc.
Poland
PJWWP

Institute of Geophysics, Polish Academy of Sciences
Poland
WAR

Instituto Dom Luiz, University of Lisbon
Portugal
IGIL

Sistema de Vigilância Sismológica dos Açores
Portugal
SVSA

Instituto Português do Mar e da Atmosfera, I.P.
Portugal
INMG

Centre of Geophysical Monitoring of the National Academy of Sciences of Belarus
Republic of Belarus
BELR

Inst. of Seismology and Geodynamics, V.I. Vernadsky Crimean Federal University
Republic of Crimea
CFUSG

Korea Meteorological Administration
Republic of Korea
KMA

National Institute for Earth Physics
Romania
BUC

North Eastern Regional Seismological Centre, Magadan, GS RAS
Russia
NERS

Federal Center for Integrated Arctic Research
Russia
FCIAR

Kola Regional Seismic Centre, GS RAS
Russia
KOLA

Kamchatka Branch of the Geophyical Survey of the RAS
Russia
KRSC

Baykal Regional Seismological Centre, GS SB RAS
Russia
BYKL

Yakutiya Regional Seismological Center, GS SB RAS
Russia
YARS

Altai-Sayan Seismological Centre, GS SB RAS
Russia
ASRS

Sakhalin Experimental and Methodological Seismological Expedition, GS RAS
Russia
SKHL

Geophysical Survey of Russian Academy of Sciences
Russia
MOS

Mining Institute of the Ural Branch of the Russian Academy of Sciences
Russia
MIRAS

Saudi Geological Survey
Saudi Arabia
SGS

Republicki seizmoloski zavod
Serbia
BEO

Geophysical Institute, Slovak Academy of Sciences
Slovakia
BRA

Slovenian Environment Agency
Slovenia
LJU

Council for Geoscience
South Africa
PRE

Real Instituto y Observatorio de la Armada
Spain
SFS

Instituto Geográfico Nacional
Spain
MDD

Institut Cartogràfic i Geològic de Catalunya
Spain
MRB

University of Uppsala
Sweden
UPP

Swiss Seismological Service (SED)
Switzerland
ZUR

Thai Meteorological Department
Thailand
BKK

The Seismic Research Centre
Trinidad and Tobago
TRN

Institut National de la Météorologie
Tunisia
TUN

Disaster and Emergency Management Presidency
Turkey
AFAD

Kandilli Observatory and Earthquake Research Institute
Turkey
ISK

IRIS Data Management Center
U.S.A.
IRIS

The Global CMT Project
U.S.A.
GCMT

National Earthquake Information Center
U.S.A.
NEIC

Texas Seismological Network, University of Texas at Austin
U.S.A.
TXNET

Pacific Northwest Seismic Network
U.S.A.
PNSN

Pacific Tsunami Warning Center
U.S.A.
PTWC

Red Sísmica de Puerto Rico
U.S.A.
RSPR

Subbotin Institute of Geophysics, National Academy of Sciences
Ukraine
SIGU

Main Centre for Special Monitoring
Ukraine
MCSM

Dubai Seismic Network
United Arab Emirates
DSN

International Seismological Centre
United Kingdom
ISC

British Geological Survey
United Kingdom
BGS

International Seismological Centre Probabilistic Point Source Model
United Kingdom
ISC-PPSM

Institute of Seismology, Academy of Sciences, Republic of Uzbekistan
Uzbekistan
ISU

Fundación Venezolana de Investigaciones Sismológicas
Venezuela
FUNV

Institute of Geophysics, Viet Nam Academy of Science and Technology
Viet Nam
PLV

Goetz Observatory
Zimbabwe
BUL

2.7 ISC Staff

Listed below are the staff (and their country of origin) who were employed at the ISC during the time period when the ISC worked on the data covered by this issue of the Summary.

- Dmitry Storchak
- Director
- Russia / United Kingdom

- Lynn Elms
- Administration Officer
- United Kingdom

- James Harris
- Senior System and Database Administrator
- United Kingdom

- Oliver Rea
- System Administrator
- United Kingdom

- Calum Clague
- Data Collection Officer
- South Africa

- Domenico Di Giacomo
- Senior Seismologist
- Italy/UK

- Tom Garth
- Seismologist / Senior Developer
- United Kingdom

- Ryan Gallacher
- Seismologist / Developer
- United Kingdom

- Natalia Poiata
- Seismologist / Developer
- Moldova

- Adrian Armstrong
- Software Engineer
- United Kingdom

- Rosemary Hulin
- Analyst
- United Kingdom

- Blessing Shumba
- Seismologist / Senior Analyst
- Zimbabwe

- Rebecca Verney
- Analyst
- United Kingdom

- Elizabeth Ayres
- Analyst / Historical Data Officer
- United Kingdom

- Kathrin Lieser
- Analyst Administrator / Summary Editor / Seismologist
- Germany

- Burak Sakarya
- Seismologist / Analyst
- Turkey

- Rian Harris
- Historical Data Officer
- United Kingdom

- Susana Carvalho
- Historical Data Officer
- Portugal

3

Availability of the ISC Bulletin

The ISC Bulletin is available from the following sources:

- Web searches
  The entire ISC Bulletin is available directly from the ISC website via tailored searches.
  (www.isc.ac.uk/iscbulletin/search)

  - Bulletin search - provides the most verbose output of the ISC Bulletin in ISF or QuakeML.
  - Event catalogue - only outputs the prime hypocentre for each event, producing a simple list of events, locations and magnitudes.
  - Arrivals - search for arrivals in the ISC Bulletin. Users can search for specific phases for selected stations and events.

- CD-ROMs/DVD-ROMs

  CDs/DVDs can be ordered from the ISC for any published volume (one per year), or for all back issues of the Bulletin (not including the latest volume). The data discs contain the Bulletin as a PDF, in IASPEI Seismic Format (ISF), and in Fixed Format Bulletin (FFB) format. An event catalogue is also included, together with the International Registry of seismic station codes.

- FTP site

  The ISC Bulletin is also available to download from the ISC ftp site, which contains the Bulletin in PDF, ISF and FFB formats.
  (ftp://www.isc.ac.uk)
  and
  (http://download.isc.ac.uk)

4

Citing the International Seismological Centre

Data from the ISC should always be cited. This includes use by academic or commercial organisations, as well as individuals. A citation should show how the data were retrieved and may be in one of these suggested forms:

The ISC is named as a valid data centre for citations within American Geophysical Union (AGU) publications. As such, please follow the AGU guidelines when referencing ISC data in one of their journals. The ISC may be cited as both the institutional author of the Bulletin and the source from which the data were retrieved.

4.1 The ISC Bulletin

International Seismological Centre (2023), On-line Bulletin, `https://doi.org/10.31905/D808B830`

The procedures used for producing the ISC Bulletin have been described in a number of scientific articles. Depending on the use of the Bulletin, users are encouraged to follow the citation suggestions below:

a) For current ISC location procedure:

Bondár, I. and D.A. Storchak (2011). Improved location procedures at the International Seismological Centre, *Geophys. J. Int.*, *186*, 1220-1244, `https://doi.org/10.1111/j.1365-246X.2011.05107.x`

b) For Rebuilt ISC Bulletin:

Storchak, D.A., Harris, J., Brown, L., Lieser, K., Shumba, B., Verney, R., Di Giacomo, D., Korger, E. I. M. (2017). Rebuild of the Bulletin of the International Seismological Centre (ISC), part 1: 1964–1979. *Geosci. Lett.* (2017) 4: 32. `https://doi.org/10.1186/s40562-017-0098-z`

Storchak, D.A., Harris, J., Brown, L., Lieser, K., Shumba, B., Di Giacomo, D. (2020) Rebuild of the Bulletin of the International Seismological Centre (ISC), part 2: 1980–2010. *Geosci. Lett.* (2020) 7: 18, `https://doi.org/10.1186/s40562-020-00164-6`

c) For principles of the ISC data collection process:

R J Willemann, D A Storchak (2001). Data Collection at the International Seismological Centre, *Seis. Res. Lett.*, *72*, 440-453, `https://doi.org/10.1785/gssrl.72.4.440`

d) For interpretation of magnitudes:

Di Giacomo, D., and D.A. Storchak (2016). A scheme to set preferred magnitudes in the ISC Bulletin, *J. Seism.*, *20(2)*, 555-567, `https://doi.org/10.1007/s10950-015-9543-7`

e) For use of source mechanisms:

Lentas, K., Di Giacomo, D., Harris, J., and Storchak, D. A. (2020). The ISC Bulletin as a comprehensive source of earthquake source mechanisms, *Earth Syst. Sci. Data*, *11*, 565-578,https://doi.org/10.5194/essd-11-565-2020

Lentas, K. (2018). Towards routine determination of focal mechanisms obtained from first motion P-wave arrivals, *Geophys. J. Int.*, *212(3)*, 1665–1686.https://doi.org/10.1093/gji/ggx503

f) For use of the original (pre-Rebuild) ISC Bulletin as a historical perspective:

Adams, R.D., Hughes, A.A., and McGregor, D.M. (1982). Analysis procedures at the International Seismological Centre. *Phys. Earth Planet. Inter. 30:* 85-93,https://doi.org/10.1016/0031-9201(82)90093-0

4.2 The Summary of the Bulletin of the ISC

International Seismological Centre (2023), Summary of the Bulletin of the International Seismological Centre, July - December 2020, *57(II)*,https://doi.org/10.31905/1QE2K1QP

4.3 The historical printed ISC Bulletin (1964-2009)

International Seismological Centre, Bull. Internatl. Seismol. Cent., 46(9-12), Thatcham, United Kingdom, 2009.

4.4 The IASPEI Reference Event List

International Seismological Centre (2023), IASPEI Reference Event (GT) List, https://doi.org/10.31905/32NSJF7V

Bondár, I. and K.L. McLaughlin (2009). A New Ground Truth Data Set For Seismic Studies, *Seismol. Res. Lett.*, *80*, 465-472, https://doi.org/10.1785/gssrl.80.3.465

Bondár, E. Engdahl, X. Yang, H. Ghalib, A. Hofstetter, V. Kirichenko, R. Wagner, I. Gupta, G. Ekström, E. Bergman, H. Israelsson, and K. McLaughlin (2004). Collection of a reference event set for regional and teleseismic location calibration, *Bull. Seismol. Soc. Am.*, *94*, 1528-1545, https://doi.org/10.1785/012003128

Bondár, E. Bergman, E. Engdahl, B. Kohl, Y.-L. Kung, and K. McLaughlin (2008). A hybrid multiple event location technique to obtain ground truth event locations, *Geophys. J. Int.*, *175*, https://doi.org/10.1111/j.1365-246X.2011.05011.x

4.5 The ISC-GEM Catalogue

International Seismological Centre (2023), ISC-GEM Earthquake Catalogue, https://doi.org/10.31905/d808b825, 2023.

Depending on the use of the Catalogue, to quote the appropriate scientific articles, as suggested below.

a) For a general use of the catalogue, please quote the following three papers (Storchak et al., 2013; 2015; Di Giacomo et al., 2018):

Storchak, D.A., D. Di Giacomo, I. Bondár, E.R. Engdahl, J. Harris, W.H.K. Lee, A. Villaseñor and P. Bormann (2013). Public Release of the ISC-GEM Global Instrumental Earthquake Catalogue (1900-2009). *Seism. Res. Lett.*, *84*, 5, 810-815, https://doi.org/10.1785/0220130034

Storchak, D.A., D. Di Giacomo, E.R. Engdahl, J. Harris, I. Bondár, W.H.K. Lee, P. Bormann and A. Villaseñor (2015). The ISC-GEM Global Instrumental Earthquake Catalogue (1900-2009): Introduction, *Phys. Earth Planet. Int.*, *239*, 48-63, https://doi.org/10.1016/j.pepi.2014.06.009

Di Giacomo, D., E.R. Engdahl and D.A. Storchak (2018). The ISC-GEM Earthquake Catalogue (1904–2014): status after the Extension Project, *Earth Syst. Sci. Data*, *10*, 1877-1899, https://doi.org/10.5194/essd-10-1877-2018

b) For use of location parameters, please quote (Bondár et al., 2015):

Bondár, I., E.R. Engdahl, A. Villaseñor, J. Harris and D.A. Storchak, 2015. ISC-GEM: Global Instrumental Earthquake Catalogue (1900-2009): II. Location and seismicity patterns, *Phys. Earth Planet. Int.*, *239*, 2-13, https://doi.org/10.1016/j.pepi.2014.06.002

c) For use of magnitude parameters, please quote (Di Giacomo et al., 2015a; 2018):

Di Giacomo, D., I. Bondár, D.A. Storchak, E.R. Engdahl, P. Bormann and J. Harris (2015a). ISC-GEM: Global Instrumental Earthquake Catalogue (1900-2009): III. Re-computed MS and mb, proxy MW, final magnitude composition and completeness assessment, *Phys. Earth Planet. Int.*, *239*, 33-47, https://doi.org/10.1016/j.pepi.2014.06.005

Di Giacomo, D., E.R. Engdahl and D.A. Storchak (2018). The ISC-GEM Earthquake Catalogue (1904–2014): status after the Extension Project, *Earth Syst. Sci. Data*, *10*, 1877-1899, https://doi.org/10.5194/essd-10-1877-2018

d) For use of station data from historical bulletins, please quote (Di Giacomo et al., 2015b; 2018):

Di Giacomo, D., J. Harris, A. Villaseñor, D.A. Storchak, E.R. Engdahl, W.H.K. Lee and the Data Entry Team (2015b). ISC-GEM: Global Instrumental Earthquake Catalogue (1900-2009), I. Data collection from early instrumental seismological bulletins, *Phys. Earth Planet. Int.*, *239*, 14-24, https://doi.org/10.1016/j.pepi.2014.06.005

Di Giacomo, D., E.R. Engdahl and D.A. Storchak (2018). The ISC-GEM Earthquake Catalogue (1904–2014): status after the Extension Project, *Earth Syst. Sci. Data*, *10*, 1877-1899, https://doi.org/10.5194/essd-10-1877-2018

e) For use of direct values of M0 from the literature, please quote (Lee and Engdahl, 2015):

Lee, W.H.K. and E.R. Engdahl (2015). Bibliographical search for reliable seismic moments of large earthquakes during 1900-1979 to compute MW in the ISC-GEM Global Instrumental Reference Earthquake Catalogue (1900-2009), *Phys. Earth Planet. Int.*, *239*, 25-32, https://doi.org/10.1016/j.pepi.2014.06.004

4.6 The ISC-EHB Dataset

International Seismological Centre (2023), ISC-EHB Dataset, https://doi.org/10.31905/PY08W6S3

Engdahl, E.R., R. van der Hilst, and R. Buland (1998). Global teleseismic earthquake relocation with improved travel times and procedures for depth determination, *Bull. Seism. Soc. Am.*, *88*, 3, 722-743. http://www.bssaonline.org/content/88/3/722.abstract

Weston, J., Engdahl, E.R., Harris, J., Di Giacomo, D. and Storchack, D.A. (2018). ISC-EHB: Reconstruction of a robust earthquake dataset, *Geophys. J. Int.*, *214*, 1, 474-484, https://doi.org/10.1093/gji/ggy155

Engdahl, E. R., Di Giacomo, D., Sakarya, B., Gkarlaouni, C. G., Harris, J., and Storchak, D. A. (2020). ISC-EHB 1964-2016, an Improved Data Set for Studies of Earth Structure and Global Seismicity, *Earth and Space Science*, *7(1)*, e2019EA000897, https://doi.org/10.1029/2019EA000897

4.7 The ISC Event Bibliography

International Seismological Centre (2023), On-line Event Bibliography, https://doi.org/10.31905/EJ3B5LV6

Also, please reference the following SRL article that describes the details of this service:

Di Giacomo, D., Storchak, D.A., Safronova, N., Ozgo, P., Harris, J., Verney, R. and Bondár, I., 2014. A New ISC Service: The Bibliography of Seismic Events, *Seismol. Res. Lett.*, *85*, 2, 354-360, https://doi.org/10.1785/0220130143

4.8 International Registry of Seismograph Stations

International Seismological Centre (2023), International Seismograph Station Registry (IR), https://doi.org/10.31905/EL3FQQ40

4.9 Seismological Dataset Repository

International Seismological Centre (2023), Seismological Dataset Repository, https://doi.org/10.31905/6TJZECEY

4.10 Data transcribed from ISC CD-ROMs/DVD-ROMs

International Seismological Centre, Bulletin Disks 1-30 [CD-ROM], Internatl. Seismol. Cent., Thatcham, United Kingdom, 2023.

5

Invited Article

5.1 A Brief History of Broadband Seismometry – Part I

Horst Rademacher
formerly Seismologisches Zentralobservatorium Gräfenberg, Germany and
Berkeley Seismology Laboratory, University of California, Berkeley (retired)

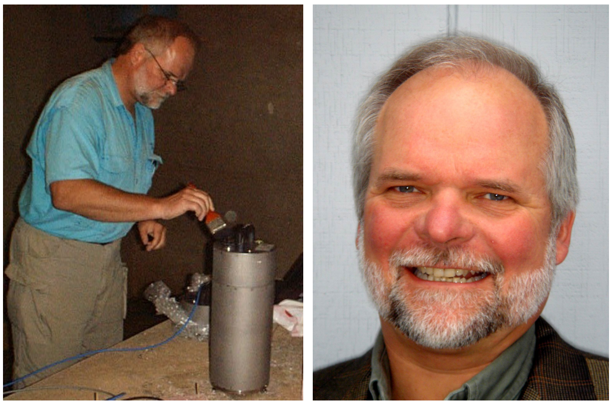

Horst Rademacher

5.2 Introduction

Almost five decades ago a new paradigm swept over the world of seismology like a tsunami. At a time when the theory of Plate Tectonics was still in its infancy and when the nuclear powers, engaged in a bitterly frozen Cold War, were testing atomic weapons several times a month, seismologists realised how ill equipped they were to measure the rumblings of the Earth, be they natural or caused by nuclear detonations.

No doubt, the data collected at that time by the World Wide Standard Seismograph Network (WWSSN) had considerably improved our abilities to record earthquakes and detect underground explosions (*Kerr*, 1985). But during its operation, which started as part of the Vela project by the US Department of Defense in the mid 1960's, it became clear that the WWSSN had major shortcomings. Each of the approximately 120 stations of the network was equipped with at least six separate seismometers, each one augmented by its own galvanometer. The data were recorded on light sensitive paper, requiring the equivalent of a darkroom at each station. Keeping such a complex system of equipment in running order became a maintenance nightmare (*Peterson and Hutt*, 2014).

Despite the words "World Wide" in its name, the WWSSN did not cover the complete globe by any means. Given the geopolitical situation at the time, no stations were deployed in what was then the

Soviet Union, in countries in the Soviet sphere of influence in Eastern Europe or in China. This led to a substantial gap in coverage. However, in 1965 the Council of Seismology of the former USSR began setting up its own network of identical seismic stations. By 1969 a total of 168 stations were deployed in the USSR and neighbouring countries. Each one was equipped with three sets of three component sensors covering the short, medium and long period parts of the seismic spectrum, thus recording in analogue form a broader frequency range than was possible with the standard WWSSN equipment (*Storchak et al.*, 2015). However, in contrast to the data collected by the WWSSN, the data from the Soviet network were not available in the rest of the world.

Despite its shortcomings the WWSSN was the top of the line seismic network of its time. The situation in most earthquake observatories around the world was worse. Operated mostly by universities and other research institutions, their equipment was often a mixture of different types and models of mechanical seismographs, each with different magnification and its own unique transfer function.

Many seismologists realised at that time that changes, even a completely new approach to the measurement of ground motion was necessary. But what was really needed?

Despite today's general perception that completely new seismic sensors were needed at the time, the most pressing issue was the way ground motion was recorded. For instance, the data of the stations of the WWSSN were recorded on photographic paper and later transferred in analogue form to microfilm. The analogue outputs of other sensors were quite often still recorded on sooted paper, posing a health hazard to the operators. In any case, these recordings were fixed and could not be manipulated further to improve their analysis. In addition, once the passband of a seismic sensor included the period range between 6 and 15 sec, the ocean microseisms dominated the recordings, masking most other seismic information. Hence making use of the rapidly developing computer technology four decades ago allowed the recording of seismic data in digital form, broadly opening the doors to the capacity to apply digital filtering and other computer-based analysis techniques.

Another item on the wishlist was the development of seismic instruments which would cover a wider frequency range, encompassing at least the same seismic band for which the stations of the WWSSN needed two separate sets of seismometers. In addition it was desirable to have the response of such a sensor be linear and flat across that broader frequency range.

In this two part contribution I will attempt to recount the development of what later became known as *modern broadband seismometry*. This technology is without a doubt the dominant tool in the world of seismology today. In the first part, I will describe the efforts of several groups of scientists and engineers in Europe and the United States who were working to implement some of the basic new ideas in the design of new sensors. Their endeavours led to the first operational broadband seismometers. In the second instalment I will describe the developments of digital recording methods, several subsequent technological developments in sensor design and the effects this new technique of measuring and recording ground motion had on the science of seismology.

Many of the original contributors are either no longer with us or are no longer working on these questions, while others are still pushing the frontiers of seismometry. New players have entered and with them new ideas have surfaced. Given the fierce competition in this field I will endeavour to stay as neutral as possible. Mention of specific instruments shall not be interpreted as endorsement. And in no way will

I judge the quality of the products developed and built by the various manufacturers referred to in the text. This call must be made by each seismologist planning to acquire and use broadband systems.

5.3 The Basic Concept of Seismometry

Ground motions associated with elastic waves can be measured in two ways, either with strain meters or with inertial pendulums. While the former allow a direct measurement of differential ground displacement, a complex transfer function has to be considered for the latter to gain meaningful information about the true movement of the ground in both amplitude and phase. This computational procedure is necessary because the actual output signal of an inertial pendulum seismometer is proportional to the relative motion between the internally suspended inertial mass and the frame of the instrument which should be well coupled to the ground. This important step is commonly referred to as the removal of the instrument response or in more mathematical terms as a deconvolution of the seismogram. Despite this complexity, inertial pendulum seismometers have been the dominant tool in seismology for more than a century.

Early instruments, like those developed by Ewing, Wiechert or Omori around the turn of the 20th century, were purely mechanical devices. The motion of their respective masses relative to the frame of the instrument - and hence the ground - was recorded on sooted paper by a system of levers and styluses (*Dewey and Byerly*, 1969). Such mechanical instruments, the seismographs, are not in operational use anymore. However many are still in working condition and can be found in museums or as exhibition pieces in seismic observatories.

It was *Galitzin* (1914), who in the early part of the 20th century first coupled the suspended mass of an inertial pendulum with an electromagnetic (EM) transducer, thereby creating the first seismometer. When its mass moves relative to the instrument frame, it induces an electrical current in the coil. This current is proportional to the velocity of the relative motion (see Figs. 5.1 and 5.2).

All seismic instruments used in the WWSSN were seismometers with electromagnetic transducers. Their

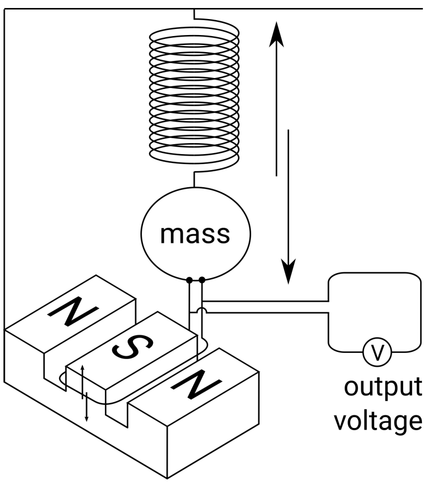

Figure 5.1: *Schematic depiction of an EM-transducer coupled to an inertial pendulum.*

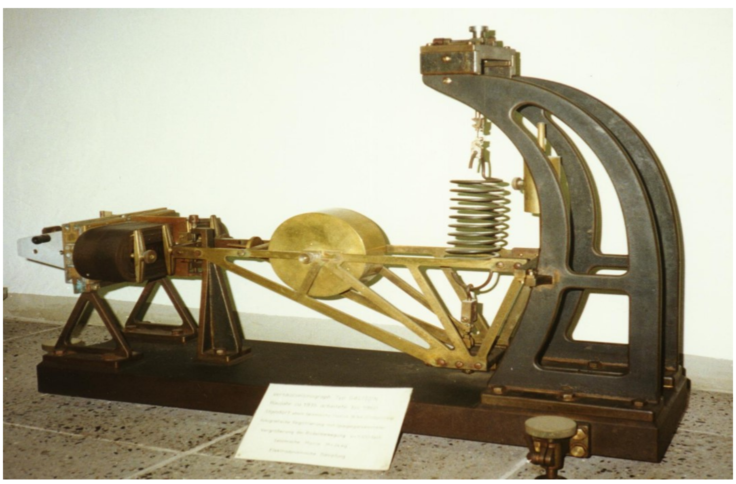

Figure 5.2: *Replica of Galitzin's instrument with the EM-transducer at the left end of the instrument. (Photo: Horst Rademacher)*

output current was fed into galvanometers, electromagnetic-optical devices, which act as very sensitive current meters. They converted the electric signal into the mechanical motion of a mirror, the movement of which was recorded as the deflection of a beam of light on light-sensitive paper or film.

Thus, recording the ground motion with a seismometer-galvanometer system is a complex series of conversions. Initially, the ground motion is converted into a mechanical displacement between the suspended mass and the instrument frame. The EM transducer converts this motion into an electrical current. The galvanometer reconverts the current into a mechanical motion and then via optical transmission into a record on light sensitive paper. In addition to the limitations mentioned in the introduction, this is another example of the complexity of seismic recording systems from past decades.

Each of these conversions is plagued by various shortcomings, which reduce the quality and fidelity of the seismic measurements. As galvanometers and optical recordings have been replaced by digital data handling and thus become obsolete, we will not discuss these aspects of the old instrumentation any further. Instead we focus on the shortcomings of inertial pendulum devices themselves. Their two main limitations are the non-linearity of the movement of the suspended mass, and clipping or saturation of the EM-transducer when the ground motion amplitudes are too large. *Wielandt* (2002) describes the causes of the non-linearity as *"imperfections in the spring and the hinges"* as well as the limited space inside a seismometer housing. The clipping has *"geometrical and electronic"* causes.

5.4 Open Loop vs. Forced Feedback Systems

Looking at an inertial pendulum seismometer through the lens of a cyberneticist we may say that it consists of two dynamic systems: the inertial mass and the transducer. The inertial mass (system A in Figure 5.3) reacts to the movement of the ground and the transducer (system B) converts this reaction into a measurable quantity. In seismometers such as those invented by Galitzin or used in the WWSSN, system A influences system B significantly, while system B has only a very minor effect on system A. Such an arrangement is defined as an open loop system (*Aström and Murray*, 2008). Modern geophones and many short period sensors operate under such an open loop arrangement.

If one could find a way to have system B also influence system A, i.e. by somehow passing the output of the transducer back into the moving inertial mass, one would get a closed loop arrangement. In

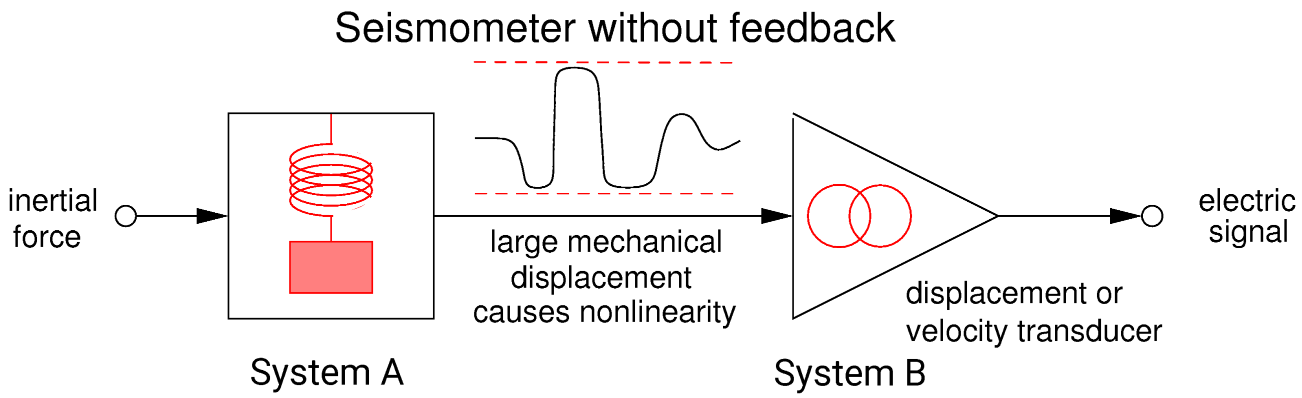

Figure 5.3: *Block diagram of the core elements of an open loop seismometer. Drawing by Erhard Wielandt* `http://www.software-for-seismometry.de/textfiles/Seismometry/BroadbandDesign.pdf`

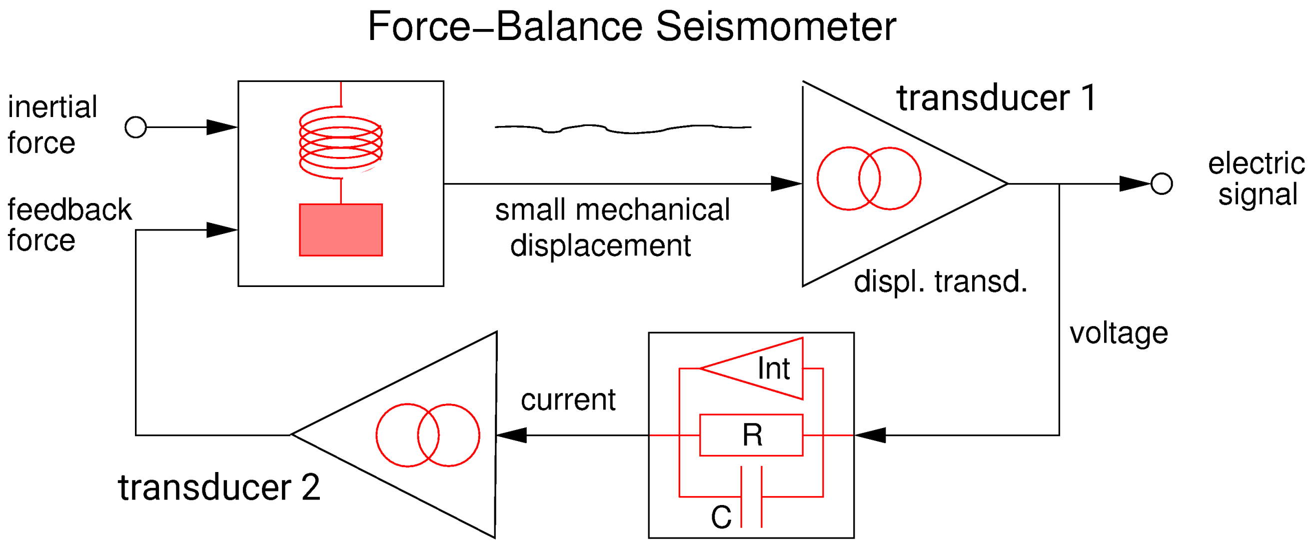

Figure 5.4: *Block diagram of a force-balance feedback seismometer. Drawing by Erhard Wielandt* `http://www.software-for-seismometry.de/textfiles/Seismometry/BroadbandDesign.pdf`

cybernetics this is called a feedback loop. If done right, such a loop can stabilise both systems. At least in theory, this concept opens the door to better seismometers, if one can find a good way to feed the transducer's output back into the system involving the inertial mass.

This becomes possible by equipping the inertial mass with a second transducer. While the first one converts the mechanical movement of the mass into an electric signal, the second transducer takes this electrical signal and converts it back into mechanical motion. If this force is exactly opposite to the amplitude and phase of the force of the original motion, one has created a negative feedback loop, also called a force-balance system.

According to the laws of cybernetics, loops with negative feedback are a necessary step to stabilise the entire system. But why would that lead to a better seismometer? The answer can be seen in the wiggly lines at the center of Figures 5.3 and 5.4. In the case of the open loop seismometer (Fig. 5.3), the amplitude of the relative motion of the mass with respect to the frame (mechanical displacement) can be very large. In contrast it is much smaller, even close to a flat line in the case of the seismometer with a feedback loop. Effectively, the feedback transducer forces the inertial mass not to move.

At first glance this is counter-intuitive. After all, we want to measure the motion of the ground. How can this be achieved, if the test mass is forced to remain still, while the ground is shaking? However, it confirms the statement of *Aström and Murray* (2008), that *"simple causal reasoning about a feedback system is difficult because the first system influences the second and the second system influences the first, leading to a circular argument. This makes reasoning based on cause and effect tricky, and it is necessary to analyse the system as a whole. A consequence of this is that the behavior of feedback systems is often counter intuitive, and it is therefore necessary to resort to formal methods to understand them".*

Without going into these formal methods, the simple way to understand how a feedback sensor can measure ground motion even without the inertial mass moving, is to look at the forces involved. In most modern feedback seismometers, the first transducer is either a capacitive sensor or a linear variable differential transformer (LVDT). The second transducer is always an EM-transducer in a coil-magnet arrangement, which uses magnetic forces to balance the inertial motion of the mass. The larger the motion to be compensated, the stronger the magnetic force must be. A stronger current through the coil is necessary to increase the strength of the magnetic field that balances the force from the ground attempting to cause the relative movement of the mass – hence the strength of the feedback current is a direct measure of the ground acceleration acting on the inertial mass.

In order to get the actual output signal of a feedback seismometer, the current is passed through a resistor which causes a voltage drop that changes depending on the variation in the strength of the current. It is this voltage variation, which when digitised and recorded, gives us the representation of the ground acceleration in form of a seismogram.

But why would a seismometer based on a force-balance feedback system be better than a seismic sensor with an open loop arrangement? The main reason is the much reduced motion of the inertial mass in a seismometer with feedback. In order to understand why this has a dramatic effect, let's look at what we want to achieve with a seismometer. When an elastic wave travels through the ground, each small volume element can move in six different ways. These are the three perpendicular translatory directions and the three rotational motions (pitch, roll and yaw). As we are not describing rotational sensors in this paper, we will focus only on the translatory motions. In order to measure the full translatory ground motion in three dimensions, we usually deploy three independent sensors oriented orthogonal to each other. Theoretically, each sensor measures the movement of the ground in exactly one direction. A vector addition of the three measurements then gives us the truly three dimensional ground motion.

But because the inertial masses and their suspensions are mechanical devices, they are plagued by limitations. A few examples are the uniformity of the material of the springs which determines their internal friction, the friction in hinges (pivots), the linearity of motion within the transducer and way the inertial mass responds to ground motion over a wide range of frequencies. The larger the amplitude of the movement of the inertial mass, the more pronounced these limitations become, despite the best efforts of seismometer manufacturers to keep them small. In contrast, if the mass moves very little, these shortcomings remain less important and the seismometer records the ground motion with high quality.

5.5 The First Feedback Seismometers

Probably the very first feedback seismograph in the world was developed in the early part of the 1920's in Zürich by the two Swiss physicists Alfred de Quervain and Auguste Piccard. They built a mechanical three-component seismograph with a single mass of 21 tons with its position stabilised with water ballast (*de Quervain and Piccard*, 1927). As this "water feedback" was purely mechanical and was not recorded as described above, I will not consider it any further.

Instead it was Hugo Benioff, one of the grand masters of geophysical instrumentation in the 20th century, who first mentioned the use of an electronic feedback system to improve the performance of a seismometer. Without directly using the words feedback or force-balancing, *Benioff* (1955) described a *"pendulum stabilizing circuit"* in which he used magnetic forces to reduce the long period pendulum drift, particularly on horizontal seismometers. Benioff claimed this to be *"useful in applications such as portable installations where the pendulum drift may be large"*.

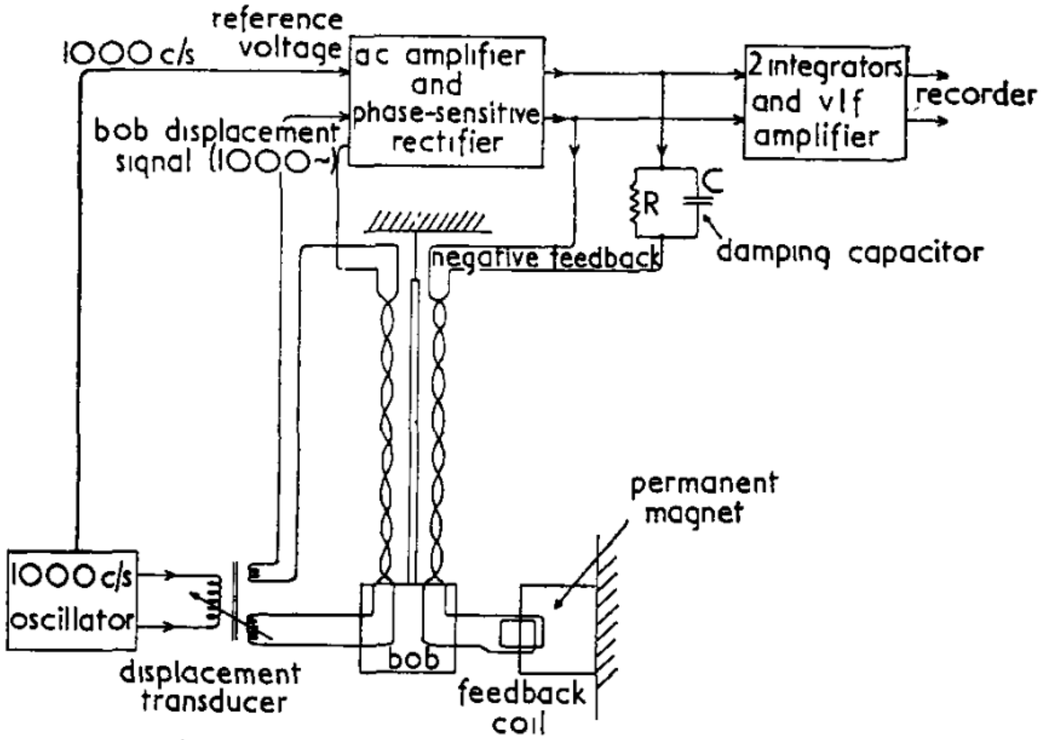

Figure 5.5: *Schematics of Tucker's first feedback seismometer. From* Tucker (1958) © IOP Publishing. Reproduced with permission. All rights reserved.

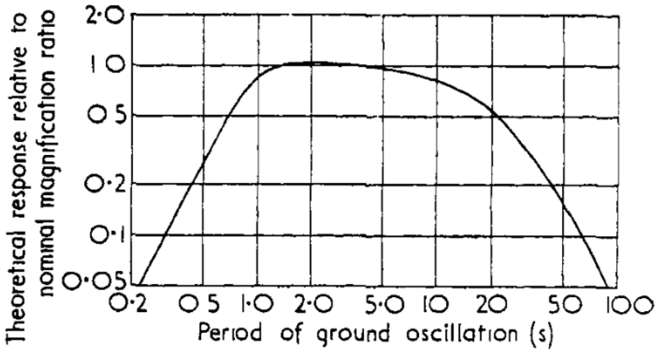

Figure 5.6: *Frequency response of Tucker's sensor. From* Tucker (1958) © IOP Publishing. Reproduced with permission. All rights reserved.

The first feedback seismometer based on this idea that I know of was built in the late 1950's at the British National Institute of Oceanography in Wormley (Surrey). Referring to Benioff's description *Tucker* (1958) constructed a long period pendulum which had several elements of modern feedback seismometers. The movements of the pendulum's bob were measured by a displacement transducer and then controlled by a feedback coil (Fig. 5.5).

The instrument was specifically developed for measuring the ocean microseisms. Hence its feedback loop was tailored for that frequency range. It gave the instrument a reasonably flat frequency response for periods between 1.5 and 12 sec (Fig. 5.6). It is not known if and where this instrument was ever deployed and if more than a prototype or two were ever built.

Shortly after Tucker's development, researchers at what is now the Lamont-Doherty Earth Observatory in

Palisades, New York, began using feedback loops to tackle a big problem which had plagued seismometry for decades: How could one build a compact, long-period seismograph to be deployed at remote sites? While long-period seismographs had existed for quite some time, they could only be used in a controlled observatory setting, where operators would adjust them when needed.

Such adjustments were necessary because any long-period elastic suspension is subject to long-term drift due to several causes. Among them are:

- thermal effects, which change the spring constant and the dimensions of the metal elements of a sensor,
- deformation of the structural elements of a seismometer over time due to fatigue or creep, and
- variations in the barometric pressure, which exert forces on the inertial mass of the sensor.

All of these influences can cause the mass to drift with amplitudes higher than those of the long-period seismic waves of interest.

To compensate for such long-term drift, the group at Lamont used a feedback loop and developed an *"integrated, triaxial long-period seismometer"* (*Sutton and Latham*, 1964). In it, the displacement of the inertial mass from its center position was measured by a differential capacitive plate, which generated a voltage proportional to the displacement of the mass. After some amplification and electronic filtering this output signal was fed into the coil of the coil and magnet assembly originally provided for the damping of the seismometer. The resulting magnetic force acted to restore the seismic mass into its electrical center position, where the output of the capacitive transducer is zero, thus completing the feedback loop.

This design was soon to be tested on a truly remote place, namely the Moon. The Apollo astronauts installed several of these seismometers – the space agency NASA called them *"mid-period sensors"* - on the lunar surface during most of their landings on the moon between 1969 and 1972. Many of them transmitted data back to Earth well into 1977 (*Nunn et al.*, 2020). However, the end of the Apollo program was also the end of the seismometer design efforts by the Lamont group. This sensor type was not developed further for use on Earth.

While the Apollo astronauts were busy on the Moon, several other groups of seismologists and engineers in Europe and in the United States worked independently on improving seismometers for use on Earth by applying feedback loops to various existing seismometer designs. Among them were *Block and Moore* (1966), at Princeton University, who applied a feedback system to a standard LaCoste-Romberg survey gravimeter and used the output to measure the extremely long period modes of free oscillation of the Earth.

Another example is Axel Plešinger and his group at what was then called the Czechoslovakian Academy of Sciences in Prague. In 1967 they outfitted several Russian built Kirnos seismometers with feedback loops (Figure 5.7). Compared to the original open loop Kirnos sensor, this endeavour led to a seismometer system with a flat amplitude response to ground motion over a large period range. The complete response curve of the feedback system is shown in Figure 5.8. Its response to ground velocity between 3 Hz and 300 sec was essentially flat with a fall off of ω^2 at even longer periods (*Plešinger and Horalek*, 1976).

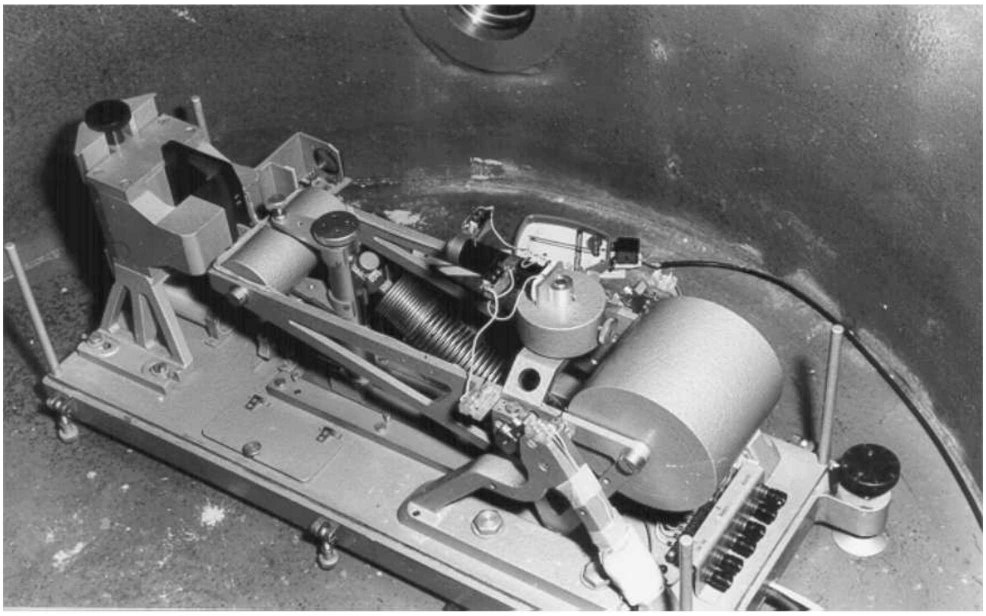

Figure 5.7: *Kirnos Seismometer with Plešinger's feedback loop (Photo: Plešinger)*

Dziewonski characterises this response as giving the instruments *"enough sensitivity to record not only the gravest modes of free oscillations of the Earth, but also the tides. At short periods, frequencies up to 5 Hz could be easily captured, and thus the entire band needed to record teleseismic signals could be accommodated"* (*Dziewonski*, 1989).

The first of these instruments was deployed in 1972 near Bishkek (then called Frunze) in Kyrgyzstan. A year later the group deployed another set at the very quiet Czech seismic station Kašperské Hory (station code KHC) in the Bohemian Forest. The signals of these three component (Z, N/S and E/W) stations were recorded locally on magnetic tape using FM modulation. The feedback-augmented seismometers at KHC operated continuously between 1973 and 1986, making it the very first broadband station in the world. A third set of these seismometers was deployed in 1976 at the station Ksiaz (station code KSP) in southwestern Poland (Fig. 5.9), about 270 km north-east of KHC.

While Plešinger's feedback sensors and other comparable alterations of existing open loop seismometers worked well and were successfully deployed at several locations, these instruments were never manufactured commercially. Hence, despite their - at that time - unique broadband performance they remain singularities in global seismometry.

5.6 Broadband Seismometry Goes Worldwide

While the Czech Group successfully operated their seismic broadband station in the Bohemian Forest for 13 years, their pioneering endeavours were barely recognised in the West. The Iron Curtain, which separated Europe during the Cold War, ran a mere 15 km west of the station KHC, effectively blocking any meaningful open scientific exchange between seismologists on either side of the line. Despite the political deep freeze, Plešinger had good personal contacts to seismologists in what was then West-Germany. Through their national science foundation, the Deutsche Forschungsgemeinschaft (DFG), the West Germans had inherited an old seismic array set-up and operated by the US Air Force in the southeastern corner of West-Germany near the small town of Gräfenberg, less than 180 km north-west of KHC. The original purpose of this array was to monitor underground Soviet nuclear weapons tests. But in the late 1960's, the station and most of its equipment was abandoned by the US military and turned over to German seismologists.

At the same time Hans Berckhemer, the long time chair of the Institute of Meteorology and Geophysics at the University of Frankfurt (Germany) proposed his concept of *"wide band seismometry"* at a meeting of the European Seismological Commission in Luxembourg. He made the case that having a seismometer that covered a spectral range of ground motion between at least 10 Hz and 300 sec was necessary to answer fundamental questions in seismology. He suggested several theoretical realizations, albeit without demonstrating the concepts with his own engineering solutions. However, his contribution was published (*Berckhemer*, 1971) in a small Belgian journal and therefore not widely read.

While the German seismologists were debating what to do with the abandoned array, Plešinger showed them seismograms collected with his broadband instruments - and the German group was impressed. In their discussion strongly influenced by Berckhemer's paper and Plešinger's data, it became very clear to the group that they wanted to rebuild the array and bring it up to the most modern standards of the time. That meant:

1. using highly sensitive broadband seismometers based on the feedback principle,
2. digitizing analogue outputs of the seismometers directly in the field and
3. transmitting the digital data in real time to a central location for recording, initial analysis and archival.

Given the state of seismometry in the world in the 1970s, these were indeed lofty and ambitious goals. In addition, this group of seismologists was just a loose federation of researchers from academia and government institutions which called itself "Forschungskollegium Physik des Erdkörpers" (Research Group for the Study of the Physics of the Solid Earth) - FKPE for short. It had no formal function within Germany's post World War II scientific hierarchy.

Nevertheless, the FKPE convinced the German funding agencies to finance a project which today would undoubtedly be labelled as truly high risk science. At the core of the uncertainty was the fact that, at that time no commercial broadband seismometer existed anywhere in the world. It was Erhard Wielandt, a German physicist who was then working in the Institute of Geophysics at the Swiss Federal Institute of Technology (ETH) in Zürich, who took on the challenge. Inspired by Plešinger's results, Wielandt and his student Gunnar Streckeisen set out to develop a completely new seismic sensor with an integrated feedback loop from scratch. The result of their work became the famous STS-1 (*Wielandt and Streckeisen*, 1982). After some initial tests of the new sensor, the German group decided to use the STS-1 as the heart of its new array.

Beginning with the first deployment in 1975 a total of 19 STS-1 seismometers were installed in the 13 stations of what became known as the Gräfenberg Array (station code GRF). Three of the stations were equipped with three components each, the rest had only vertical components as shown in the left panel in Figure 5.10. Initially the seismometers had a flat response to ground velocity between 20 sec and

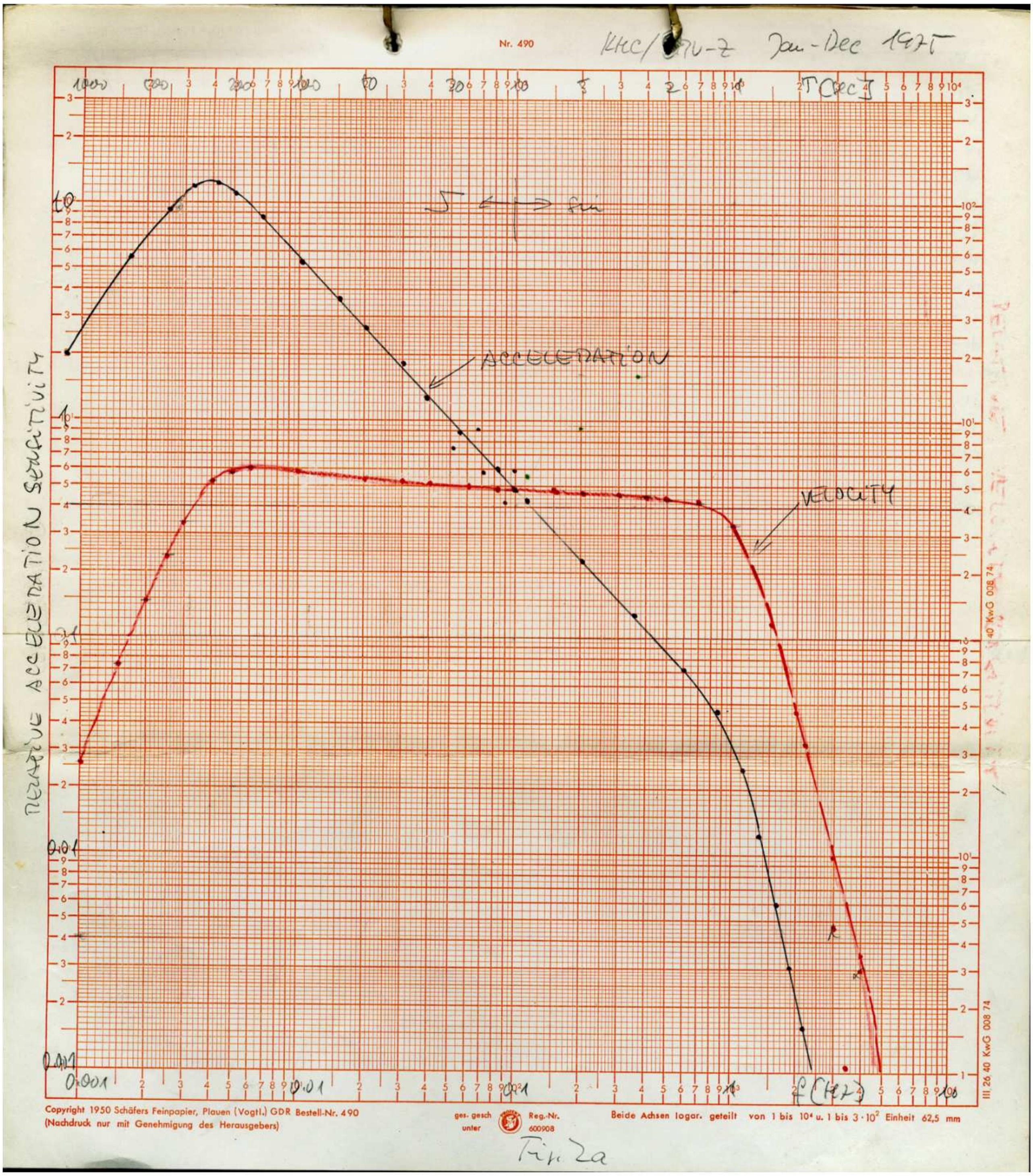

Figure 5.8: *Original measurements of the amplitude frequency response of Plešinger's complete system at KHC. The red line shows the nearly flat response of the system to ground velocities in the bandwidth of 300 sec to 3 Hz. Note that all data points were drawn by hand on log-log paper. From* Kolář, P., The KHC Seismic Station: The Birthplace of Broadband Seismology, Seismol. Res. Lett., *91*, 1057 – 1063, 2020, `https://doi.org/10.1785/0220190326` © Seismological Society of America.

Figure 5.9: *Three component Plešinger feedback sensors in sealed pressure housings in Ksiaz, Poland (Photo: Plešinger)*

5 Hz. Some of them were later upgraded to record ground motion at ultra long periods of up to 360 sec. The upper corner was eventually extended to 15-20 Hz. All data were digitised on site with a 16 bit AD converter with gain ranging. It gave the system a dynamic range of 138 dB, a value completely unheard of in seismology until then.

Finally, the digital data were telemetered over dedicated telephone lines to the central observatory site in the town of Erlangen (*Harjes and Seidl*, 1978). There, all data were archived continuously and are still available today through the German Federal Agency for Geosciences (BGR) in Hanover (`http://eida.bgr.de/fdsnws/dataselect/1/`); data from the station GRA1 is also available through the IRIS Data Management Center. After nearly thirty years of continuous operation, the STS-1 seismometers at GRF showed signs of ageing and in the early 2000's all 13 stations were upgraded with second generation, three component broadband seismometers from Streckeisen.

This unique set-up made the Gräfenberg Array the first continuously recorded, digital broadband array in the world. Because of its impressive results GRF became - at least for a while - the go-to site for seismologists from all over the world, who wanted to learn more about operating a complex array of these newly available broadband seismometers and about digital data acquisition and processing. It also helped Streckeisen, Wielandt's former student, to launch his own company manufacturing the STS-1, short for Streckeisen-Seismometer 1. Within a few years, these sensors became standard equipment for new, top of the line global networks, like the American operated Global Seismic Network (GSN) or the French GEOSCOPE and some of them are still operating today. More information on the Gräfenberg Array and the operational procedures of BGR can be found in their ISC Summary article (*Hartmann et al.*, 2018).

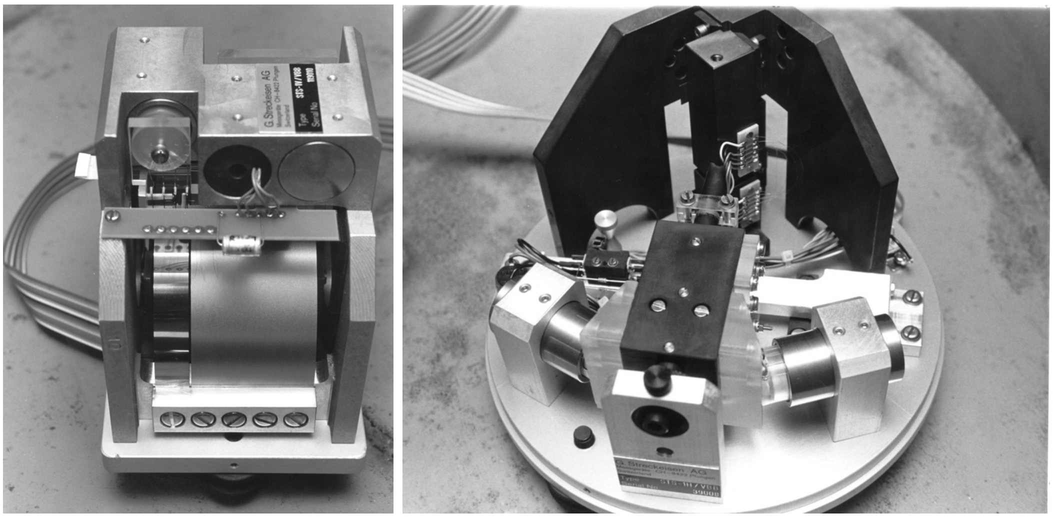

Figure 5.10: *The STS-1 seismometer. The vertical component with its famous leaf spring is shown on the left, a horizontal component on the right. (Photos: Rick McKenzie, UC Berkeley)*

5.7 A Broadband Borehole Seismometer

In the meantime scientists and engineers on the opposite side of the Atlantic were also busy developing seismic sensors with feedback systems. The most consequential work took place in the early 1970's at the Teledyne-Geotech Company in Garland, Texas. Under a contract with the Advanced Research Projects Agency (ARPA) of the US Department of Defense, the engineers at the company designed a broadband, three-component borehole seismometer with the goal of upgrading or replacing some stations of the WWSSN. The new concept was called Seismic Research Observatory (SRO) and in addition to using broadband seismometers, the plan was to record all data digitally. A borehole solution was chosen to help reduce the ever present long period seismic noise at the Earth's surface.

The new borehole seismometers contained three orthogonally oriented sensor modules and their associated electronics (see Fig. 5.11). It was mainly developed by two Geotech engineers, B.M. Kirkpatrick and O.D. Starkey. The mechanical configuration of the sensors was of conventional design; a LaCoste suspension was used for the vertical and "garden-gate" suspensions were used for the horizontal components. The sensors were of a force-balance type with capacitive transducers, based on the concept of *Block and Moore* (1966). As the signal of such capacitive transducers is proportional to mass displacement rather than mass velocity, their output was higher at low frequencies when compared to conventional seismometers (for a full description of the SRO stations see *Peterson et al.*, 1976). The instrument was named KS-36000, using the initials of the last names of the principal developers.

Despite the fact that each of the sensors in the KS-36000 had an output proportional to displacement over the frequency range from 50 sec to 1 Hz, this output signal was filtered at the wellhead to produce the short- and long-period signals, which were finally recorded (see Figure 5.12). While this arrangement had the advantage of almost completely blocking out the mostly unwanted ocean microseisms with periods of 6-8 secs, it also diminished the inherent "broadbandedness" of the seismometer. When compared, for example, to the amplitude frequency response of Plešinger's seismometer (Fig. 5.8) it is clear, that the filtering process prevented the SRO station from collecting the full information contained in the Earth's ground motions in the seismically relevant band.

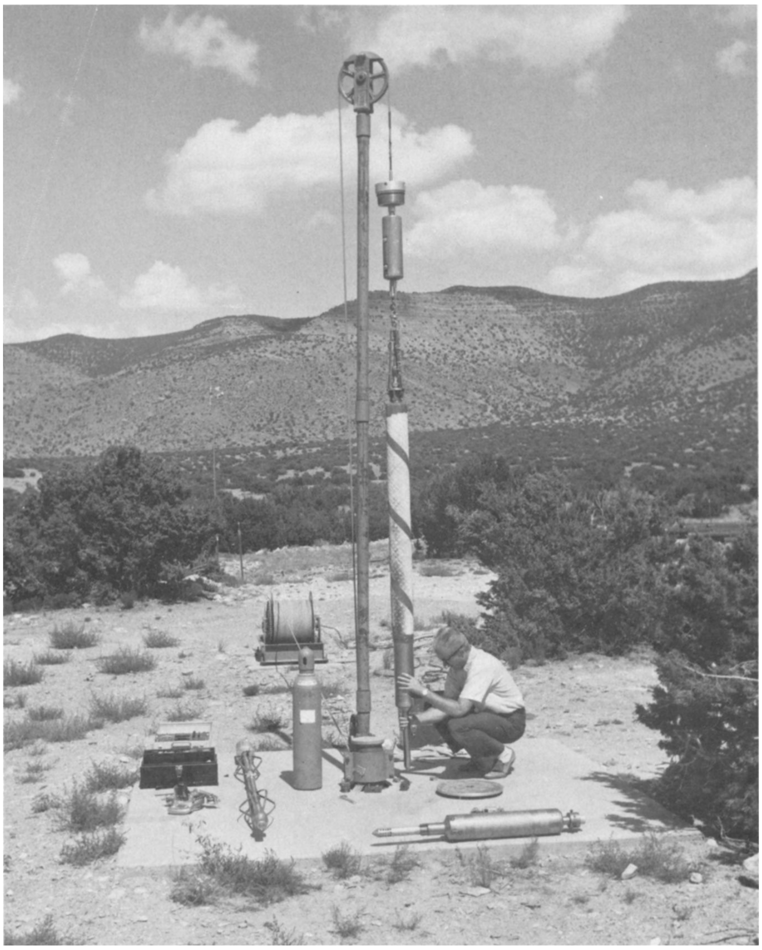

Figure 5.11: *The first broadband borehole sensor, named KS-36000, was installed in a borehole at the Albuquerque Seismology Laboratory in July 1974. From* Peterson et al., The Seismic Research Observatory, Bull. Seismol. Soc. Am., 66(6), 2049 – 2068, 1976, `https://doi.org/10.1785/BSSA0660062049` © Seismological Society of America.

The initial preproduction SRO-System was deployed for testing at the Albuquerque Seismological Laboratory in New Mexico in July 1974 (Fig. 5.11, right). In the following years a total of 13 stations were installed globally, one of which was installed in a 150 m deep borehole at the main station of the Gräfenberg Array in the village of Haidhof (station code GRFO).

Both broadband sensors, the STS-1 and the KS-36000, brought seismological data acquisition to a completely new level. These sensors and their digital data recording systems made it possible to collect seismic data over a much wider frequency range using just one instrument. But both systems were extremely complex, very difficult to manufacture and hard to install, even by skilled personnel. For instance, each component of an STS-1 had be installed in an air tight arrangement under an evacuated glass bell. This vacuum was necessary to prevent pressure changes in the seismic vault from affecting the sensor's long period performance. They also had to be well protected from any temperature fluctuations and shielded against variations in the magnetic field. To reduce the effects of the dissipated heat generated by the feedback loop within the KS-36000, each borehole instrument casing was filled with Helium and wrapped with foam insulation before being lowered into the borehole. During the manufacturing process, each individual KS-36000 sensor was sealed in containers *"baked and evacuated to lessen the possibility of internal convections"* (*Peterson et al.*, 1976). In addition the systems were

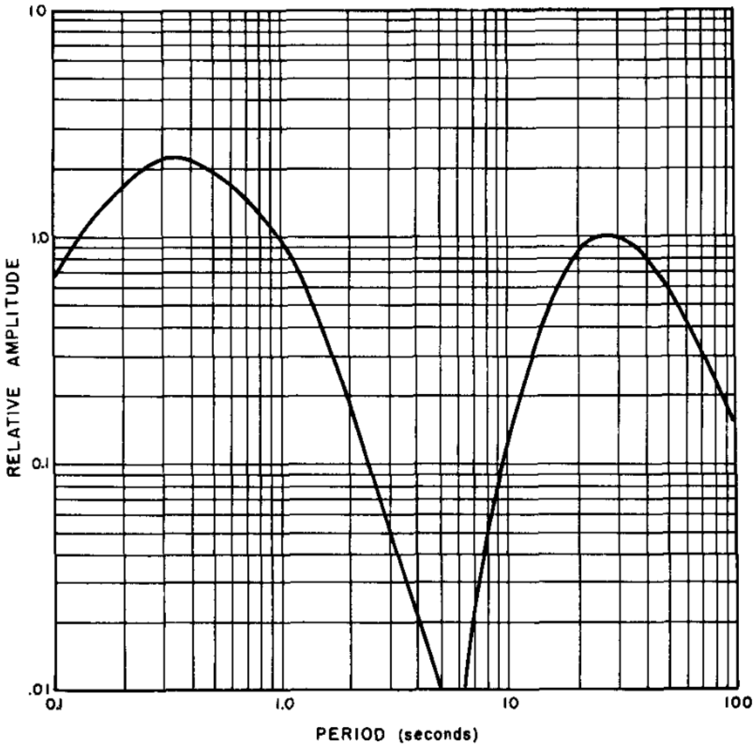

Figure 5.12: The final output transfer function of the SRO stations. From Peterson et al., The Seismic Research Observatory, Bull. Seismol. Soc. Am., 66(6), 2049 – 2068, 1976, https://doi.org/10.1785/BSSA0660062049 © Seismological Society of America.

fairly big. The entire KS-36000 arrangement deployed in an SRO borehole was almost 4 m long, and the three separate components of the STS-1 each under its own glass bell needed several square meters of space on a seismic pier. In short, like Plešinger's seismometers, this first generation of commercial broadband sensors was anything but field worthy. They had to be carefully installed and maintained in boreholes or in seismic observatories in well constructed seismic vaults and on well built piers.

5.8 Small, Compact, Field Worthy and still Broadband

Most of the people whose contributions to the development of broadband seismometers controlled by feedback circuits described above were either seismologists or engineers with long experience with building seismic measuring equipment. While their equipment worked very well and certainly lifted seismology to new levels, it may take scientific outsiders to bring fundamentally new ideas into an established scientific field like seismometry. Two such outsiders to Earth science were Peter Fellgett and Mike Usher at the University of Reading in England. Fellgett had a lifelong interest in scientific instruments. He was however rather critical about the processes in which most of these instruments were developed, particularly about the widespread discrepancy between their performance "in theory" versus the actual results. He claimed this not to be *"good science, which demands that if theory and practice differ, then one or both must be improved"* (*Fellgett*, 1984).

With this premise in 1964 Fellgett became Professor of Cybernetics and Instrument Physics in Reading and the first director of the department. There, his interest in instrument science continued and he encouraged Mike Usher, one of the cyberneticists working in his department, to develop a rather small seismometer which should be able to record ground motions with very long periods.

Usher enlisted the help of R.F. Burch from the Blacknest Seismological Centre operated by the British Atomic Weapons Research Establishment in nearby Aldermaston to design and built a horizontal component "wideband miniature seismometer". This sensor was small indeed, measuring just a few centimetres across (see Fig. 5.13). The position of the small inertial mass of only 40 g was measured relative to the instrument frame by a differential capacitance transducer and controlled by a negative feedback loop using a coil-magnet arrangement (*Usher et al.*, 1977). Usher's graduate student Cansun Guralp took this design to a new level by designing and building a complete, three component, broadband miniature seismometer (*Usher et al.*, 1978).

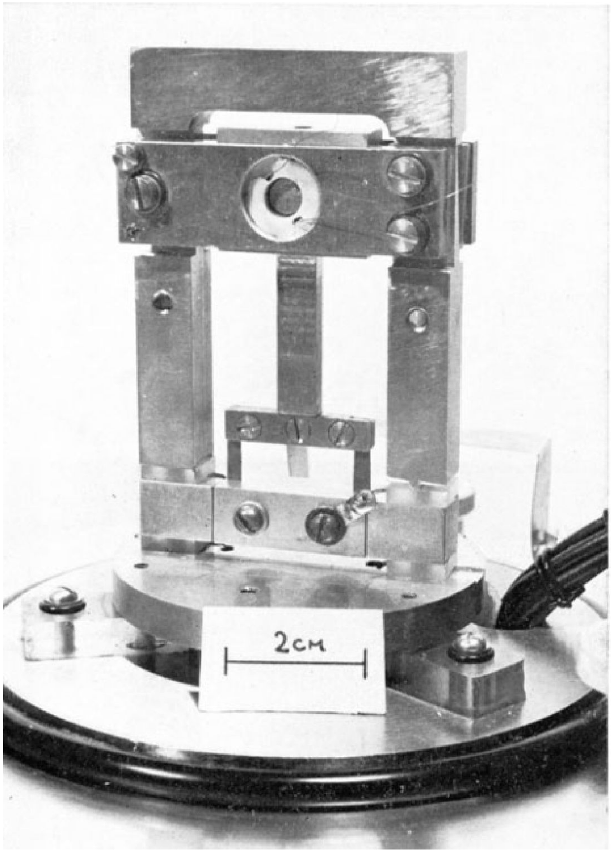

Figure 5.13: *The mechanics of Usher's horizontal miniature broadband seismic sensor. From* Usher et al., (1977) © IOP Publishing. Reproduced with permission. All rights reserved.

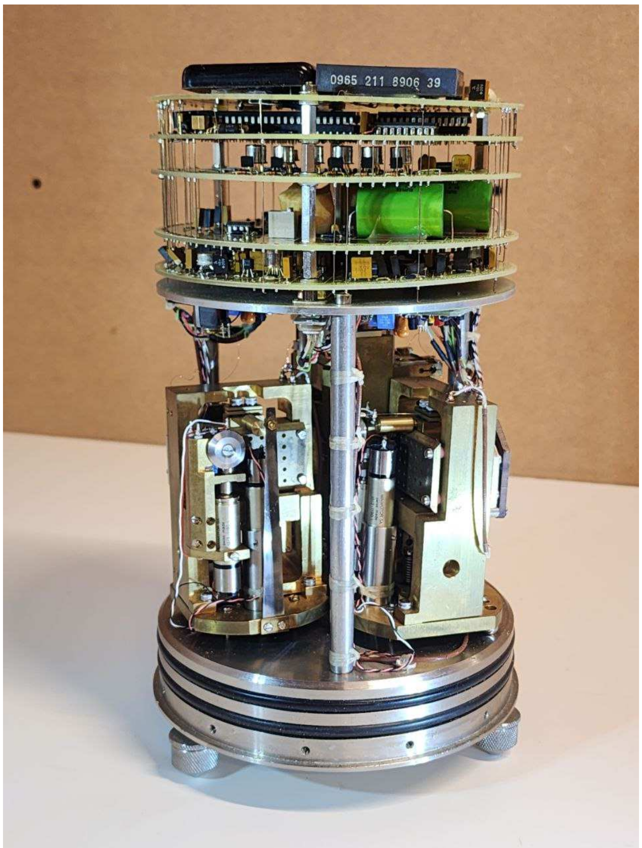

Figure 5.14: *The very first production model of the Guralp 3T seismometer without its casing. It was the first portable triaxial broadband seismometer. (Photo: Horst Rademacher)*

After obtaining his Ph. D. from Reading in 1980 with a thesis on designing a three component wideband borehole seismometer, Guralp founded his own company. There, he arranged the three components and the respective feedback electronics of the miniature wideband sensor into one cylindrical package with a diameter of just 17 cm and a height of less than 30 cm. The result was the Guralp 3T, the very first portable three component broadband seismometer (Fig. 5.14). It did not need to be installed in an observatory vault, but could be deployed even under rough field conditions. Its standard version had a flat response to ground velocity between 120 sec and 50 Hz. Over the decades, more than a thousand of these seismometers have been built in various versions, and as of this writing, the instrument is still in production.

5.9 An Initial Look at Broadband Seismograms

Despite the convincing theoretical underpinnings of the new developments and the technological advances described above, broadband seismograms were not accepted immediately in the broader seismological community. I will never forget the reaction of my former thesis adviser at the University of Cologne (Germany), when I showed him one of the first broadband seismograms we had collected at the Gräfenberg-Array in the late 1970's: This record is horribly noisy, he remarked, referring to the strong ocean microseisms dominating the seismogram. He was used to analysing only seismograms from short period seismometers, which did not record these microseisms with periods above six seconds - and also nothing else in the long-period range of the seismic spectrum. As previously mentioned, this criticism was the main reason why the initial output of the broadband borehole seismometers of the SRO stations was notch filtered to eliminate the ocean microseisms (Fig. 5.12).

Over time, however, the treasures hidden in the recordings of broadband seismometers became clear. In one of the first analyses of broadband data from the Gräfenberg Array, *Kind and Seidl* (1982) showed example records from medium sized earthquakes in the Chile-Bolivia border area recorded at GRF at an epicentral distance of almost 100 deg. Figure 5.15 shows three 15 sec long traces of the P-wave arrival of a M=6.5 quake in that region. The bottom trace depicts the unfiltered broadband recording of the vertical component at one of the GRF stations. The two traces above are digital simulations of how standard WWSSN seismometers would have recorded this P-wave train with the long period (LP) instrument (middle trace) and the short period (SP) (top trace) WWSSN sensors.

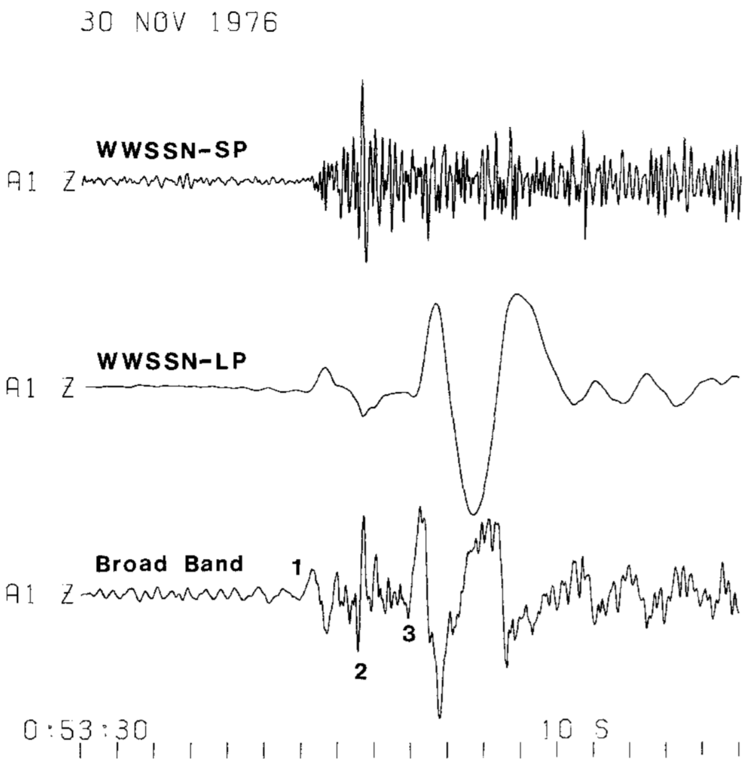

Figure 5.15: *15 sec long recording of the arrival of the P-wave of a M=6.5 earthquake in the Chile-Bolivia border region at the vertical component of GRF station A1. The bottom trace depicts the unfiltered broadband data, the traces above are digital simulations of WWSSN LP- and SP-seismometers, respectively. From* Kind, R. and Seidl, D., Analysis of Broadband Seismograms from the Chile-Peru Area, Bull. Seismol. Soc. Am., 72(6), 2131 – 2145, 1982, `https://doi.org/10.1785/BSSA07206A2131`, © Seismological Society of America.

There was of course no real WWSSN station in Gräfenberg. Instead the authors programmed bandpass filters which had the same characteristics as the transfer functions of the SP- and LP-WWSSN seismometers respectively. After applying these filters numerically to the broadband data, they were able to simulate the WWSSN recordings. With appropriate filters, almost any of the open loop seismometers existing at that time could be simulated. This, of course was only possible because of the inherent broadbandedness of the sensors and the digital recording of their outputs.

5.10 Summary

I have tried to recount the early development of broadband seismometry in the late 1970's and early 1980's. In this part, I focussed on the instrumentation, first by explaining the basic principles of feedback seismometers and then describing the work of various groups in Europe and in the United States in designing and building such sensors. In a second instalment I will focus on the digital recordings and describe some of the techniques used to apply broadband data to seismological analysis. I will also attempt to describe later technological development in the field of broadband seismometry and finally give an overview of how data from these instruments have contributed to the advancement of seismology in general and to our understanding of the Earth's interior and of earthquake source processes.

Acknowledgements

The topics covered in this contribution were drawn from a graduate course on Seismic Instrumentation I gave in the Department of Earth and Planetary Science at the University of California, Berkeley. I thank Dmitry Storchak (International Seismological Centre, UK) for suggesting this expose. I am very grateful to Erhard Wielandt (Prof. em., University of Stuttgart, Germany), Axel Plešinger (formerly Czech Academy of Sciences) and Cansun Guralp (Gaiacode Ltd., UK) for critically reading the text. Their suggestions led to major improvements. I also thank Axel Plešinger and the staff of the Berkeley Seismological Laboratory (UC Berkeley) for providing me with photos of some of the early broadband instruments. Editor Kathrin Lieser (International Seismological Centre, UK) diligently pointed out inconsistencies in the text and secured all copyright permissions. Despite having such high level help, I am solely responsible for all errors - big and small - the reader may find in the text. If any reader has additional information about the early days of broadband seismometry, please drop me a note (`horst@berkeley.edu`). I always like to learn more...

References

Aström, K. J. and R.M. Murray (2008) Feedback Systems: An Introduction for Scientists and Engineers, Princeton University Press, 408p.

Benioff, H. (1955), Earthquake Seismographs and Associated Instruments, *Advances in Geophysics*, *2*, 219 – 275, `https://doi.org/10.1016/S0065-2687(08)60314-3`.

Berckhemer, H. (1971) The Concept of Wideband Seismometry, *Comm. Obs. Royal de Belgique*, Sér. A, No. 13, Sér. Géoph. No. 101, 214 – 220.

Block, B. and RD. Moore (1966) Measurements in the Earth Mode Frequency Range by an Electrostatic Sensing and Feedback Gravimeter, *J. Geophys. Res.*, *71*(18), 4361 – 4375, https://doi.org/10.1029/JZ071i018p04361.

de Quervain, A. and A. Piccard (1927), Déscription du séismographe universel de 21 tonnes système de Quervain-Piccard, *Publ. Bureau Centr. Séism. Int. Sér. A*, *4*(32).

Dewey, J. and P. Byerly (1969), The Early History of Seismometry (to 1900), *Bull. Seismol. Soc. Am.*, *59*(1), 183 – 227, https://doi.org/10.1785/BSSA0590010183.

Dziewonski, A. M. (1989), The Global Seismographic Network: Progress and Promise, in J.J. Litehiser (Ed.), *Observatory Seismology*, University of California Press, Berkeley, California, http://ark.cdlib.org/ark:/13030/ft7m3nb4pj/.

Fellgett, P.B (1984), Three concepts make a million points, *Infrared Physics*, *24*(2–3), 95 – 98, https://doi.org/10.1016/0020-0891(84)90053-8.

Galitzin, B. (1914), Vorlesungen über Seismometrie, Teubner Verlag, Leipzig und Berlin, 538 p. (in German).

Harjes, H.-P. and D. Seidl (1978), Digital recording and analysis of broad-band seismic data at the Gräfenberg (GRF) array, *J. Geophys.*, 44, 511 – 523.

Hartmann, G., Th. Plenefisch and K. Stammler (2018), Seismological Central Observatory (SZO) of BGR, Germany, *Summ. Bull. Internatl. Seismol. Cent.*, July - December 2015, *52*(II), pp. 27 – 43, https://doi.org/10.31905/GQZM5DJ3.

Kerr, A.U. (Ed.) (1985), The VELA Program, A Twenty-Five Year Review of Basic Research, Defense Technical Information Center, ADA22289, 985p.

Kind, R. and D. Seidl (1982), Analysis of Broadband Seismograms from the Chile-Peru Area, *Bull. Seismol. Soc. Am.*, *72*(6), 2131 – 2145, https://doi.org/10.1785/BSSA07206A2131.

Kolář, P. (2020), The KHC Seismic Station: The Birthplace of Broadband Seismology, *Seismol. Res. Lett.*, *91*, 1057 – 1063, https://doi.org/10.1785/0220190326.

Nunn, C., R.F. Garcia, Y. Nakamura, A.G. Marusiak, T. Kawamura, D. Sun, L. Margerin, R. Weber, M. Drilleau, M.A. Wieczorek and A. Khan (2020), Lunar Seismology: A Data and Instrument Review, *Space Sci Rev*, *216*(89), https://doi.org/10.1007/s11214-020-00709-3.

Peterson, J., H.M. Butler, L.G. Holcomb and C.R. Hutt (1976), The Seismic Research Observatory, *Bull. Seismol. Soc. Am.*, *66*(6), 2049-2068, https://doi.org/10.1785/BSSA0660062049.

Peterson, J. and C.R. Hutt (2014), World-Wide Standardized Seismograph Network: A data users guide, *U.S. Geological Survey Open-File Report 2014–1218*, 74 p., https://doi.org/10.3133/ofr20141218.

Plešinger, A. and J. Horalek (1976), The seismic broadband recording and data processing system FBV/DPS and its seismological applications, *J. Geophys.*, 42, 201 – 217.

Storchak, D.A., D. Di Giacomo, E.R. Engdahl, J. Harris, I. Bondár, W.H.K. Lee, P. Bormann, and A. Villaseñor (2015), The ISC-GEM Global Instrumental Earthquake Catalogue (1900–2009): Introduction, *Phys. Earth planet. Interiors*, 239, 48 – 63, https://doi.org/10.1016/j.pepi.2014.06.009.

Sutton, G.H. and G.V. Latham (1964), Analysis of a feedback-controlled seismometer, *J. Geophys. Res.*, *69*(18), 3865 – 3882, https://doi.org/10.1029/JZ069i018p03865.

Tucker, M.J. (1958), An electronic feedback seismograph, *J. Sci. Instrum.*, 35, 167-171, https://doi.org/10.1088/0950-7671/35/5/306.

Usher, M.J., I.W. Buckner and R.F. Burch (1977), A miniature wideband horizontal-component feedback seismometer, *J. Phys. E: Sci. Instrum.*, *10*, 1253 – 1260, https://doi.org/10.1088/0022-3735/10/12/020.

Usher, M.J., C. Guralp and R.F. Burch (1978), The design of miniature wideband seismometers, *Geophys. J. Int.*, *55*(3), 605 – 613, https://doi.org/10.1111/j.1365-246X.1978.tb05930.x.

Wielandt, E. (2002), Seismometry, in W.H.K. Lee et al (Ed.), *International Handbook of Earthquake and Engineering Seismology, Part A*, Ch. 18, p. 283 – 304, https://doi.org/10.1016/S0074-6142(02)80221-2.

Wielandt, E. and G. Streckeisen (1982), The Leaf-Spring Seismometer: Design and Performance, *Bull. Seismol. Soc. Am.*, *72*(6), 2349 – 2367, https://doi.org/10.1785/BSSA07206A2349.

6

Summary of Seismicity, July – December 2020

The period between July and December 2020 produced 5 earthquakes with $M_W \geq 7$; these are listed in Table 6.2. The two largest events occurred in Alaska in the Shumagin Islands region with magnitudes of M_W 7.8 and 7.6. The first and larger megathrust event ruptured the plate boundary along the Alaska subduction zone on 22nd July 2020 (06:12:43.49 UTC, 55.0056°N, 158.5615°W, 22.5 km, 3184 stations (ISC)). About three month later, on 19th October 2020 (20:54:39.70 UTC, 54.6127°N, 159.6792°W, 32.9 km, 3110 stations (ISC)) another major event struck the Shumagin region about 80 km south-west of the July epicentre. This event, however, was somewhat unusual as (1) it was an intraplate strike-slip event in the downgoing Pacific plate (*Herman and Furlong*, 2021; *Jiang et al.*, 2022); and (2) the event triggered a tsunami that was larger than the one triggered by the main shock in July. Usually, strike-slip events rarely reach magnitudes as large as this aftershock and cause smaller tsunamis than thrust events because they produce lower vertical seafloor deformation. *Bai et al.* (2023) explained this unusual occurrence in their study by a very complex source mechanism involving a weak tsunamigenic fast rupture of two intraplate faults below and most likely above the plate boundary, along with an induced strong tsunamigenic slow thrust slip on a third fault near the shelf break.

The most discussed earthquake in the scientific community during this Summary's time period was the M_W7 Samos event, Greece (30/10/2020 11:51:27.32 UTC, 37.9051°N, 26.7559°E, 16 km, 3226 stations (ISC)) with currently 79 entries in the ISC Event Bibliography (*Di Giacomo et al.*, 2014; *International Seismological Centre*, 2023). It was the largest earthquake in the eastern Aegean Sea and western Turkiye for decades. The mainshock occurred offshore along an E-W striking north-dipping normal fault north of Samos Island and caused severe damage in Samos and the greater Izmir area, Turkiye (e.g., *Papadimitriou et al.*, 2020; *Zúñiga and Tan*, 2021).

A non-tectonic event that was not only discussed by the scientific community (23 entries in the ISC Event Bibliography) but also the media and public, was the devastating explosion of 2750 t of ammonium nitrate that were stored in a warehouse in the port of Beirut, Lebanon on 04/08/2020 (15:08:18.06 UTC, 33.9719°N, 35.4965°E, depth fixed to surface, 118 stations (ISC)). P phases of the blast could be observed up to teleseismic distances (GERES array, 22 degrees epicentral distance). The explosion caused heavy destruction in the surrounding neighbourhoods, killed more than 200 people, injured 7000 and left 300,000 people homeless (*Human Rights Watch*, 2021).

The number of events in this Bulletin Summary categorised by type are given in Table 6.1.

Figure 6.1 shows the number of moderate and large earthquakes in the second half of 2020. The distribution of the number of earthquakes should follow the Gutenberg-Richter law.

Figures 6.2 to 6.5 show the geographical distribution of moderate and large earthquakes in various magnitude ranges.

Table 6.1: Summary of events by type between July and December 2020.

felt earthquake	6472
known earthquake	141808
known chemical explosion	8053
known induced event	2831
known landslide	2
known mine explosion	2071
known rockburst	535
known experimental explosion	74
suspected collapse	3
suspected earthquake	121005
suspected chemical explosion	5586
suspected induced event	222
suspected landslide	1
suspected mine explosion	5691
suspected rockburst	206
suspected experimental explosion	504
suspected ice-quake	164
unknown	5
total	295233

Table 6.2: Summary of the earthquakes of magnitude Mw $\geq$ 7 between July and December 2020.

Date	lat	lon	depth	Mw	Flinn-Engdahl Region
2020-07-22 06:12:43	55.01	-158.56	22	7.8	Alaska Peninsula
2020-10-19 20:54:39	54.61	-159.68	32	7.6	South of Alaska
2020-07-17 02:50:22	-7.95	147.74	85	7.1	Eastern New Guinea region
2020-09-01 04:09:28	-27.99	-71.17	16	7.0	Near coast of northern Chile
2020-10-30 11:51:27	37.91	26.76	16	7.0	Dodecanese Islands

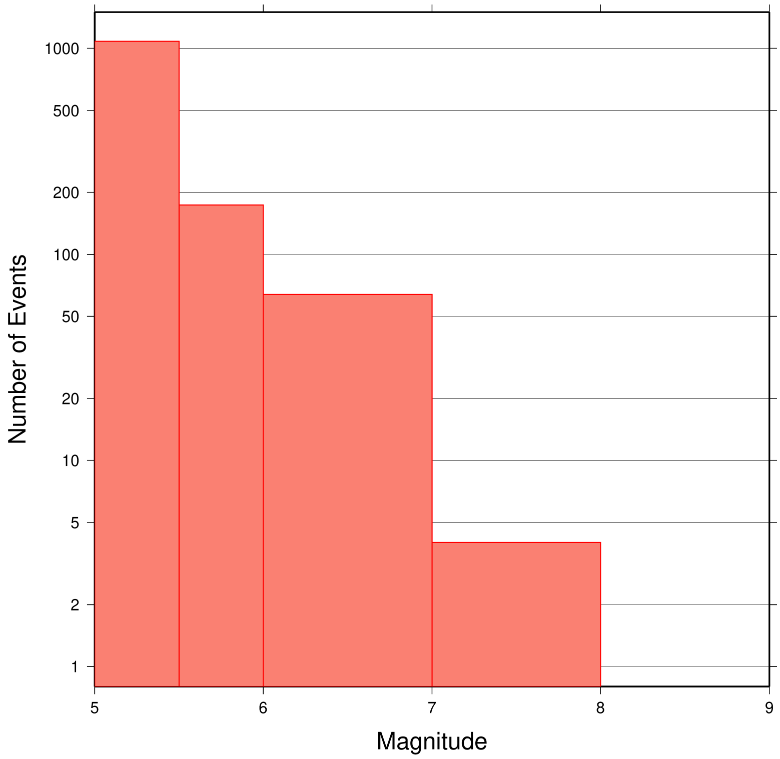

Figure 6.1: *Number of moderate and large earthquakes between July and December 2020. The non-uniform magnitude bias here correspond with the magnitude intervals used in Figures 6.2 to 6.5.*

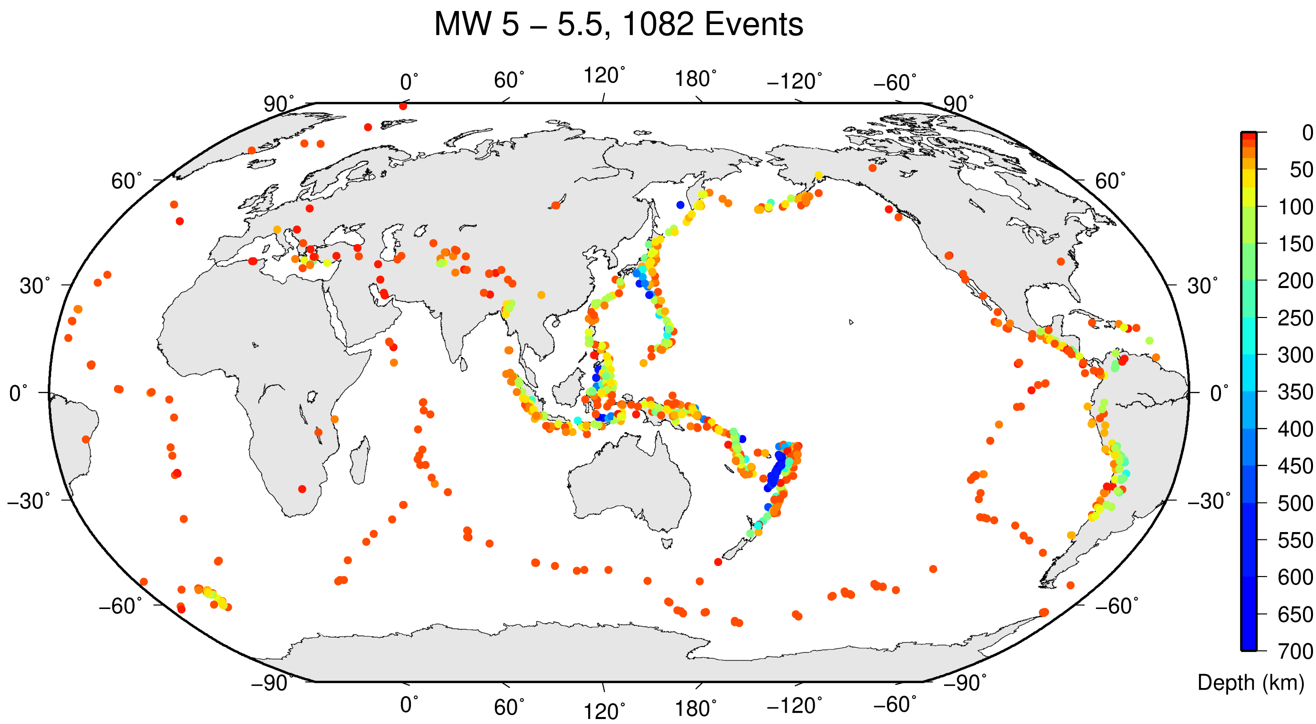

Figure 6.2: *Geographic distribution of magnitude 5-5.5 earthquakes between July and December 2020.*

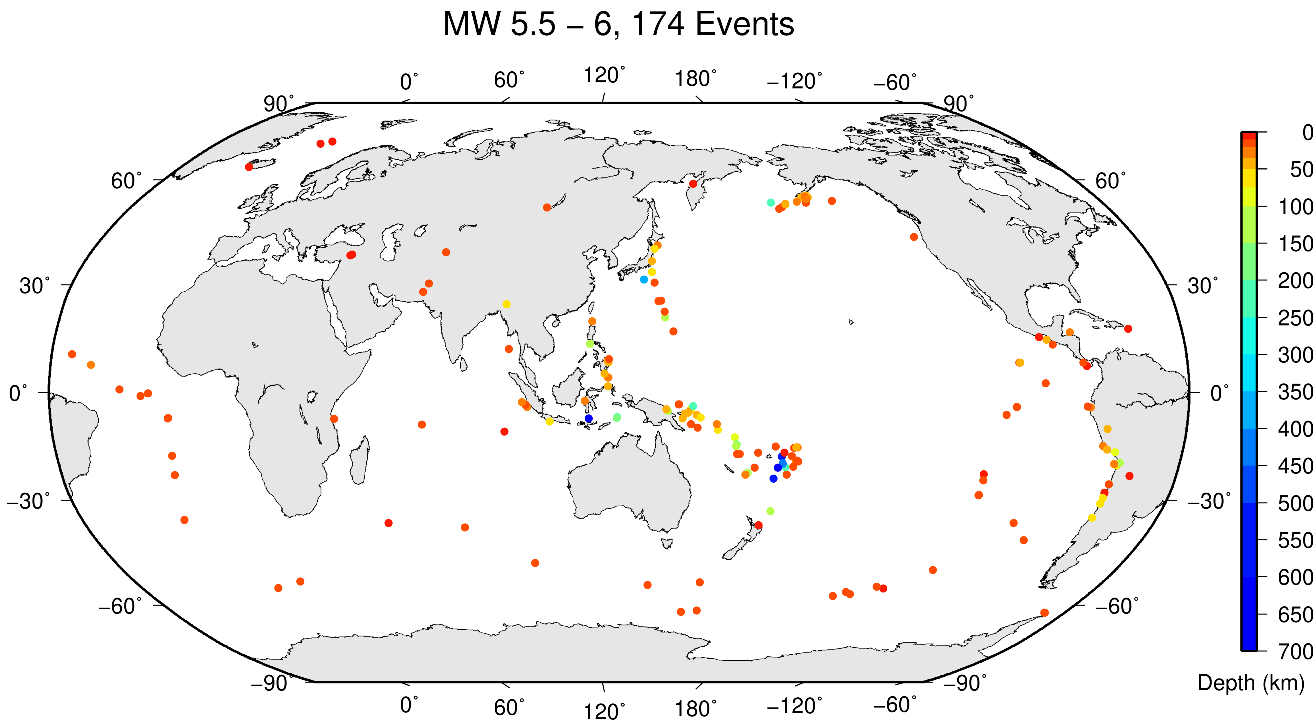

Figure 6.3: *Geographic distribution of magnitude 5.5-6 earthquakes between July and December 2020.*

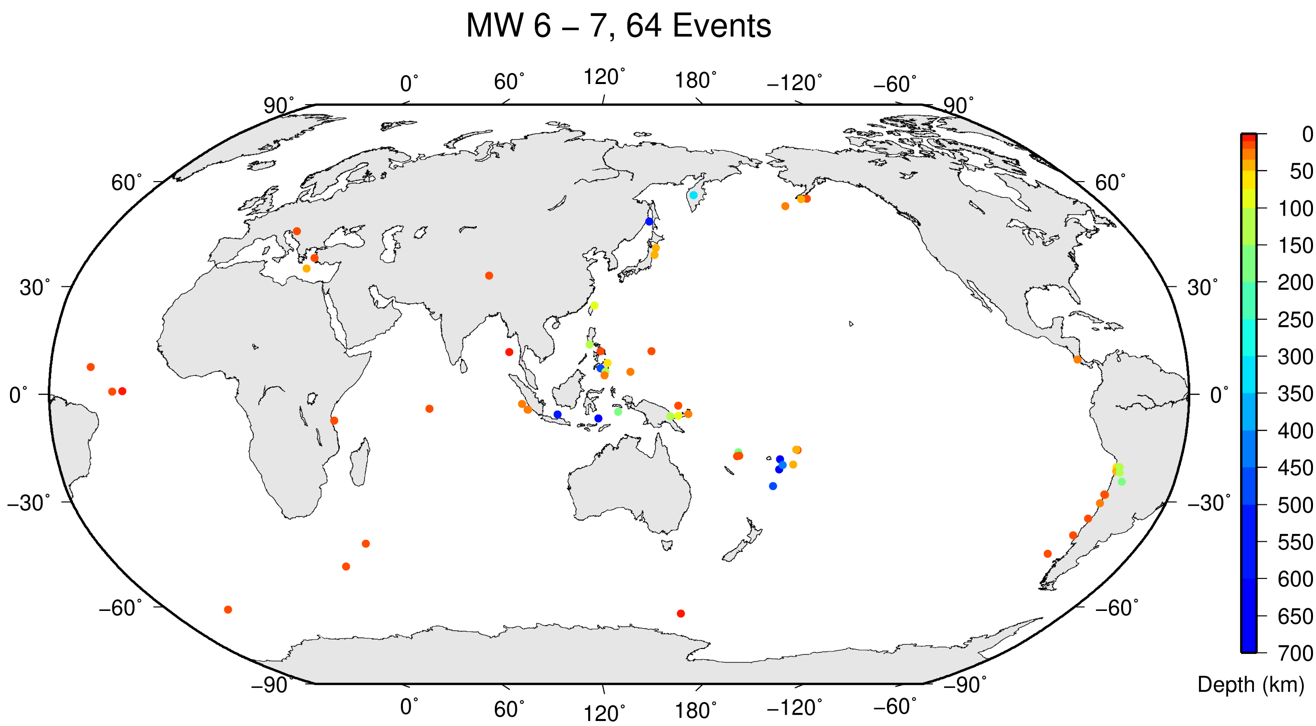

Figure 6.4: *Geographic distribution of magnitude 6-7 earthquakes between July and December 2020.*

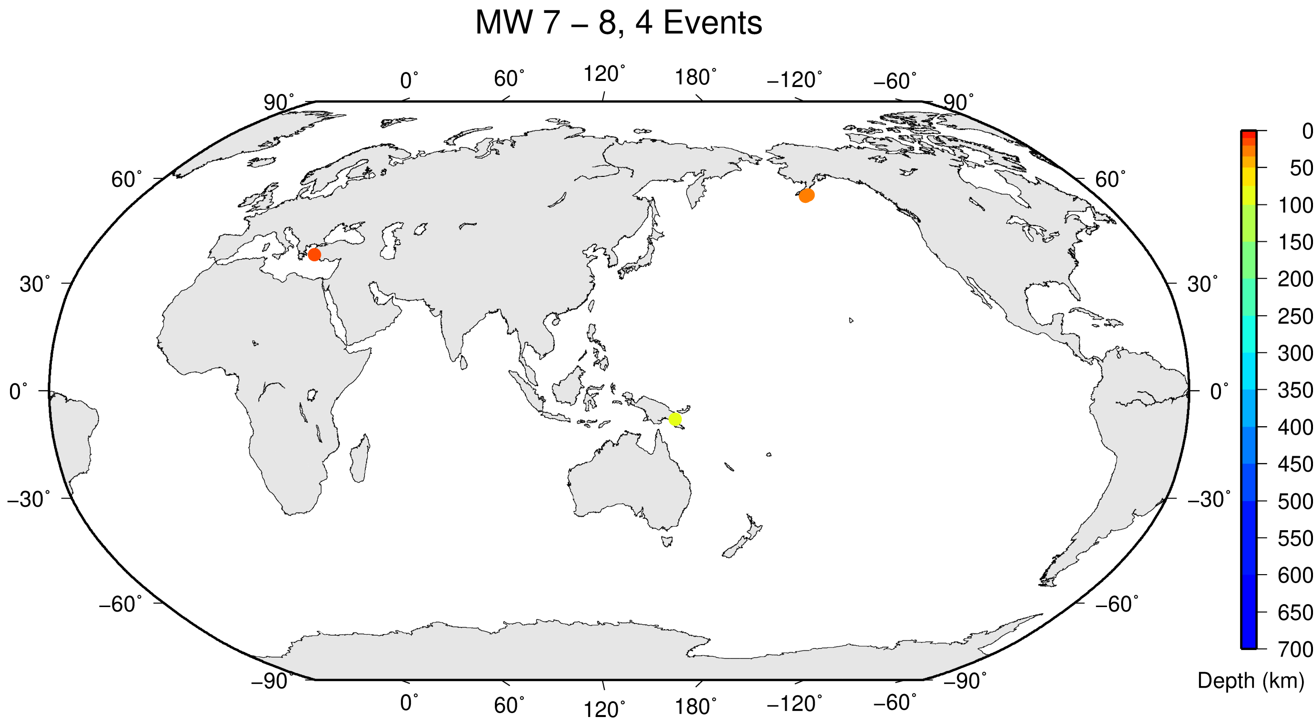

Figure 6.5: *Geographic distribution of magnitude 7-8 earthquakes between July and December 2020.*

References

Bai, Y., C. Liu, T. Lay, K.F. Cheung and Y. Yamazaki (2023), Fast and slow intraplate ruptures during the 19 October 2020 magnitude 7.6 Shumagin earthquake, *Nat Commun*, *14*(2015), https://doi.org/10.1038/s41467-023-37731-2.

Di Giacomo, D., D.A. Storchak, N. Safronova, P. Ozgo, J. Harris, R. Verney and I. Bondár (2014), A New ISC Service: The Bibliography of Seismic Events, *Seismol. Res. Lett.*, *85*(2), 354–360, https://doi.org/10.1785/0220130143.

Herman, M.W. and K.P. Furlong (2021), Triggering an unexpected earthquake in an uncoupled subduction zone, *Sci. Adv.*,*7*, eabf7590, https:://doi.org/10.1126/sciadv.abf7590.

Human Rights Watch (2021), "They Killed Us from the Inside" An Investigation into the August 4 Beirut Blast, p. 706, ISBN: 978-1-62313-931-5, https://www.hrw.org/sites/default/files/media_2021/08/lebanon0821_web.pdf.

International Seismological Centre (2023), On-line Event Bibliography, https://doi.org/10.31905/EJ3B5LV6.

Jiang, Y., P.J. González and Roland Bürgmann (2022), Subduction earthquakes controlled by incoming plate geometry: The 2020 M > 7.5 Shumagin, Alaska, earthquake doublet, *Earth Planet. Sci. Lett.*, *584*, 117447, https://doi.org/10.1016/j.epsl.2022.117447.

Papadimitriou, P., V. Kapetanidis, A. Karakonstantis, I. Spingos, I. Kassaras, V. Sakkas, V. Kouskouna, A. Karatzetzou, K. Pavlou, G. Kaviris and N. Voulgaris (2020), First Results on the Mw=6.9 Samos Earthquake of 30 October 2020, *Bull. geol. Soc. Greece*, *56*(1), 251-279, https://doi.org/10.12681/bgsg.25359.

Zúñiga, F.R. and O. Tan (2021), Introduction to the special issue on the October 30, 2020, Mw7.0, Samos Island, Greece, earthquake, *Acta Geophys.* *69*, 975–977, https://doi.org/10.1007/s11600-021-00612-7.

7

Statistics of Collected Data

7.1 Introduction

The ISC Bulletin is based on the parametric data reports received from seismological agencies around the world. With rare exceptions, these reports include the results of waveform review done by analysts at network data centres and observatories. These reports include combinations of various bulletin elements such as event hypocentre estimates, moment tensors, magnitudes, event type and felt and damaging data as well as observations of the various seismic waves recorded at seismic stations.

Data reports are received in different formats that are often agency specific. Once an authorship is recognised, the data are automatically parsed into the ISC database and the original reports filed away to be accessed when necessary. Any reports not recognised or processed automatically are manually checked, corrected and re-processed. This chapter describes the data that are received at the ISC before the production of the reviewed Bulletin.

Notably, the ISC integrates all newly received data reports into the automatic ISC Bulletin (available on-line) soon after these reports are made available to ISC, provided it is done before the submission deadline that currently stands at 12 months following an event occurrence.

With data constantly being reported to the ISC, even after the ISC has published its review, the total data shown as collected, in this chapter, is limited to two years after the time of the associated reading or event, i.e. any hypocentre data collected two years after the event are not reflected in the figures below.

7.2 Summary of Agency Reports to the ISC

A total of 150 agencies have reported data for July 2020 to December 2020. The parsing of these reports into the ISC database is summarised in Table 7.1.

Table 7.1: *Summary of the parsing of reports received by the ISC from a total of 150 agencies, containing data for this summary period.*

	Number of reports
Total collected	7479
Automatically parsed	6479
Manually parsed	1000

Data collected by the ISC consists of multiple data types. These are typically one of:

- Bulletin, hypocentres with associated phase arrival observations.

- Catalogue, hypocentres only.
- Unassociated phase arrival observations.

In Table 7.2, the number of different data types reported to the ISC by each agency is listed. The number of each data type reported by each agency is also listed. Agencies reporting indirectly have their data type additionally listed for the agency that reported it. The agencies reporting indirectly may also have 'hypocentres with associated phases' but with no associated phases listed - this is because the association is being made by the agency reporting directly to the ISC. Summary maps of the agencies and the types of data reported are shown in Figure 7.1 and Figure 7.2.

Table 7.2: *Agencies reporting to the ISC for this summary period. Entries in bold are for new or renewed reporting by agencies since the previous six-month period.*

Agency	Country	Directly or indirectly reporting (D/I)	Hypocentres with associated phases	Hypocentres without associated phases	Associated phases	Unassociated phases	Amplitudes
TIR	Albania	D	735	0	11432	82	2560
CRAAG	Algeria	D	315	1	2776	15	0
LPA	Argentina	D	0	0	0	1392	0
SJA	Argentina	D	1180	1	54137	1	16516
NSSP	Armenia	D	37	1	678	0	0
AUST	Australia	D	1755	2	167522	0	162417
CUPWA	Australia	D	32	0	342	0	0
IDC	Austria	D	15757	0	595539	0	505507
VIE	Austria	D	6385	108	66968	3129	68552
AZER	Azerbaijan	D	3811	0	47220	0	0
UCC	Belgium	D	1493	0	8700	19	2518
SCB	Bolivia	D	700	0	9231	0	1263
RHSSO	Bosnia and Herzegovina	D	723	0	9618	3538	0
BGSI	Botswana	D	246	1	2924	0	891
OSUNB	Brazil	D	116	0	4275	0	0
VAO	Brazil	D	856	13	22644	0	0
SOF	Bulgaria	D	343	0	3931	1779	0
OTT	Canada	D	1423	33	36777	0	5116
PGC	Canada	I OTT	698	0	20262	0	0
GUC	Chile	D	4386	442	122376	8688	36353
BJI	China	D	1380	40	103174	24726	69647
ASIES	Chinese Taipei	D	0	35	0	0	0
TAP	Chinese Taipei	D	10557	0	688200	0	0
RSNC	Colombia	D	13954	70	228433	301	33973
UCR	Costa Rica	D	543	0	20437	0	0
ZAG	Croatia	D	0	0	0	68240	0
SSNC	Cuba	D	2716	0	36628	0	14567
NIC	Cyprus	D	315	0	9760	0	3899
IPEC	Czech Republic	D	636	0	9579	24322	3201
PRU	Czech Republic	D	4776	0	54744	143	12792
WBNET	Czech Republic	D	2093	0	45024	0	45020
KEA	Democratic People's Republic of Korea	D	192	0	2438	0	1261
DNK	Denmark	D	2118	1039	25996	24076	7707
OSPL	Dominican Republic	D	1510	5	18694	0	6367
SDD	Dominican Republic	D	1863	0	36750	457	13561
IGQ	Ecuador	D	120	0	5822	0	0
HLW	Egypt	D	207	0	1917	0	0
SNET	El Salvador	D	1277	4	16542	31	348
EST	Estonia	I HEL	183	20	0	0	0
FIA0	Finland	I HEL	0	7	0	0	0
HEL	Finland	D	6466	1460	165743	0	32298
CSEM	France	I PRU	2602	120	0	0	0
IPGP	France	D	0	131	0	0	0
LDG	France	D	2626	69	41402	0	14248

Table 7.2: *(continued)*

Agency	Country	Directly or indirectly reporting (D/I)	Hypocentres with associated phases	Hypocentres without associated phases	Associated phases	Unassociated phases	Amplitudes
STR	France	D	4197	0	77265	31	0
PPT	French Polynesia	D	1232	25	7214	5	6713
TIF	Georgia	D	0	110	0	1890	0
AWI	Germany	D	5959	16	24067	1526	12750
BGR	Germany	D	650	304	18565	0	5771
BNS	Germany	I BGR	7	37	0	0	0
BRG	Germany	D	0	0	0	9869	3171
CLL	Germany	D	1309	0	6654	4259	3679
GDNRW	Germany	I BGR	0	6	0	0	0
GFZ	Germany	D	2402	859	134370	0	123168
HLUG	Germany	I BGR	1	3	0	0	0
LEDBW	Germany	I BGR	33	10	0	0	0
ATH	Greece	D	8022	23	318980	0	76148
THE	Greece	D	4600	2	129988	3358	69955
UPSL	Greece	D	0	7	0	0	0
GCG	Guatemala	D	971	1	8976	12	459
HKC	Hong Kong	D	0	0	0	27	0
KRSZO	Hungary	D	875	34	14671	0	5202
REY	Iceland	D	62	1	2681	0	0
HYB	India	D	794	53	2595	0	84
NDI	India	D	944	445	29338	614	9206
DJA	Indonesia	D	4923	102	75312	0	59710
TEH	Iran	D	1419	0	15667	0	0
THR	Iran	D	73	0	2224	0	999
ISN	Iraq	D	95	0	549	8	203
DIAS	Ireland	D	0	0	0	845	0
GII	Israel	D	1884	0	38501	0	0
GEN	Italy	D	941	0	20846	30	0
MED_RCMT	Italy	D	0	91	0	0	0
RISSC	Italy	D	7	0	135	0	0
ROM	Italy	D	8305	324	720466	246575	479829
SARA	Italy	D	290	0	3829	0	0
TRI	Italy	D	0	0	0	10131	0
JSN	Jamaica	D	239	0	2191	4	0
JMA	Japan	D	92534	10304	572432	0	10076
NIED	Japan	D	0	561	0	0	0
SYO	Japan	D	0	0	0	1125	0
JSO	Jordan	D	543	5	8493	0	6292
NNC	Kazakhstan	D	8807	0	77738	0	73142
SOME	Kazakhstan	D	5630	114	63327	10	53748
KNET	Kyrgyzstan	D	895	0	7429	0	2963
KRNET	Kyrgyzstan	D	2640	0	47391	6	0
LVSN	Latvia	D	144	0	2099	0	1215
GRAL	Lebanon	D	123	0	1209	922	0
LIT	Lithuania	D	972	964	5487	793	4
MCO	Macao, China	D	0	0	0	25	0
TAN	Madagascar	D	984	0	8537	2	0
ECX	Mexico	D	814	0	21274	0	4223
MEX	Mexico	D	12538	114	216306	0	1
PDG	Montenegro	D	415	0	10945	0	4541
CNRM	Morocco	D	1792	0	21787	0	0
NAM	Namibia	D	121	0	1362	6	423
DMN	Nepal	D	79	0	1950	0	631
DBN	Netherlands	I BGR	0	3	0	0	0
NOU	New Caledonia	D	4108	6	75957	0	4880
WEL	New Zealand	D	10080	57	540622	85746	243894
CATAC	Nicaragua	D	2400	0	90567	53	0
SKO	North Macedonia	D	0	579	3747	1900	1550
BER	Norway	D	2284	1638	46760	4135	10436
NAO	Norway	D	2067	791	5610	0	1875
OMAN	Oman	D	518	0	25510	0	0
UPA	Panama	D	1386	95	23773	190	600
ARE	Peru	I RSNC	2	0	0	0	0
MAN	Philippines	D	14	6464	1922	76666	14735
QCP	Philippines	D	0	0	0	168	0
PJWWP	Poland	D	130	1	274	0	18

Table 7.2: *(continued)*

Agency	Country	Directly or indirectly reporting (D/I)	Hypocentres with associated phases	Hypocentres without associated phases	Associated phases	Unassociated phases	Amplitudes
WAR	Poland	D	0	0	0	6101	293
IGIL	Portugal	D	783	0	3421	0	1062
INMG	Portugal	D	1625	0	79818	4862	40146
SVSA	Portugal	D	860	0	28628	1576	18151
BELR	Republic of Belarus	D	0	0	0	22843	7086
CFUSG	Republic of Crimea	D	100	0	2276	37	1376
KMA	Republic of Korea	D	11	0	297	0	0
BUC	Romania	D	598	0	23120	98265	8079
ASRS	Russia	D	106	3609	4615	0	1281
BYKL	Russia	D	75	0	9223	0	3072
DRS	Russia	I MOS	178	203	0	0	0
FCIAR	Russia	D	122	2	977	470	323
IDG	Russia	I MOS	0	1	0	0	0
IGKR	Russia	I MOS	0	15	0	0	0
KOLA	Russia	D	1894	128	17249	38	0
KRSC	Russia	D	635	0	19339	0	0
MIRAS	Russia	D	45	0	1144	0	579
MOS	Russia	D	2627	4133	275988	0	91324
NERS	Russia	D	72	2	1778	0	769
NORS	Russia	I MOS	52	185	0	0	0
SKHL	Russia	D	900	901	18585	0	7622
YARS	Russia	D	240	4	5110	0	3171
SGS	Saudi Arabia	D	3108	0	50672	0	0
BEO	Serbia	D	900	0	20123	0	1
BRA	Slovakia	D	0	0	0	18324	0
LJU	Slovenia	D	1439	17	15893	6563	6805
PRE	South Africa	D	2479	0	46900	305	14541
MDD	Spain	D	4922	58	103875	0	29383
MRB	Spain	D	826	0	34547	0	11016
SFS	Spain	D	1328	0	24081	36	0
UPP	Sweden	D	1522	907	15801	0	0
ZUR	Switzerland	D	1124	28	38443	0	15978
BKK	Thailand	D	257	7	2371	0	2770
TRN	Trinidad and Tobago	D	2547	6	20636	20618	0
TUN	Tunisia	D	38	0	297	0	0
AFAD	Turkey	D	14363	0	398401	0	144579
ISK	Turkey	D	14957	0	340460	393	131448
AEIC	U.S.A.	I NEIC	175	4532	132903	0	0
ANF	U.S.A.	I IRIS	34	240	0	0	0
BUT	U.S.A.	I NEIC	0	435	4863	0	0
GCMT	U.S.A.	D	0	2450	0	0	0
HVO	U.S.A.	I NEIC	2	458	19426	0	0
IRIS	U.S.A.	D	475	240	56915	0	0
NCEDC	U.S.A.	I NEIC	1	310	23960	0	0
NEIC	U.S.A.	D	21225	11844	1856325	0	906472
PAS	U.S.A.	I NEIC	0	535	43879	0	0
PMR	U.S.A.	I IRIS	7	0	0	0	0
PNSN	U.S.A.	D	0	113	0	0	0
PTWC	U.S.A.	D	219	0	3383	0	0
REN	U.S.A.	I NEIC	0	467	19529	0	0
RSPR	U.S.A.	D	3293	716	57933	0	0
SEA	U.S.A.	I NEIC	0	49	3277	0	0
SLM	U.S.A.	I NEIC	0	115	1781	0	0
TUL	U.S.A.	I NEIC	0	1	0	0	0
TXNET	U.S.A.	D	1885	3	97022	121	38407
UUSS	U.S.A.	I NEIC	0	90	1419	0	0
MCSM	Ukraine	D	1190	198	23571	520	13682
SIGU	Ukraine	D	26	26	722	0	339
DSN	United Arab Emirates	D	428	0	6114	0	0
BGS	United Kingdom	D	348	22	9873	52	4315
ISC-PPSM	United Kingdom	D	0	97	0	0	0

Table 7.2: *(continued)*

Agency	Country	Directly or indirectly reporting (D/I)	Hypocentres with associated phases	Hypocentres without associated phases	Associated phases	Unassociated phases	Amplitudes
ISU	Uzbekistan	D	725	49	3900	20	0
FUNV	Venezuela	D	804	0	7551	0	0
PLV	Viet Nam	D	39	2	531	0	224
BUL	Zimbabwe	D	362	0	2785	84	0

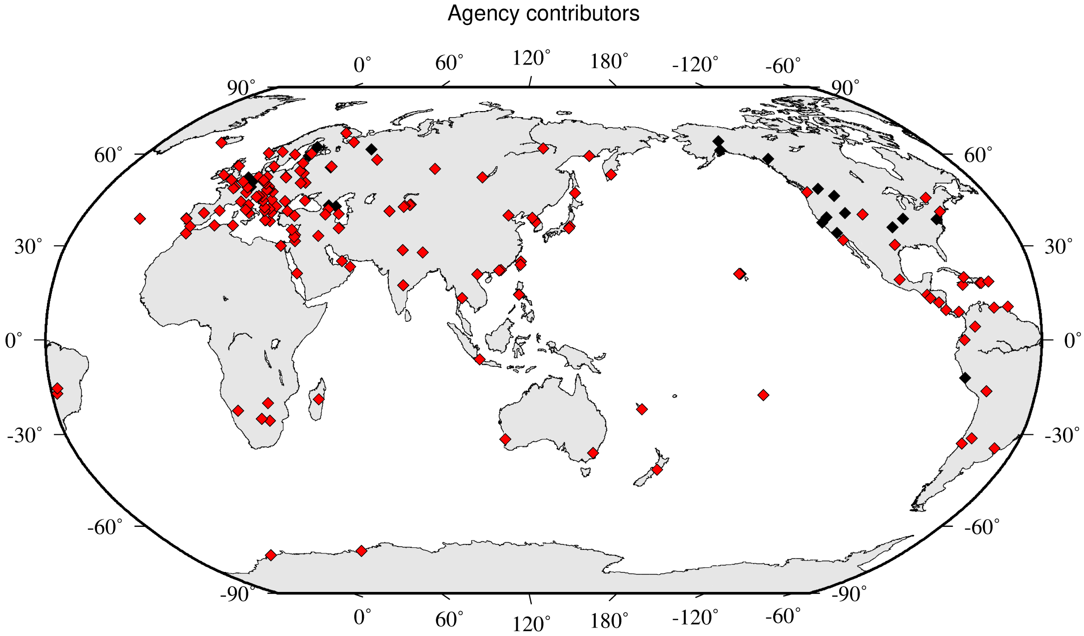

Figure 7.1: *Map of agencies that have contributed data to the ISC for this summary period. Agencies that have reported directly to the ISC are shown in red. Those that have reported indirectly (via another agency) are shown in black. Any new or renewed agencies, since the last six-month period, are shown by a star. Each agency is listed in Table 7.2.*

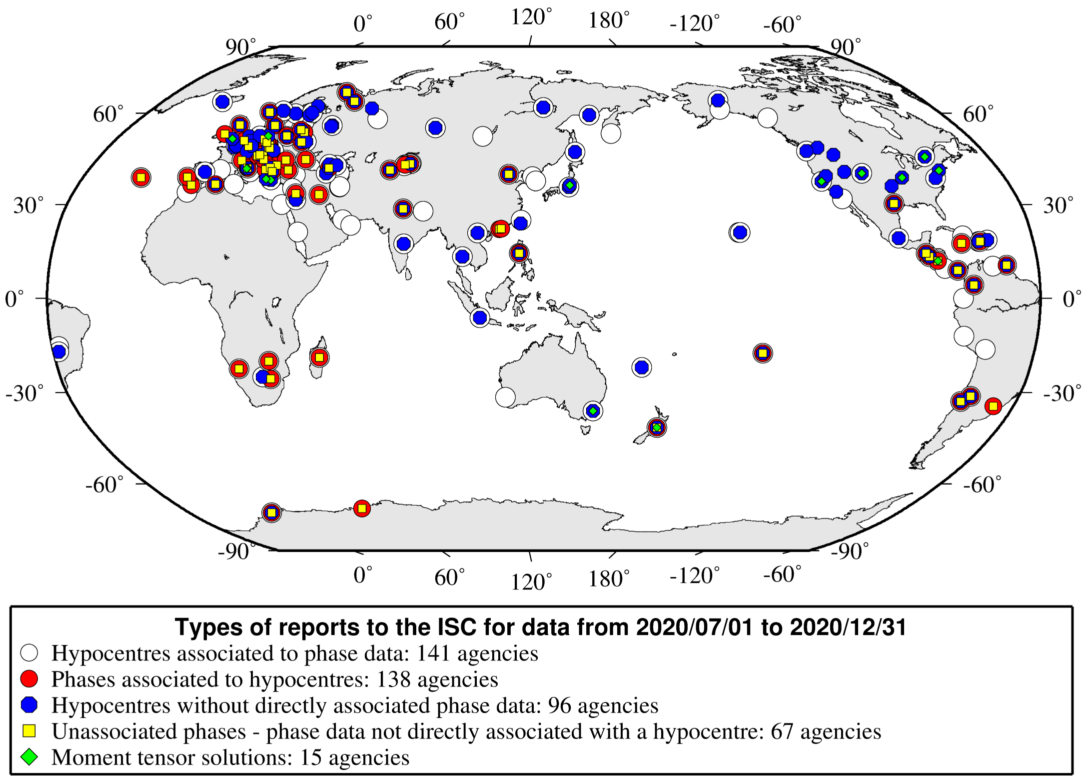

Figure 7.2: *Map of the different data types reported by agencies to the ISC. A full list of the data types reported by each agency is shown in Table 7.2.*

7.3 Arrival Observations

The collection of phase arrival observations at the ISC has increased dramatically with time. The increase in reported phase arrival observations is shown in Figure 7.3.

The reports with phase data are summarised in Table 7.3. This table is split into three sections, providing information on the reports themselves, the phase data, and the stations reporting the phase data. A map of the stations contributing these phase data is shown in Figure 7.4.

The ISC encourages the reporting of phase arrival times together with amplitude and period measurements whenever feasible. Figure 7.5 shows the percentage of events for which phase arrival times from each station are accompanied with amplitude and period measurements.

Figure 7.6 indicates the number of amplitude and period measurement for each station.

Together with the increase in the number of phases (Figure 7.3), there has been an increase in the number of stations reported to the ISC. The increase in the number of stations is shown in Figure 7.7. This increase can also be seen on the maps for stations reported each decade in Figure 7.8.

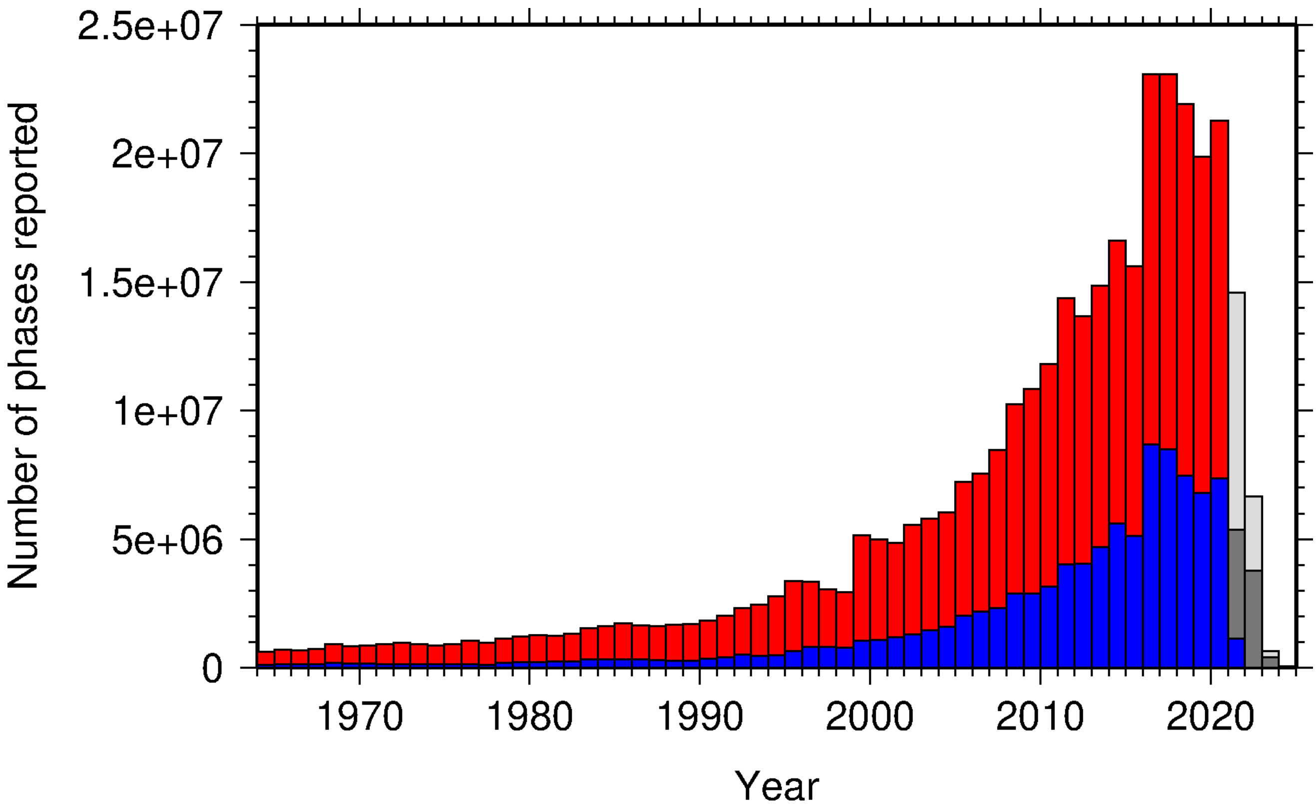

Figure 7.3: *Histogram showing the number of phases (red) and number of amplitudes (blue) collected by the ISC for events each year since 1964. The data in grey covers the current period where data are still being collected before the ISC review takes place and is accurate at the time of publication.*

Table 7.3: *Summary of reports containing phase arrival observations.*

Reports with phase arrivals	7054
Reports with phase arrivals including amplitudes	5832
Reports with only phase arrivals (no hypocentres reported)	170
Total phase arrivals received	10435565
Total phase arrival-times received	9099969
Number of duplicate phase arrival-times	788963 (8.7%)
Number of amplitudes received	3757334
Stations reporting phase arrivals	9839
Stations reporting phase arrivals with amplitude data	5697
Max number of stations per report	2409

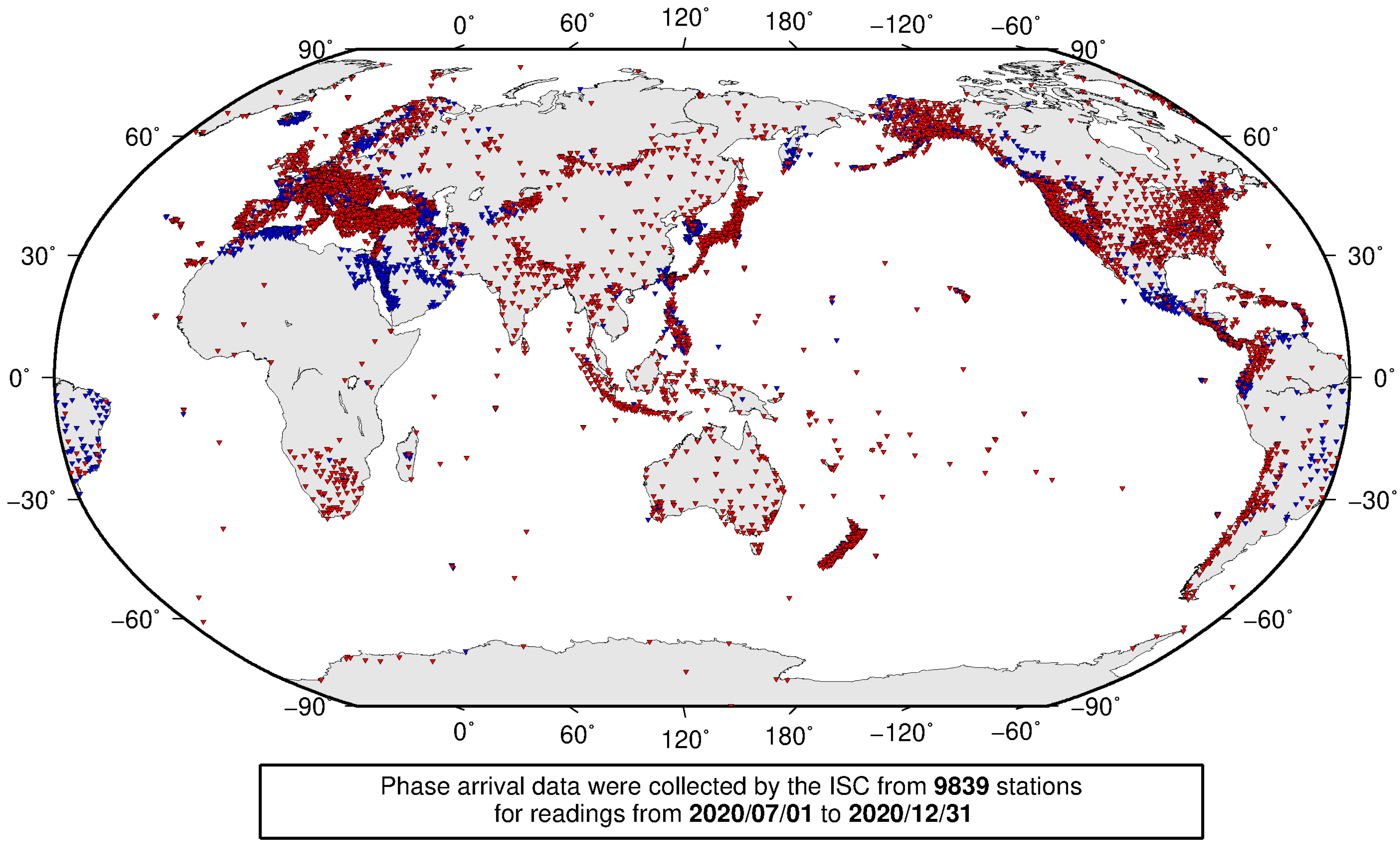

Figure 7.4: *Stations contributing phase data to the ISC for readings from July 2020 to the end of December 2020. Stations in blue provided phase arrival times only; stations in red provided both phase arrival times and amplitude data.*

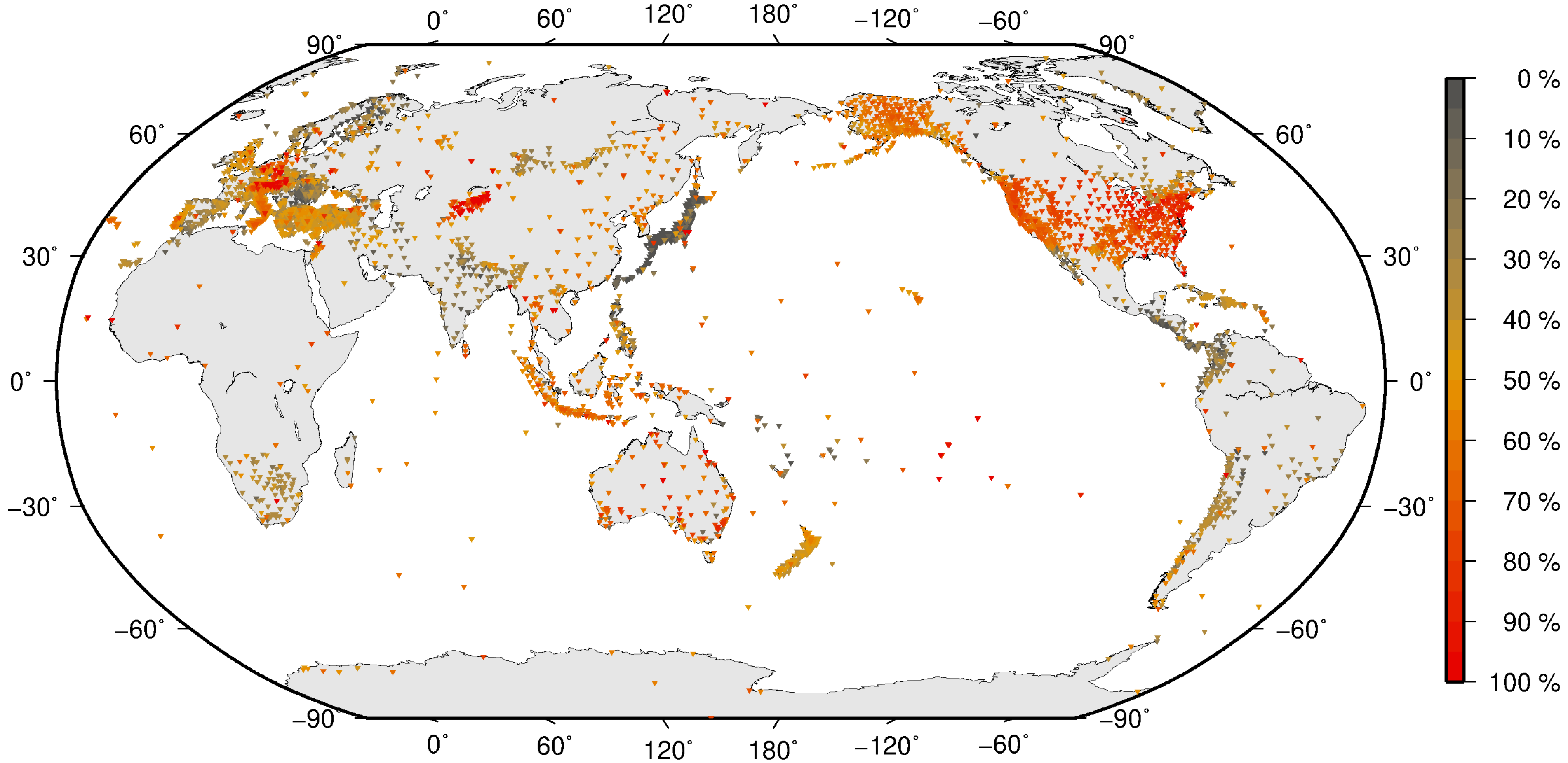

Amplitude data were collected by the ISC from **5633** stations sent by **90** agencies for readings from **2020/07/01** to **2020/12/31**

Figure 7.5: *Percentage of events for which phase arrival times from each station are accompanied with amplitude and period measurements.*

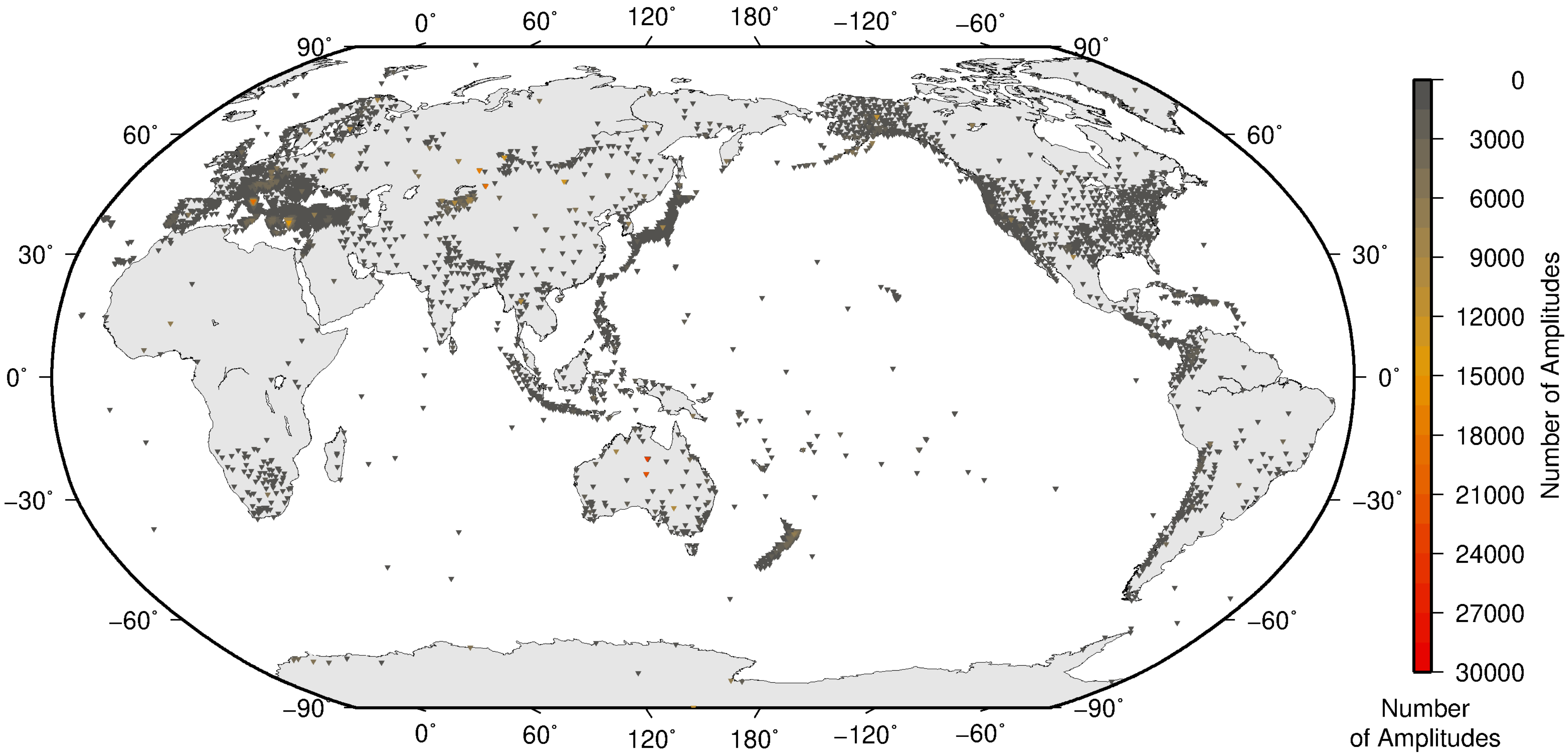

Amplitude data were collected by the ISC from **5633** stations sent by **90** agencies for readings from **2020/07/01** to **2020/12/31**

Figure 7.6: *Number of amplitude and period measurements for each station.*

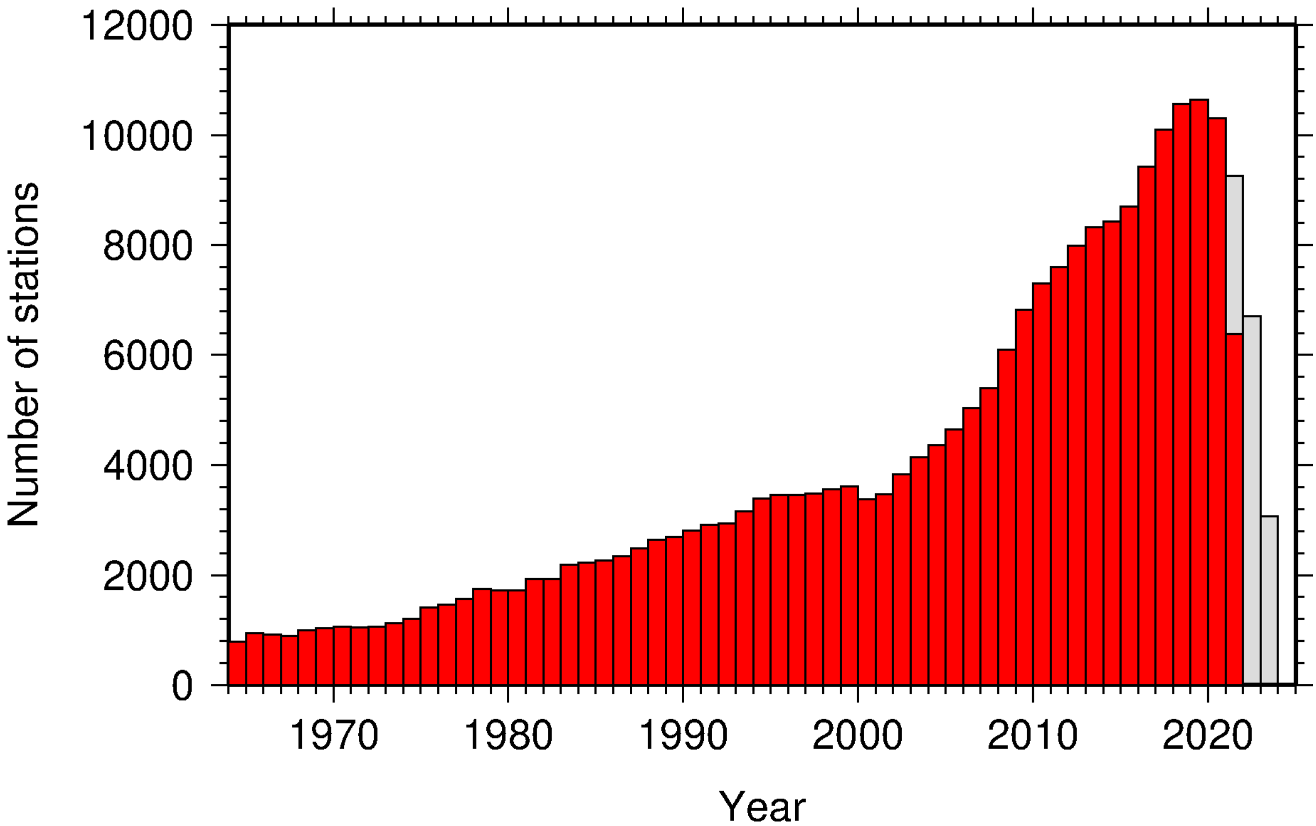

Figure 7.7: *Histogram showing the number of stations reporting to the ISC each year since 1964. The data in grey covers the current period where station information is still being collected before the ISC review of events takes place and is accurate at the time of publication.*

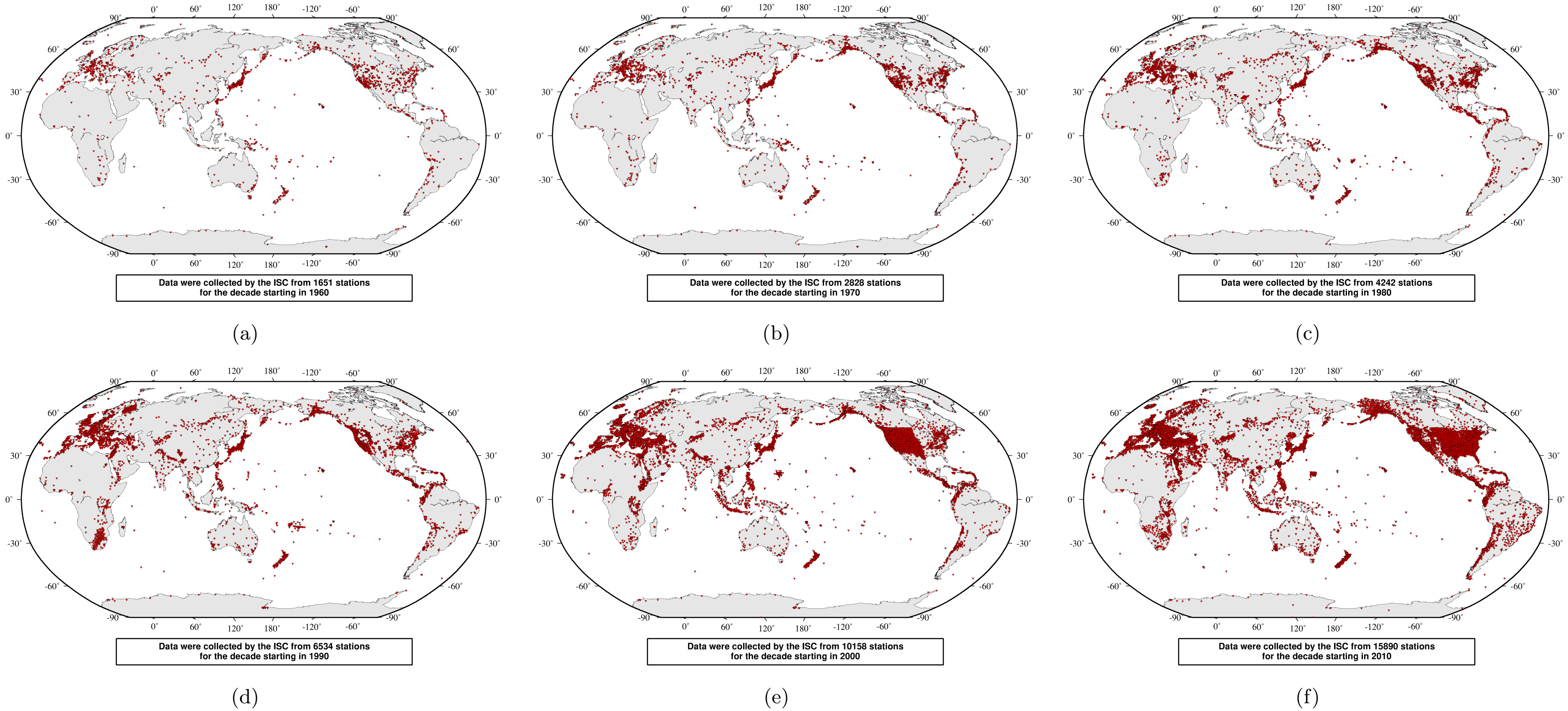

Figure 7.8: *Maps showing the stations reported to the ISC for each decade since 1960. Note that the last map covers a shorter time period.*

7.4 Hypocentres Collected

The ISC Bulletin groups multiple estimates of hypocentres into individual events, with an appropriate prime hypocentre solution selected. The collection of these hypocentre estimates are described in this section.

The reports containing hypocentres are summarised in Table 7.4. The number of hypocentres collected by the ISC has also increased significantly since 1964, as shown in Figure 7.9. A map of all hypocentres reported to the ISC for this summary period is shown in Figure 7.10. Where a network magnitude was reported with the hypocentre, this is also shown on the map, with preference given to reported values, first of M_W followed by M_S, m_b and M_L respectively (where more than one network magnitude was reported).

Table 7.4: *Summary of the reports containing hypocentres.*

Reports with hypocentres	7309
Reports of hypocentres only (no phase readings)	425
Total hypocentres received	422612
Number of duplicate hypocentres	10128 (2.4%)
Agencies determining hypocentres	162

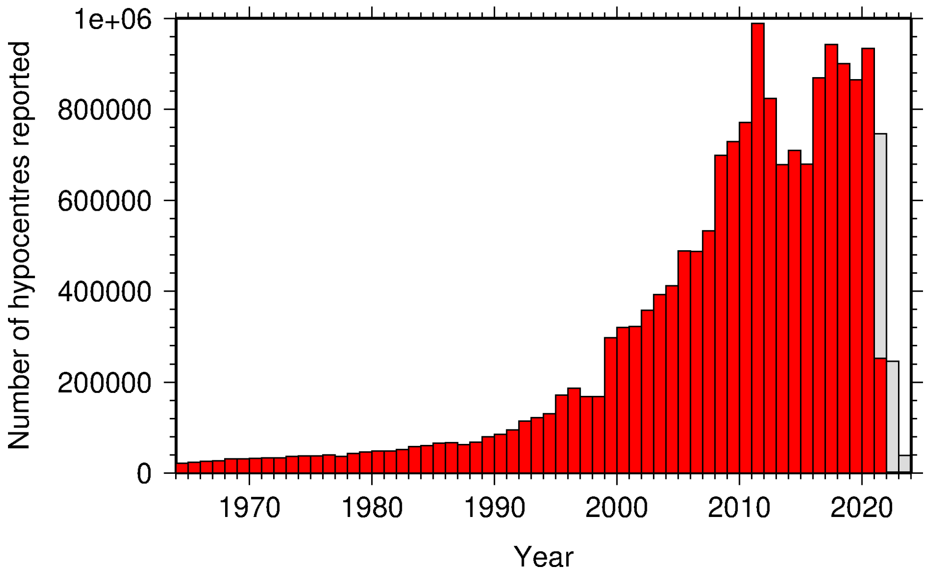

Figure 7.9: *Histogram showing the number of hypocentres collected by the ISC for events each year since 1964. For each event, multiple hypocentres may be reported.*

All the hypocentres that are reported to the ISC are automatically grouped into events, which form the basis of the ISC Bulletin. For this summary period 442909 hypocentres (including ISC) were grouped into 303782 events, the largest of these having 64 hypocentres in one event. The total number of events shown here is the result of an automatic grouping algorithm, and will differ from the total events in the published ISC Bulletin, where both the number of events and the number of hypocentre estimates will have changed due to further analysis. The process of grouping is detailed in Section 10.1.3 of Volume 57 Issue I of the ISC Summary. Figure 8.2 on page 79 shows a map of all prime hypocentres.

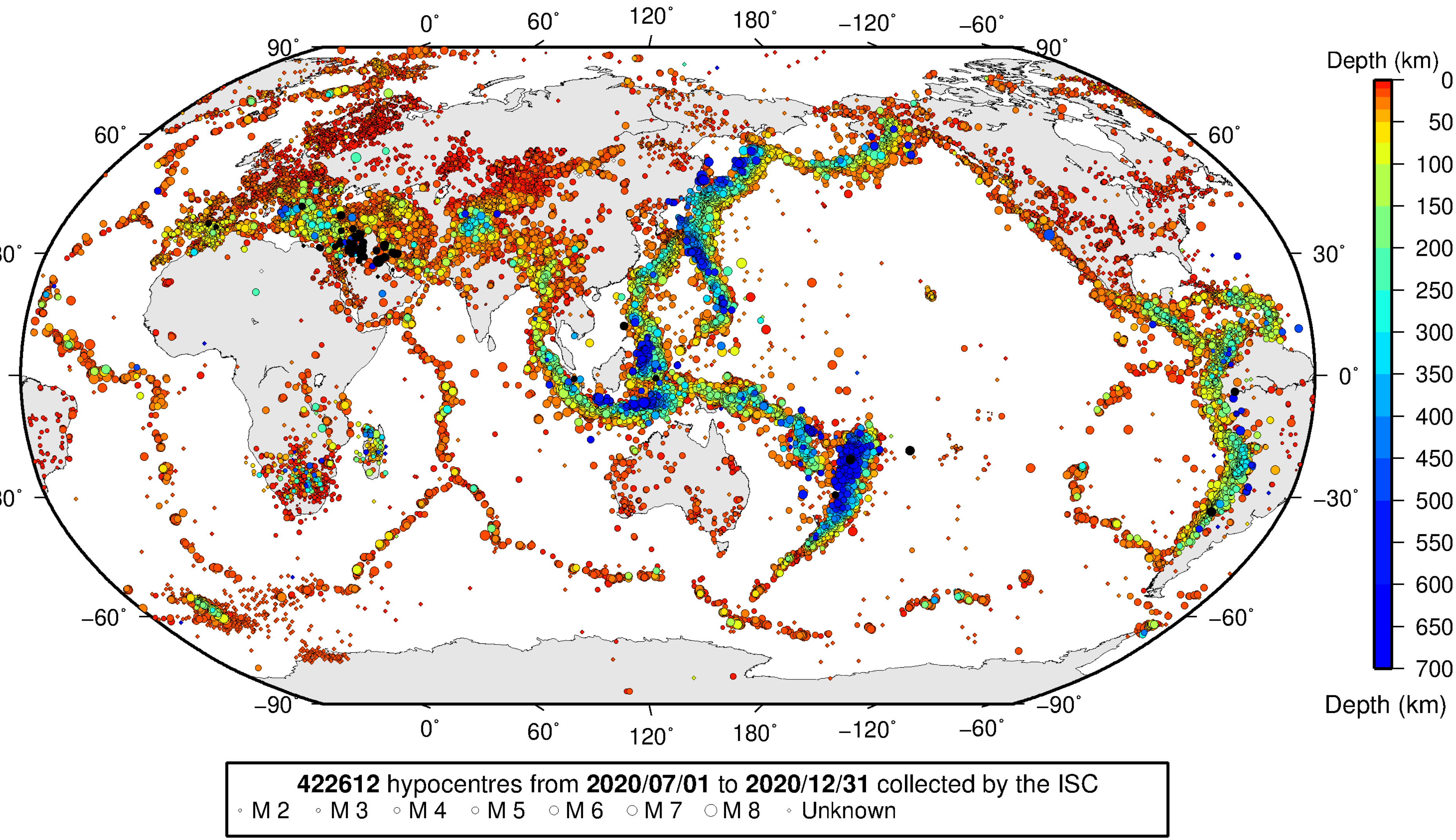

Figure 7.10: *Map of all hypocentres collected by the ISC. The scatter shows the large variation of the multiple hypocentres that are reported for each event. The magnitude corresponds with the reported network magnitude. If more than one network magnitude type was reported, preference was given to values of* M_W*,* M_S*,* m_b *and* M_L *respectively. Compare with Figure 8.2*

7.5 Collection of Network Magnitude Data

Data contributing agencies normally report earthquake hypocentre solutions along with magnitude estimates. For each seismic event, each agency may report one or more magnitudes of the same or different types. This stems from variability in observational practices at regional, national and global level in computing magnitudes based on a multitude of wave types. Differences in the amplitude measurement algorithm, seismogram component(s) used, frequency range, station distance range as well as the instrument type contribute to the diversity of magnitude types. Table 7.5 provides an overview of the complexity of reported network magnitudes reported for seismic events during the summary period.

Table 7.5: *Statistics of magnitude reports to the ISC; M – average magnitude of estimates reported for each event.*

	M<3.0	3.0≤M<5.0	M≥5.0
Number of seismic events	238653	42616	473
Average number of magnitude estimates per event	1.4	3.2	27.3
Average number of magnitudes (by the same agency) per event	1.2	1.8	3.2
Average number of magnitude types per event	1.2	2.4	11.8
Number of magnitude types	29	42	35

Table 7.6 gives the basic description, main features and scientific paper references for the most commonly reported magnitude types.

Table 7.6: *Description of the most common magnitude types reported to the ISC.*

Magnitude type	Description	References	Comments
M	Unspecified		Often used in real or near-real time magnitude estimations
mB	Medium-period and Broad-band body-wave magnitude	*Gutenberg* (1945a); *Gutenberg* (1945b); *IASPEI* (2005); *IASPEI* (2013); *Bormann et al.* (2009); *Bormann and Dewey* (2012)	
mb	Short-period body-wave magnitude	*IASPEI* (2005); *IASPEI* (2013); *Bormann et al.* (2009); *Bormann and Dewey* (2012)	Classical mb based on stations between 21°-100° distance
mb1	Short-period body-wave magnitude	*IDC* (1999) and references therein	Reported only by the IDC; also includes stations at distances less than 21°
mb1mx	Maximum likelihood short-period body-wave magnitude	*Ringdal* (1976); *IDC* (1999) and references therein	Reported only by the IDC

Table 7.6: *continued*

Magnitude type	Description	References	Comments
mbtmp	short-period body-wave magnitude with depth fixed at the surface	*IDC* (1999) and references therein	Reported only by the IDC
mbLg	Lg-wave magnitude	*Nuttli* (1973); *IASPEI* (2005); *IASPEI* (2013); *Bormann and Dewey* (2012)	Also reported as MN
Mc	Coda magnitude		
MD (Md)	Duration magnitude	*Bisztricsany* (1958); *Lee et al.* (1972)	
ME (Me)	Energy magnitude	*Choy and Boatwright* (1995)	Reported only by NEIC
MJMA	JMA magnitude	*Tsuboi* (1954)	Reported only by JMA
ML (Ml)	Local (Richter) magnitude	*Richter* (1935); *Hutton and Boore* (1987); *IASPEI* (2005); *IASPEI* (2013)	
MLSn	Local magnitude calculated for Sn phases	*Balfour et al.* (2008)	Reported by PGC only for earthquakes west of the Cascadia subduction zone
MLv	Local (Richter) magnitude computed from the vertical component		Reported only by DJA and BKK
MN (Mn)	Lg-wave magnitude	*Nuttli* (1973); *IASPEI* (2005)	Also reported as mbLg
MS (Ms)	Surface-wave magnitude	*Gutenberg* (1945c); *Vaněk et al.* (1962); *IASPEI* (2005)	Classical surface-wave magnitude computed from station between 20°-160° distance
Ms1	Surface-wave magnitude	*IDC* (1999) and references therein	Reported only by the IDC; also includes stations at distances less than 20°
ms1mx	Maximum likelihood surface-wave magnitude	*Ringdal* (1976); *IDC* (1999) and references therein	Reported only by the IDC
Ms7	Surface-wave magnitude	*Bormann et al.* (2007)	Reported only by BJI and computed from records of a Chinese-made long-period seismograph in the distance range 3°-177°
MW (Mw)	Moment magnitude	*Kanamori* (1977); *Dziewonski et al.* (1981)	Computed according to the *IASPEI* (2005) and *IASPEI* (2013) standard formula

Table 7.6: *continued*

Magnitude type	Description	References	Comments
Mw(mB)	Proxy Mw based on mB	*Bormann and Saul* (2008)	Reported only by DJA and BKK
Mwp	Moment magnitude from P-waves	*Tsuboi et al.* (1995)	Reported only by DJA and BKK and used in rapid response
mbh	Unknown		
mbv	Unknown		
MG	Unspecified type		Contact contributor
Mm	Unknown		
msh	Unknown		
MSV	Unknown		

Table 7.7 lists all magnitude types reported, the corresponding number of events in the ISC Bulletin and the agency codes along with the number of earthquakes.

Table 7.7: *Summary of magnitude types in the ISC Bulletin for this summary period. The number of events with values for each magnitude type is listed. The agencies reporting these magnitude types are listed, together with the total number of values reported.*

Magnitude type	Events	Agencies reporting magnitude type (number of values)
M	17207	WEL (9306), MOS (3347), CATAC (2264), GFZ (2138), BKK (215), IGQ (103), PRU (34), INMG (14), KRSZO (6), OTT (5), OSUNB (1), TAN (1)
MB	168	NAO (145), SCB (19), SSNC (4)
mB	2051	BJI (1084), DJA (814), WEL (277), CATAC (186), GFZ (117), BKK (79), NOU (4), OSUNB (3), SFS (2), KEA (1), IGQ (1), OTT (1)
mb	23034	IDC (14336), NEIC (7349), NNC (3653), VIE (2968), KRNET (2637), GFZ (2294), DJA (1355), MOS (1319), BJI (1130), NOU (436), VAO (354), CATAC (264), BGR (243), MDD (144), MCSM (137), OMAN (108), BKK (103), CFUSG (69), IASPEI (54), NDI (39), AUST (38), SFS (37), INMG (35), SIGU (26), DSN (22), OSUNB (13), YARS (7), THE (7), PTWC (5), IGQ (5), SSNC (4), PDG (2), THR (2), ROM (1), STR (1), BGS (1), IGIL (1), OTT (1)
mB_BB	27	BGR (27)
mb_Lg	5260	MDD (4807), NEIC (434), OTT (27)
mbR	97	VAO (97)
mbtmp	15561	IDC (15561)
Mc	25	KRSC (25)
MC	2	AFAD (2)
MD	13696	RSPR (3531), SSNC (2497), LDG (2373), SDD (1848), TRN (1040), GCG (884), ECX (739), SOF (315), JMA (256), NCEDC (222), JSN (147), ROM (145), GRAL (120), SLM (113), MEX (108), GII (100), CFUSG (94), PNSN (94), PDG (78), TIR (41), TUN (36), HLW (35), UPA (33), STR (30), SIGU (17), HVO (14), UUSS (9), JSO (6), SNET (6), OSPL (5), DNK (2), SEA (1), BUT (1)

Table 7.7: Continued.

Magnitude type	Events	Agencies reporting magnitude type (number of values)
Mjma	318	BKK (207), IGQ (103), RSNC (4), JSO (3), SFS (2), DJA (1)
ML	135569	ISK (14951), AFAD (13984), RSNC (13719), TAP (10557), WEL (8900), IDC (8746), NEIC (8445), ROM (8271), ATH (7995), HEL (6599), VIE (4959), GUC (4661), AEIC (4580), AZER (3810), SGS (3045), SSNC (2505), PRE (2337), WBNET (2085), SFS (2066), INMG (1950), UPP (1926), TXNET (1881), LDG (1863), SDD (1850), KOLA (1710), OSPL (1514), TEH (1419), SNET (1308), CNRM (1247), DNK (1185), BER (1184), LJU (1104), TIR (1081), SJA (1079), BEO (897), GEN (833), MRB (824), ECX (758), RHSSO (722), TAN (722), SCB (690), KRSZO (660), IPEC (636), KRSC (635), BUC (597), SKO (572), UPA (535), PGC (534), DJA (515), IGIL (492), PAS (490), REN (469), HVO (444), BUT (434), NDI (382), PDG (371), NAO (330), NIC (315), AUST (304), CRAAG (300), SARA (280), UCC (242), YARS (233), ANF (229), KNET (227), OMAN (206), GCG (187), BGSI (173), HLW (169), BJI (166), BGR (165), BGS (159), BKK (154), DSN (153), LVSN (140), PPT (114), ISN (92), KEA (85), NOU (85), UUSS (81), IGQ (78), SEA (75), THR (68), PTWC (63), NCEDC (60), MIRAS (45), BNS (44), PLV (39), RSPR (37), DMN (35), OTT (28), GFZ (28), CUPWA (23), CLL (21), NAM (16), JSO (13), RISSC (7), FIA0 (5), SIGU (4), VAO (2), CATAC (2), OGSO (2), PMR (2), SLM (1), CSEM (1)
MLh	5308	THE (4558), ZUR (641), ASRS (105), RSNC (4)
MLhc	273	ZUR (273)
MLSn	158	PGC (158)
MLv	24038	WEL (9558), DJA (5069), STR (4163), CATAC (2302), RSNC (1444), NOU (1124), SFS (946), BKK (244), JSO (187), MCSM (159), IGQ (111), AUST (38), GFZ (12), KRSZO (6), OTT (5), TXNET (1)
MN	695	OTT (695)
mpv	4043	NNC (4043)
MPVA	281	NORS (235), MOS (230)
mR	53	OSUNB (53)
MS	13419	IDC (7263), MAN (6453), BJI (794), MOS (410), BGR (165), NSSP (38), INMG (32), VIE (27), IASPEI (22), SOME (14), OMAN (14), YARS (10), GUC (7), DSN (5), DNK (3), IGIL (3), KEA (1), PPT (1), SSNC (1), NDI (1)
Ms(BB)	91	IGQ (85), RSNC (3), DJA (1), BKK (1), JSO (1)
Ms7	800	BJI (800)
Ms_20	174	NEIC (174)
MsBB	5	OTT (5)
MSH	85	CFUSG (85)
MV	97990	JMA (97990)
MVS	1	CATAC (27)

Table 7.7: *Continued.*

Magnitude type	Events	Agencies reporting magnitude type (number of values)
MW	7669	SDD (1798), GCMT (1224), SJA (1073), UPA (846), FUNV (576), NIED (561), GFZ (551), UCR (442), AFAD (349), NDI (327), BER (268), SSNC (215), PGC (163), IPGP (131), DJA (72), JMA (69), MED_RCMT (65), GCG (58), WEL (55), ASIES (35), ROM (22), ATH (21), INMG (20), PLV (16), UPSL (7), OSUNB (5), GUC (4), TIR (4), OSPL (2), RSNC (2)
Mw(mB)	599	WEL (249), CATAC (179), GFZ (114), BKK (73), SFS (2), IGQ (1)
Mwb	212	NEIC (212)
MwMwp	96	GFZ (50), CATAC (50), BKK (9)
Mwp	595	SARA (280), DJA (149), PTWC (146), CATAC (54), GFZ (50), RSNC (28), BKK (10), OMAN (6), ROM (1)
Mwr	557	NEIC (407), GUC (136), PAS (45), SLM (40), NCEDC (29), OTT (15)
Mws	612	GII (612)
Mww	607	NEIC (606), GUC (19)

The most commonly reported magnitude types are short-period body-wave, surface-wave, local (or Richter), moment, duration and JMA magnitude type. For a given earthquake, the number and type of reported magnitudes greatly vary depending on its size and location. The large earthquake of October 25, 2010 gives an example of the multitude of reported magnitude types for large earthquakes (Listing 7.1). Different magnitude estimates come from global monitoring agencies such as the IDC, NEIC and GCMT, a local agency (GUC) and other agencies, such as MOS and BJI, providing estimates based on the analysis of their networks. The same agency may report different magnitude types as well as several estimates of the same magnitude type, such as NEIC estimates of Mw obtained from W-phase, centroid and body-wave inversions.

Listing 7.1: *Example of reported magnitudes for a large event*

```
Event   15264887 Southern Sumatera
   Date       Time        Err   RMS Latitude Longitude  Smaj  Smin   Az Depth   Err Ndef Nsta Gap  mdist  Mdist Qual   Author      OrigID
2010/10/25 14:42:22.18   0.27 1.813  -3.5248  100.1042 4.045 3.327  54  20.0  1.37 2102 2149  23   0.76 176.43 m i de ISC       01346132
 (#PRIME)

Magnitude  Err Nsta Author      OrigID
mb      6.1        61 BJI       15548963
mB      6.9        68 BJI       15548963
Ms      7.7        85 BJI       15548963
Ms7     7.5        86 BJI       15548963
mb      5.3 0.1    48 IDC       16686694
mb1     5.3 0.1    51 IDC       16686694
mb1mx   5.3 0.0    52 IDC       16686694
mbtmp   5.3 0.1    51 IDC       16686694
ML      5.1 0.2     2 IDC       16686694
MS      7.1 0.0    31 IDC       16686694
Ms1     7.1 0.0    31 IDC       16686694
ms1mx   6.9 0.1    44 IDC       16686694
mb      6.1       243 ISCJB     01677901
MS      7.3       228 ISCJB     01677901
M       7.1       117 DJA       01268475
mb      6.1 0.2   115 DJA       01268475
mB      7.1 0.1   117 DJA       01268475
MLv     7.0 0.2    26 DJA       01268475
        7.1 0.4   117 DJA       01268475
Mwp     6.9 0.2   102 DJA       01268475
mb      6.4        49 MOS       16742129
MS      7.2        70 MOS       16742129
mb      6.5       110 NEIC      01288303
ME      7.3           NEIC      01288303
MS      7.3       143 NEIC      01288303
MW      7.7           NEIC      01288303
MW      7.8       130 GCMT      00125427
mb      5.9           KLM       00255772
ML      6.7           KLM       00255772
MS      7.6           KLM       00255772
mb      6.4        20 BGR       16815854
Ms      7.2         2 BGR       16815854
mb      6.3 0.3   250 ISC       01346132
MS      7.3 0.1   237 ISC       01346132
```

An example of a relatively small earthquake that occurred in northern Italy for which we received magnitude reports of mostly local and duration type from six agencies in Italy, France and Austria is given in Listing 7.2.

Listing 7.2: *Example of reported magnitudes for a small event*

```
Event 15089710 Northern Italy
   Date       Time        Err   RMS Latitude Longitude  Smaj  Smin  Az Depth   Err Ndef Nsta Gap  mdist  Mdist Qual   Author      OrigID
2010/08/08 15:20:46.22   0.94 0.778  45.4846    8.3212 2.900 2.539 110   28.6  9.22  172  110  82   0.41   5.35 m i ke ISC       01249414
 (#PRIME)

Magnitude  Err Nsta Author      OrigID
ML      2.4       10 ZUR       15925566
Md      2.6 0.2   19 ROM       16861451
Ml      2.2 0.2    9 ROM       16861451
ML      2.5          GEN       00554757
ML      2.6 0.3   28 CSEM      00554756
Md      2.3 0.0    3 LDG       14797570
Ml      2.6 0.3   32 LDG       14797570
```

Figure 7.11 shows a distribution of the number of agencies reporting magnitude estimates to the ISC according to the magnitude value. The peak of the distribution corresponds to small earthquakes where many local agencies report local and/or duration magnitudes. The number of contributing agencies rapidly decreases for earthquakes of approximately magnitude 5.5 and above, where magnitudes are mostly given by global monitoring agencies.

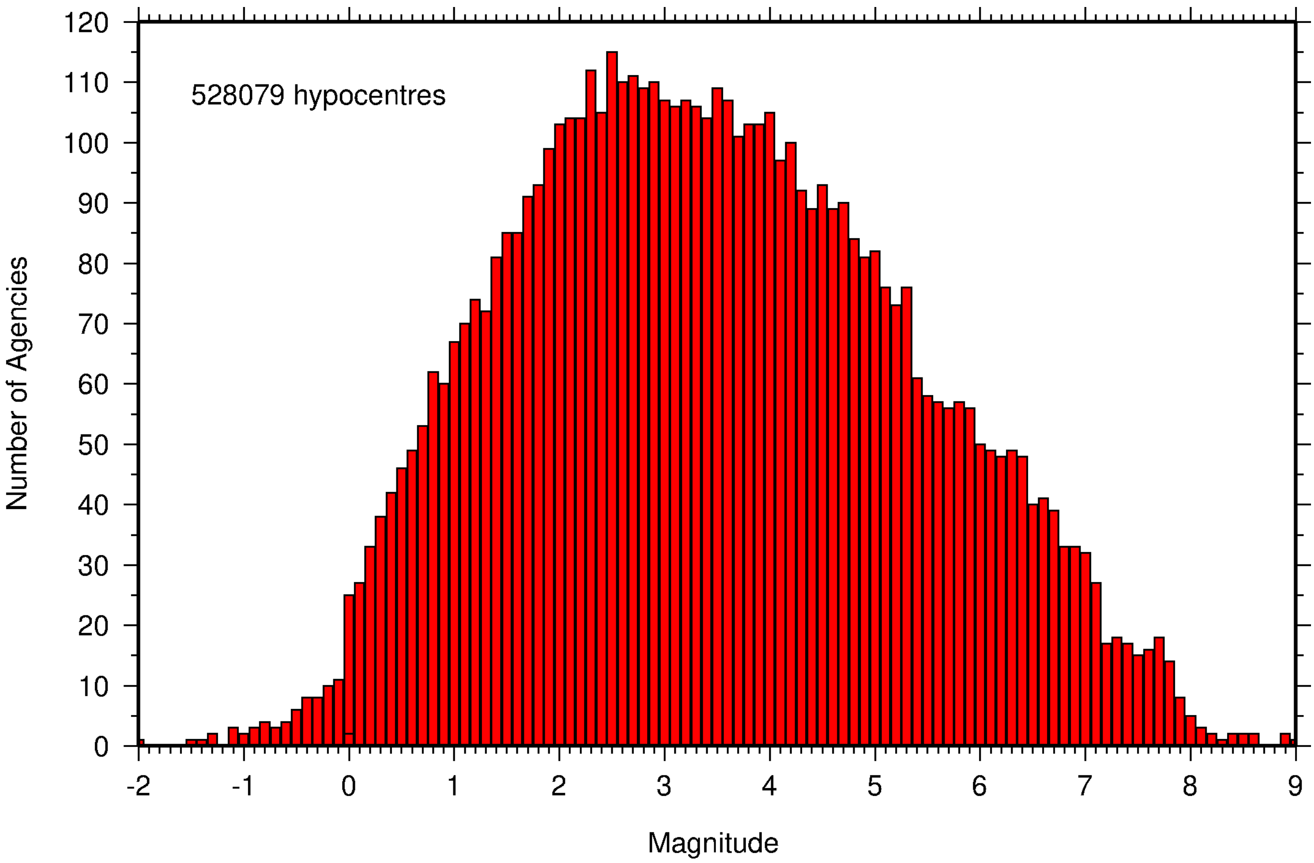

Figure 7.11: *Histogram showing the number of agencies that reported network magnitude values. All magnitude types are included.*

7.6 Moment Tensor Solutions

The ISC Bulletin publishes moment tensor solutions, which are reported to the ISC by other agencies. The collection of moment tensor solutions is summarised in Table 7.8. A histogram showing all moment tensor solutions collected throughout the ISC history is shown in Figure 7.12. Several moment tensor solutions from different authors and different moment tensor solutions calculated by different methods from the same agency may be present for the same event.

Table 7.8: *Summary of reports containing moment tensor solutions.*

Reports with Moment Tensors	1457
Total moment tensors received	9464
Agencies reporting moment tensors	15

The number of moment tensors for this summary period, reported by each agency, is shown in Table 7.9. The moment tensor solutions are plotted in Figure 7.13.

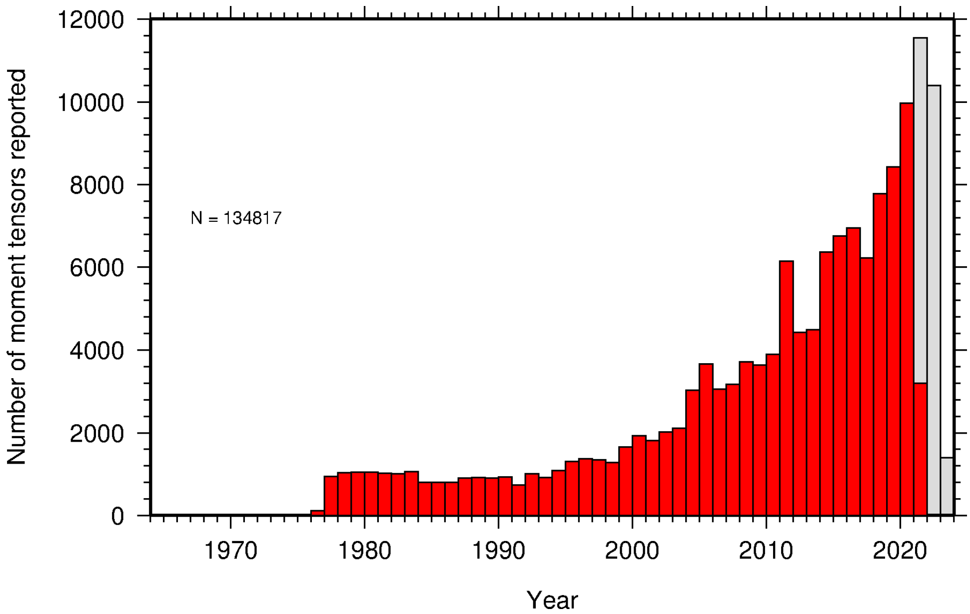

Figure 7.12: *Histogram showing the number of moment tensors reported to the ISC since 1964. The regions in grey represent data that are still being actively collected.*

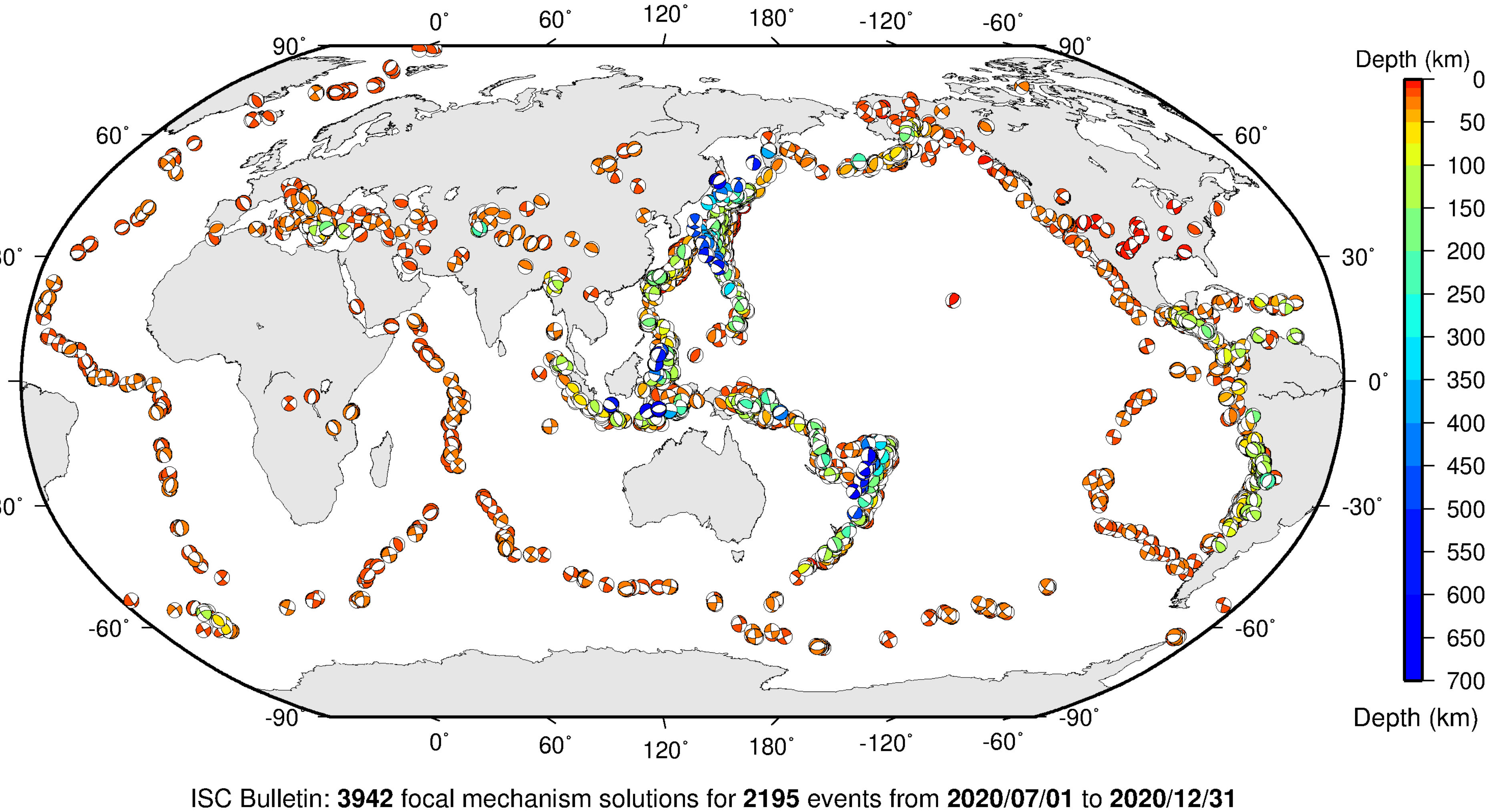

Figure 7.13: *Map of all moment tensor solutions in the ISC Bulletin for this summary period.*

Table 7.9: *Summary of moment tensor solutions in the ISC Bulletin reported by each agency.*

Agency	Number of moment tensor solutions	Agency	Number of moment tensor solutions
GCMT	1224	ROM	22
NEIC	971	ATH	21
NIED	561	UCR	19
TAN	505	MOS	18
GFZ	483	OTT	15
CATAC	369	NCEDC	12
IPGP	262	ECX	8
ISC-PPSM	97	UPSL	7
PNSN	94	GCG	5
ASIES	70	MEX	4
MED_RCMT	65	SDD	2
UPA	63	PLV	2
WEL	55	SNET	1
SLM	40		

7.7 Timing of Data Collection

Here we present the timing of reports to the ISC. Please note, this does not include provisional alerts, which are replaced at a later stage. Instead, it reflects the final data sent to the ISC. The absolute timing of all hypocentre reports, regardless of magnitude, is shown in Figure 7.14. In Figure 7.15 the reports are grouped into one of six categories - from within three days of an event origin time, to over one year. The histogram shows the distribution with magnitude (for hypocentres where a network magnitude was reported) for each category, whilst the map shows the geographic distribution of the reported hypocentres.

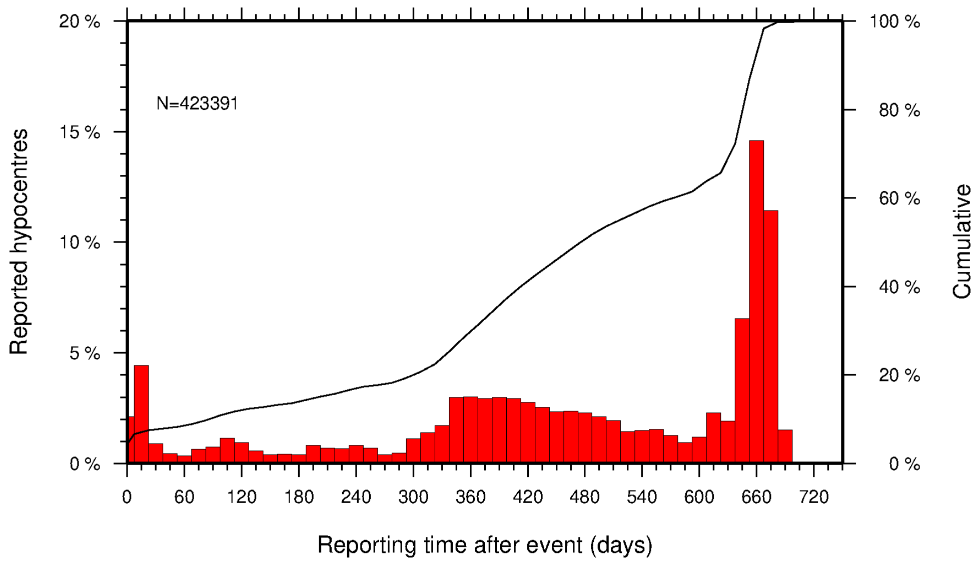

Figure 7.14: *Histogram showing the timing of final reports of the hypocentres (total of N) to the ISC. The cumulative frequency is shown by the solid line.*

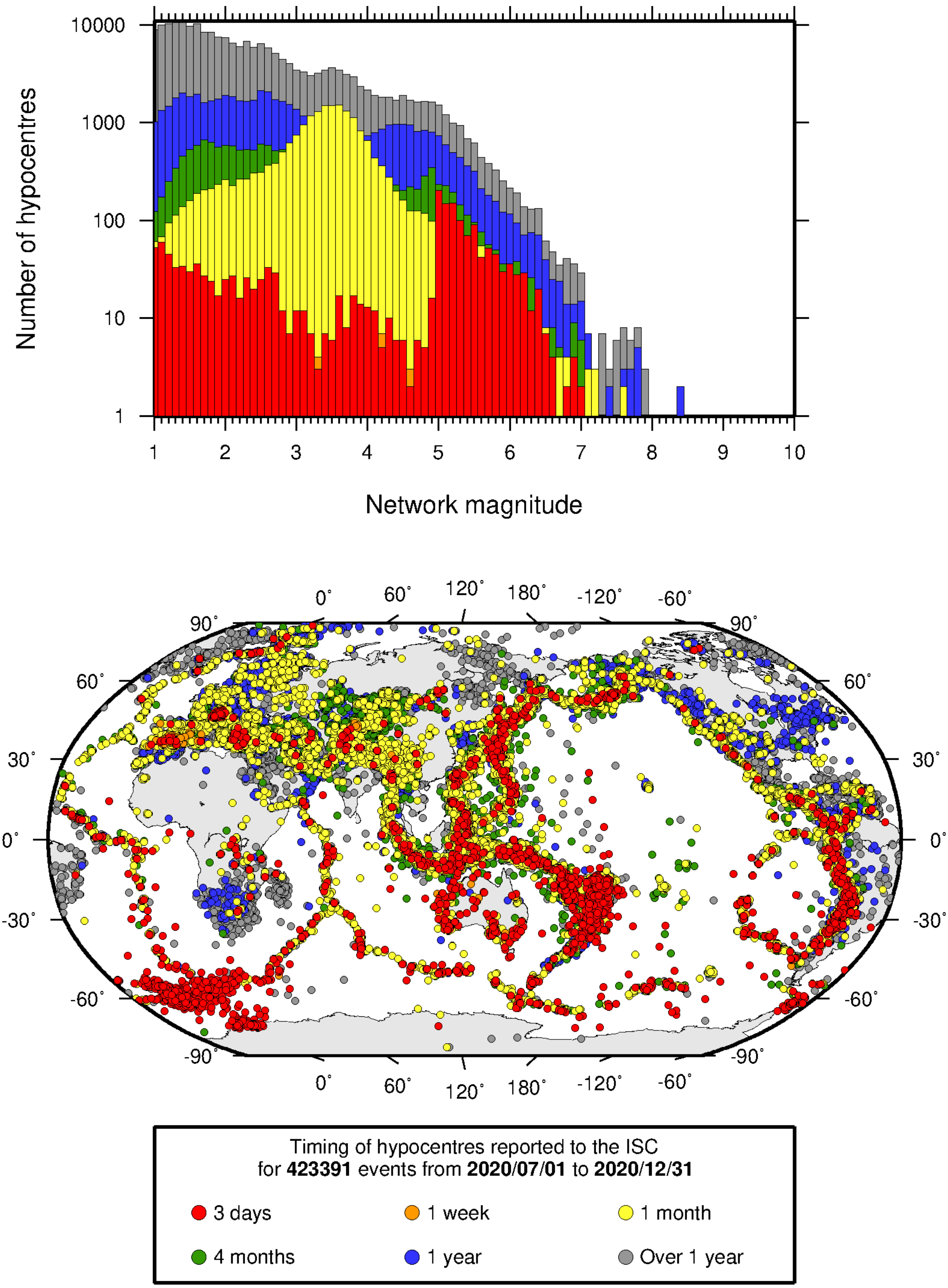

Figure 7.15: *Timing of hypocentres reported to the ISC. The colours show the time after the origin time that the corresponding hypocentre was reported. The histogram shows the distribution with magnitude. If more than one network magnitude was reported, preference was given to a value of M_W followed by M_S, m_b and M_L respectively; all reported hypocentres are included on the map. Note: early reported hypocentres are plotted over later reported hypocentres, on both the map and histogram.*

8

Overview of the ISC Bulletin

This chapter provides an overview of the seismic event data in the ISC Bulletin. We indicate the differences between all ISC events and those ISC events that are reviewed or located. We describe the wealth of phase arrivals and phase amplitudes and periods observed at seismic stations worldwide, reported in the ISC Bulletin and often used in the ISC location and magnitude determination. Finally, we make some comparisons of the ISC magnitudes with those reported by other agencies, and discuss magnitude completeness of the ISC Bulletin.

8.1 Events

The ISC Bulletin had 295233 reported events in the summary period between July and December 2020. Some 91% (269285) of the events were identified as earthquakes, the rest (25948) were of anthropogenic origin (including mining and other chemical explosions, rockbursts and induced events) or of unknown origin. As discussed in Section 10.1.3 of Volume 57 Issue I of the ISC Summary. In this summary period 8% of the events were reviewed and 6% of the events were located by the ISC. For events that are not located by the ISC, the prime hypocentre is identified according to the rules described in Section 10.1.3 of Volume 57 Issue I of the ISC Summary.

Of the 10699437 reported phase observations, 32% are associated to ISC-reviewed events, and 31% are associated to events selected for ISC location. Note that all large events are reviewed and located by the ISC. Since large events are globally recorded and thus reported by stations worldwide, they will provide the bulk of observations. This explains why only about one-fifth of the events in any given month is reviewed although the number of phases associated to reviewed events has increased nearly exponentially in the past decades.

Figure 8.1 shows the daily number of events throughout the summary period. Figure 8.2 shows the locations of the events in the ISC Bulletin; the locations of ISC-reviewed and ISC-located events are shown in Figures 8.3 and 8.4, respectively.

Figure 8.5 shows the hypocentral depth distributions of events in the ISC Bulletin for the summary period. The vast majority of events occur in the Earth's crust. Note that the peaks at 0, 10, 35 km, and at every 50 km intervals deeper than 100 km are artifacts of analyst practices of fixing the depth to a nominal value when the depth cannot be reliably resolved.

Figure 8.6 shows the depth distribution of free-depth solutions in the ISC Bulletin. The depth of a hypocentre reported to the ISC is assumed to be determined as a free parameter, unless it is explicitly labelled as a fixed-depth solution. On the other hand, as described in Section 10.1.4 of Volume 57 Issue I of the ISC Summary, the ISC locator attempts to get a free-depth solution if, and only if, there is resolution for the depth in the data, i.e. if there is a local network and/or sufficient depth-sensitive

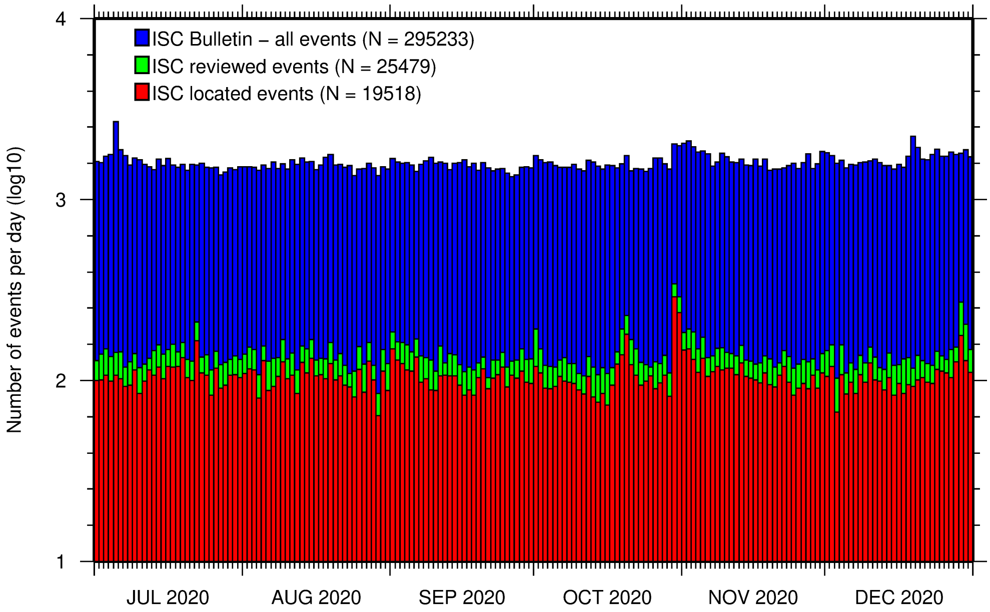

Figure 8.1: *Histogram showing the number of events in the ISC Bulletin for the current summary period. The vertical scale is logarithmic.*

phases are reported.

Figure 8.7 shows the depth distribution of fixed-depth solutions in the ISC Bulletin. Except for a fraction of events whose depth is fixed to a shallow depth, this set comprises mostly ISC-located events. If there is no resolution for depth in the data, the ISC locator fixes the depth to a value obtained from the ISC default depth grid file, or if no default depth exists for that location, to a nominal default depth assigned to each Flinn-Engdahl region (see details in Section 10.1.4 of Volume 57 Issue I of the ISC Summary). During the ISC review editors are inclined to accept the depth obtained from the default depth grid, but they typically change the depth of those solutions that have a nominal (10 or 35 km) depth. When doing so, they usually fix the depth to a round number, preferably divisible by 50.

For events selected for ISC location, the number of stations typically increases as arrival data reported by several agencies are grouped together and associated to the prime hypocentre. Consequently, the network geometry, characterised by the secondary azimuthal gap (the largest azimuthal gap a single station closes), is typically improved. Figure 8.8 illustrates that the secondary azimuthal gap is indeed generally smaller for ISC-located events than that for all events in the ISC Bulletin. Figure 8.9 shows the distribution of the number of associated stations. For large events the number of associated stations is usually larger for ISC-located events than for any of the reported event bulletins. On the other hand, events with just a few reporting stations are rarely selected for ISC location. The same is true for the number of defining stations (stations with at least one defining phase that were used in the location). Figure 8.10 indicates that because the reported observations from multiple agencies are associated to the prime, large ISC-located events typically have a larger number of defining stations than any of the reported event bulletins.

The formal uncertainty estimates are also typically smaller for ISC-located events. Figure 8.11 shows the distribution of the area of the 90% confidence error ellipse for ISC-located events during the summary period. The distribution suffers from a long tail indicating a few poorly constrained event locations.

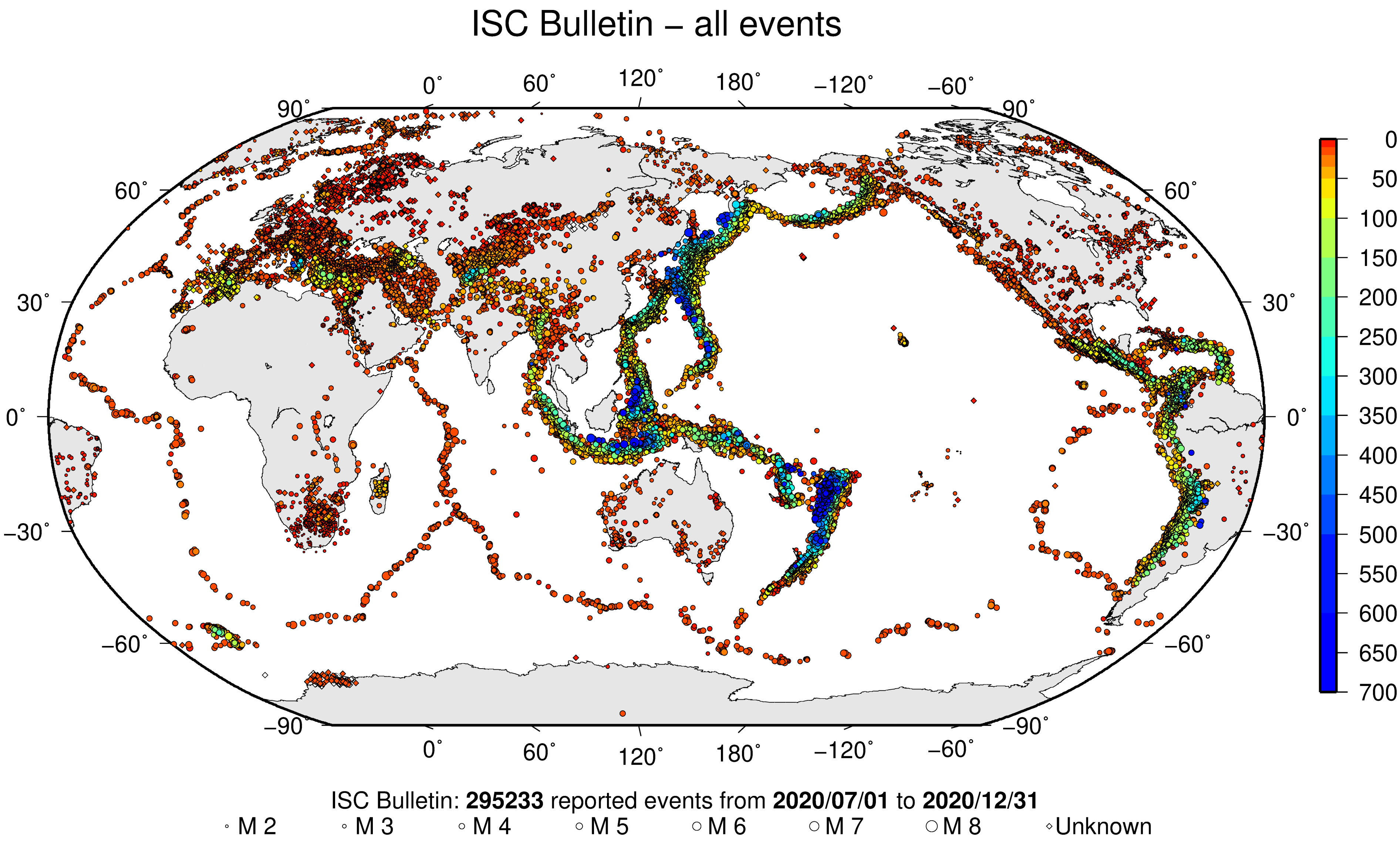

Figure 8.2: *Map of all events in the ISC Bulletin. Prime hypocentre locations are shown. Compare with Figure 7.10.*

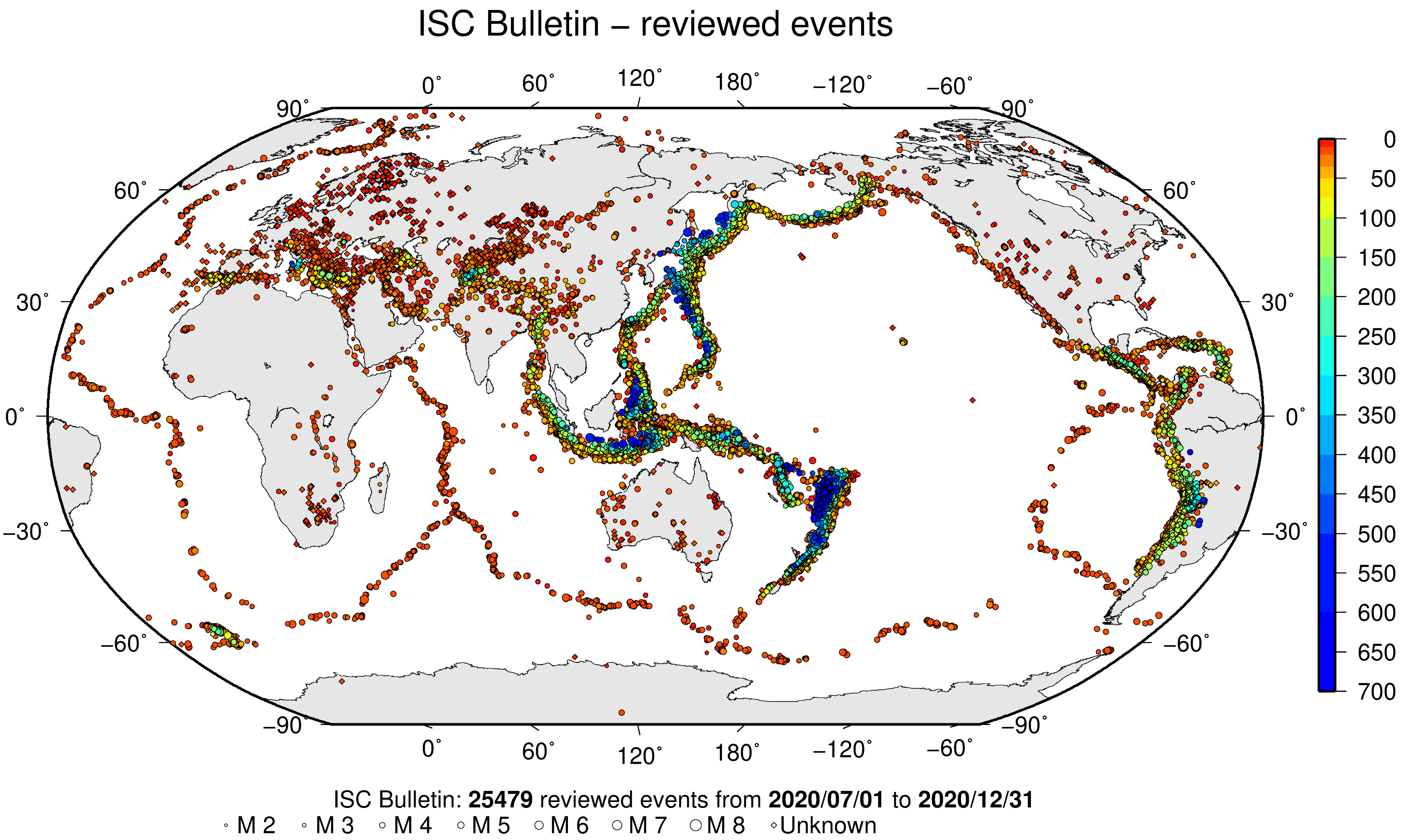

Figure 8.3: *Map of all events reviewed by the ISC for this time period. Prime hypocentre locations are shown.*

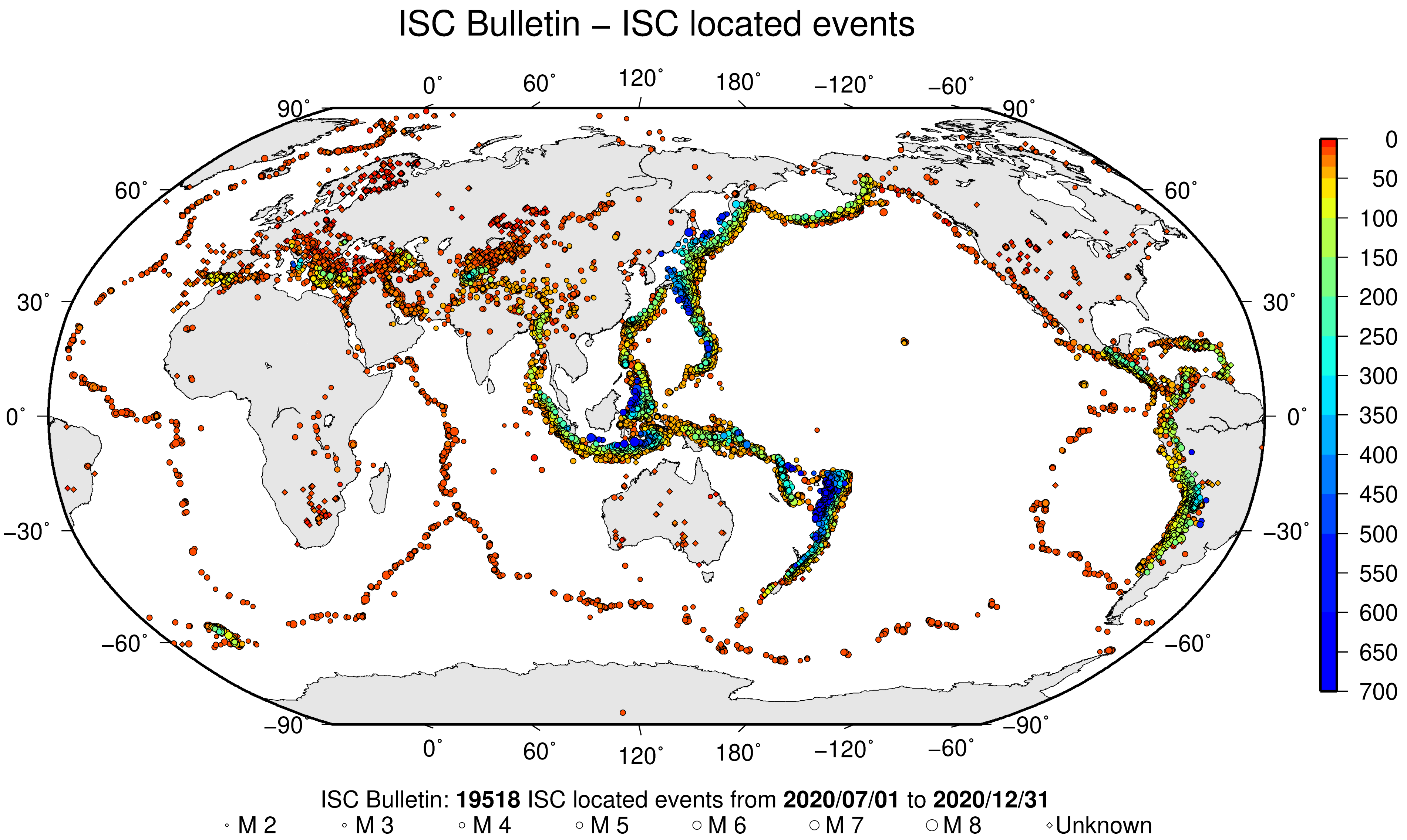

Figure 8.4: *Map of all events located by the ISC for this time period. ISC determined hypocentre locations are shown.*

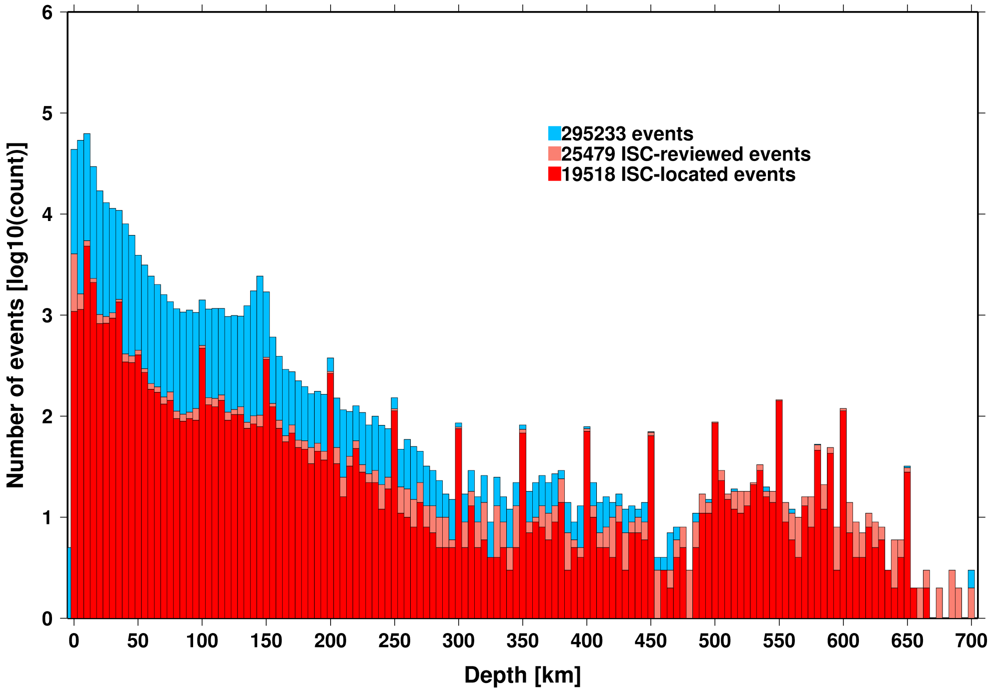

Figure 8.5: *Distribution of event depths in the ISC Bulletin (blue) and for the ISC-reviewed (pink) and the ISC-located (red) events during the summary period. All ISC-located events are reviewed, but not all reviewed events are located by the ISC. The vertical scale is logarithmic.*

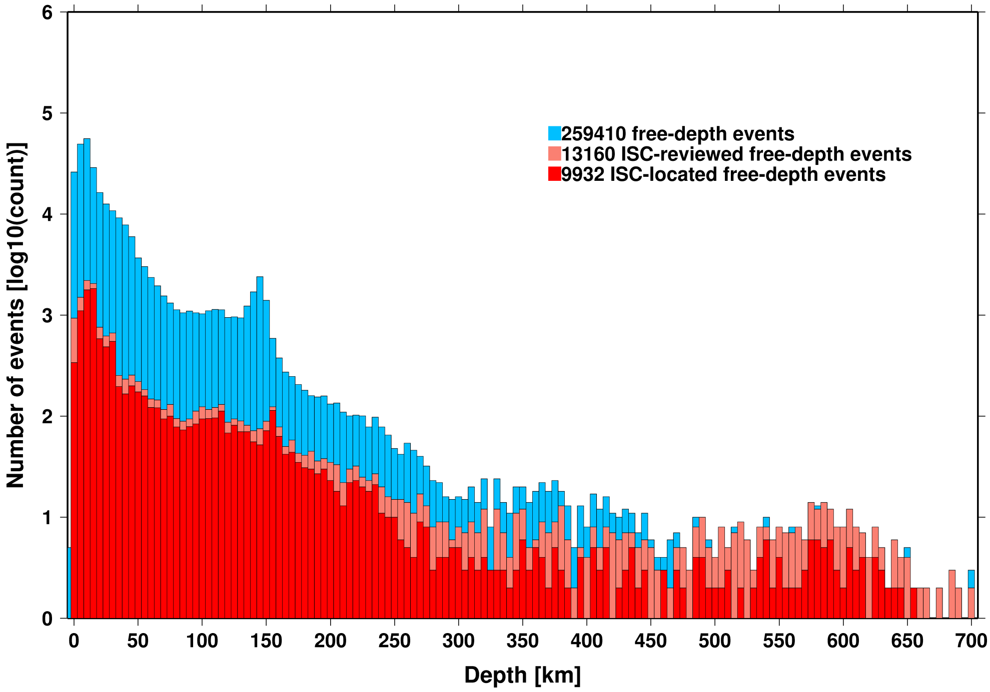

Figure 8.6: *Hypocentral depth distribution of events where the prime hypocentres are reported/located with a free-depth solution in the ISC Bulletin. The vertical scale is logarithmic.*

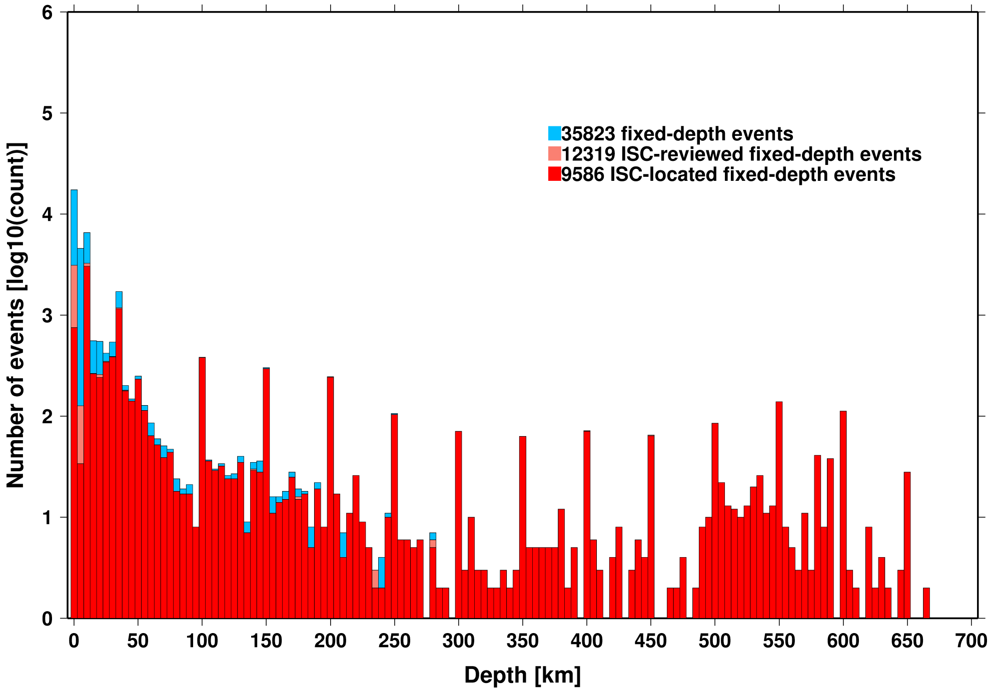

Figure 8.7: *Hypocentral depth distribution of events where the prime hypocentres are reported/located with a fixed-depth solution in the ISC Bulletin. The vertical scale is logarithmic.*

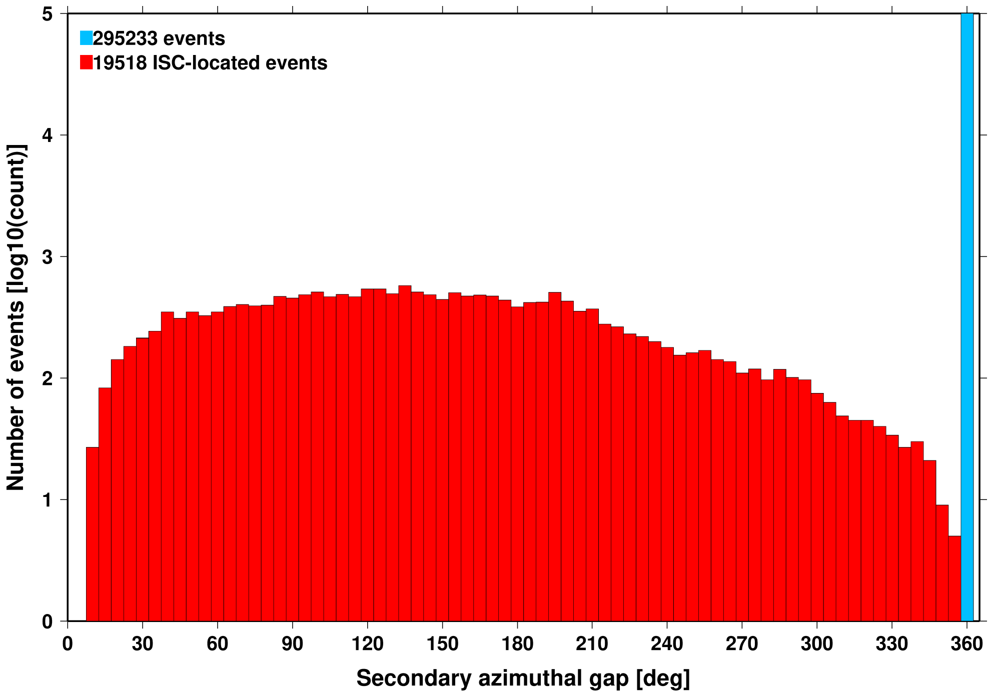

Figure 8.8: *Distribution of secondary azimuthal gap for events in the ISC Bulletin (blue) and those selected for ISC location (red). The vertical scale is logarithmic.*

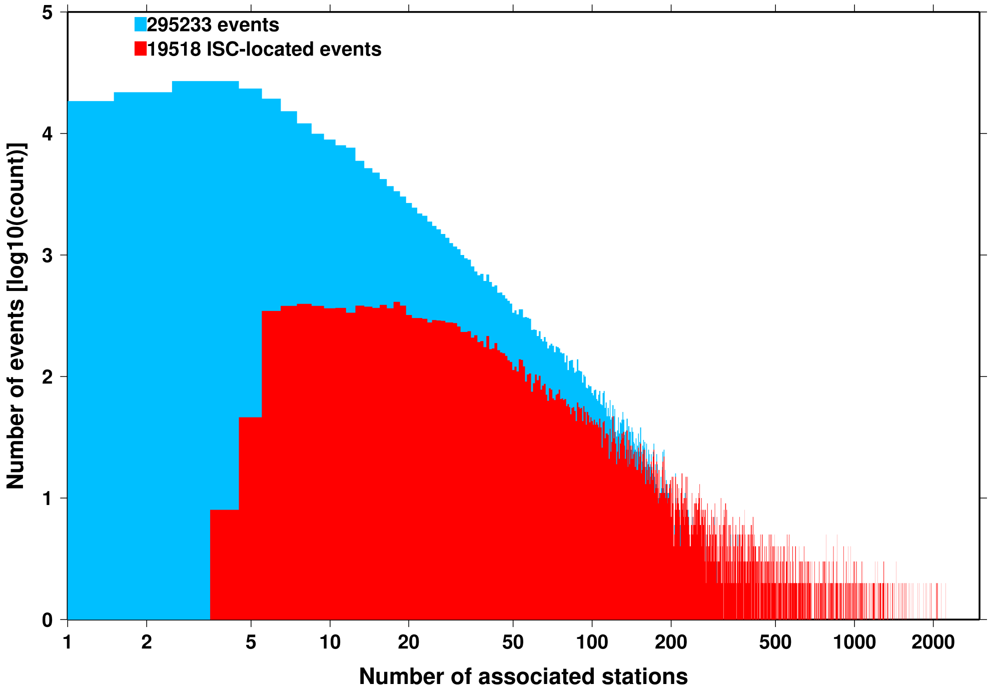

Figure 8.9: *Distribution of the number of associated stations for events in the ISC Bulletin (blue) and those selected for ISC location (red). The vertical scale is logarithmic.*

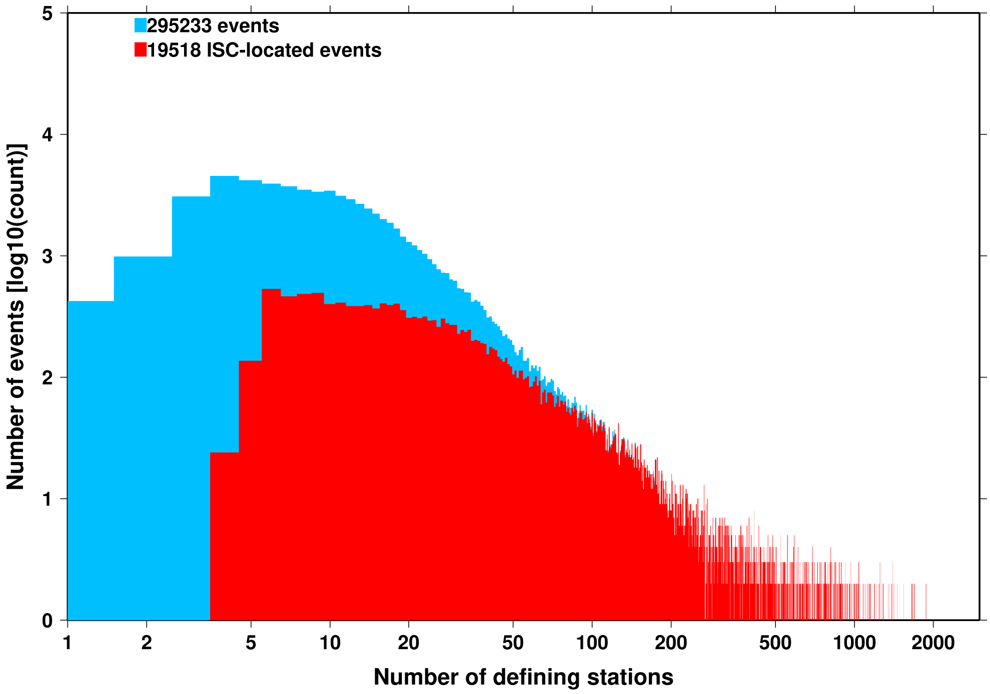

Figure 8.10: *Distribution of the number of defining stations for events in the ISC Bulletin (blue) and those selected for ISC location (red). The vertical scale is logarithmic.*

Nevertheless, half of the events are characterised by an error ellipse with an area less than 160 km^2, 90% of the events have an error ellipse area less than 1035 km^2, and 95% of the events have an error ellipse area less than 1924 km^2.

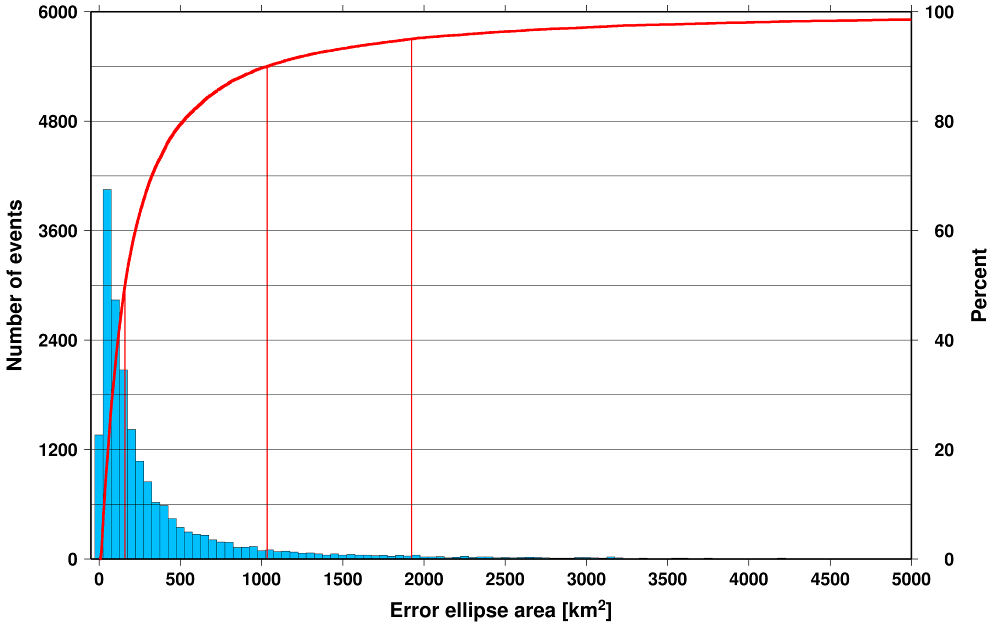

Figure 8.11: *Distribution of the area of the 90% confidence error ellipse of the ISC-located events. Vertical red lines indicate the 50th, 90th and 95th percentile values.*

Figure 8.12 shows one of the major characteristic features of the ISC location algorithm (Bondár and Storchak, 2011). Because the ISC locator accounts for correlated travel-time prediction errors due to unmodelled velocity heterogeneities along similar ray paths, the area of the 90% confidence error ellipse does not decrease indefinitely with increasing number of stations, but levels off once the information carried by the network geometry is exhausted, thus providing more realistic uncertainty estimates.

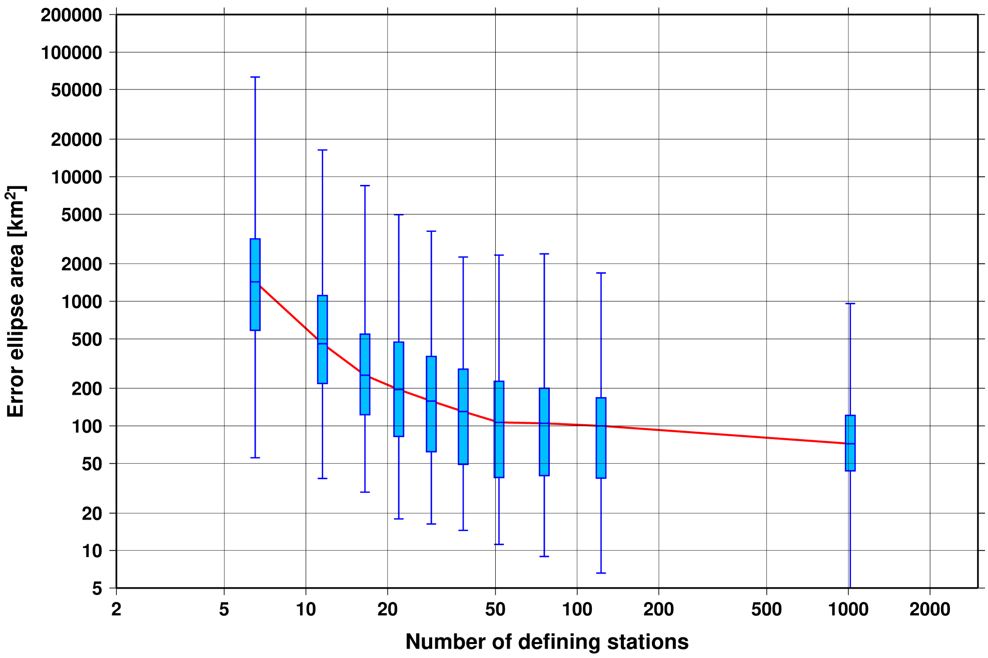

Figure 8.12: *Box-and-whisker plot of the area of the 90% confidence error ellipse of the ISC-located events as a function of the number of defining stations. Each box represents one-tenth-worth of the total number of data. The red line indicates the median 90% confidence error ellipse area.*

8.2 Seismic Phases and Travel-Time Residuals

The number of phases that are associated to events over the summary period in the ISC Bulletin is shown in Figure 8.13. Phase types and their total number in the ISC Bulletin is shown in the Appendix, Table 10.2. A summary of phase types is indicated in Figure 8.14.

In computing ISC locations, the current (for events since 2009) ISC location algorithm (*Bondár and Storchak*, 2011) uses all *ak135* phases where possible. Within the Bulletin, the phases that contribute to an ISC location are labelled as *time defining*. In this section, we summarise these time defining phases.

In Figure 8.15, the number of defining phases is shown in a histogram over the summary period. Each defining phase is listed in Table 8.1, which also provides a summary of the number of defining phases per event. A pie chart showing the proportion of defining phases is shown in Figure 8.16. Figure 8.17 shows travel times of seismic waves. The distribution of residuals for these defining phases is shown for the top five phases in Figures 8.18 through 8.22.

Table 8.1: *Numbers of 'time defining' phases (N) within the ISC Bulletin for 19518 ISC located events.*

Phase	Number of 'defining' phases	Number of events	Max per event	Median per event
P	868931	12657	2628	17
Pn	639954	17953	1096	17
Sn	207382	15381	229	7
Pb	100620	8822	152	7
Pg	81672	6931	216	7
Sb	66289	8398	119	5
Sg	59865	6651	203	6
PKPdf	46581	4140	552	3
S	38315	3401	360	3
PKiKP	27354	3104	313	2
PKPbc	20819	3314	220	2
PKPab	13760	2502	124	2
PcP	13607	3374	86	2

Table 8.1: *(continued)*

Phase	Number of 'defining' phases	Number of events	Max per event	Median per event
pP	10499	1339	180	3
PP	8689	1100	169	2
Pdif	7676	868	315	2
sP	4283	1026	72	2
ScP	4024	972	68	2
SS	4018	855	68	3
SKSac	2851	446	74	2
PKKPbc	1917	364	103	2
pwP	1804	539	50	2
SnSn	885	496	11	1
ScS	884	293	66	1
SKPbc	872	284	39	2
pPKPdf	754	270	27	1
sS	727	377	11	1
PnPn	708	417	21	1
P'P'df	647	152	28	3
SKiKP	575	257	24	1
SKPdf	425	139	29	1
PKKPdf	412	183	44	1
pPKPab	410	133	31	1
PKKPab	397	163	25	1
pPKPbc	291	139	17	1
PS	271	138	10	2
SKSdf	239	140	22	1
sPKPdf	226	129	14	1
SKPab	213	113	16	1
P'P'bc	188	111	16	1
SKKSac	183	119	13	1
SKKPbc	152	44	26	2
PnS	131	104	3	1
SP	131	38	27	1
sPKPab	112	52	11	1
PcS	110	83	6	1
Sdif	103	47	34	1
pPKiKP	96	38	10	1
sPKPbc	92	49	12	1
pPdif	86	37	10	1
pS	74	67	3	1
PKSdf	69	40	14	1
SKKSdf	64	60	2	1
P'P'ab	40	26	4	1
PbPb	33	17	12	1
SKKPdf	32	16	8	1
SKKPab	22	10	7	2
sPKiKP	21	13	7	1
sPdif	20	20	1	1
SPn	17	13	2	1
SbSb	12	11	2	1
PKSbc	6	6	1	1
sSdif	4	4	1	1
sPn	3	3	1	1
PgPg	2	2	1	1
S'S'ac	2	2	1	1
sSKSac	2	2	1	1
pSKSac	2	2	1	1
sSn	1	1	1	1
pSKSdf	1	1	1	1
SgSg	1	1	1	1

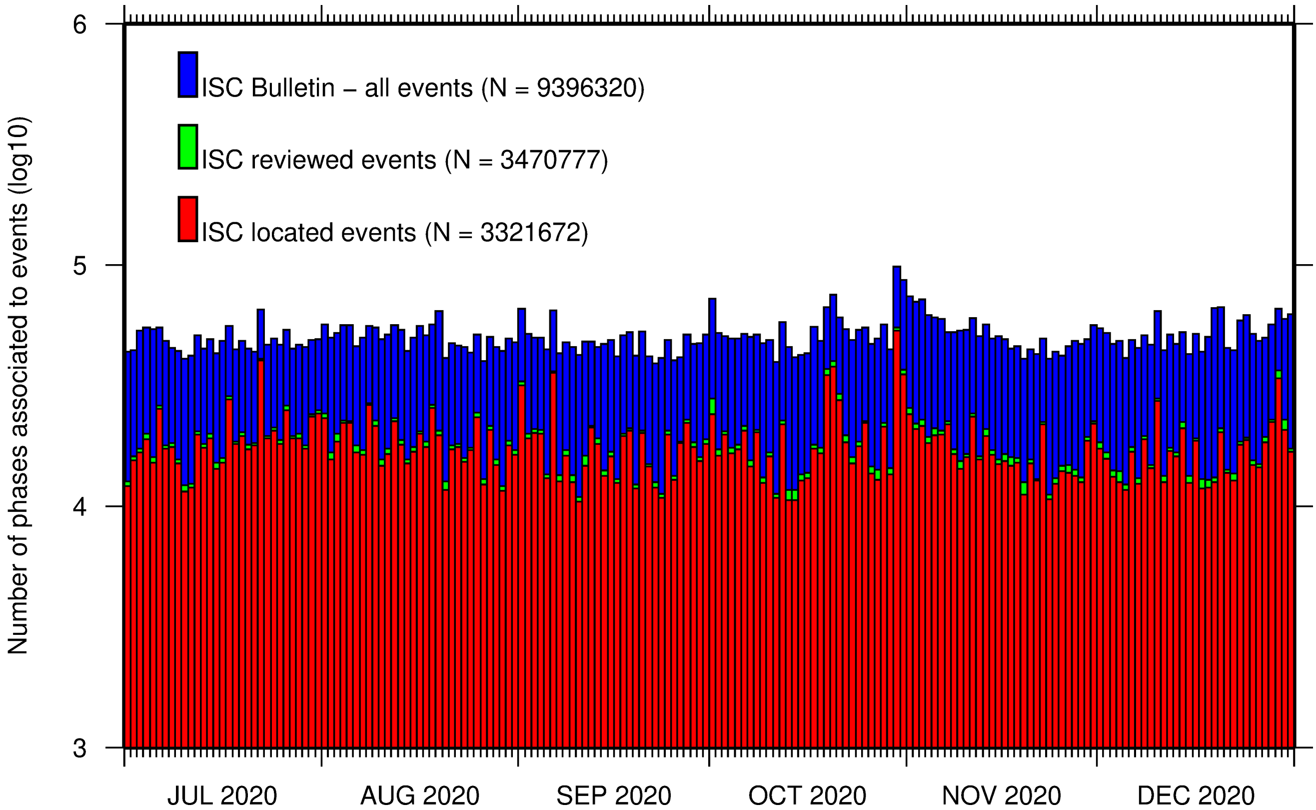

Figure 8.13: *Histogram showing the number of phases (N) that the ISC has associated to events within the ISC Bulletin for the current summary period.*

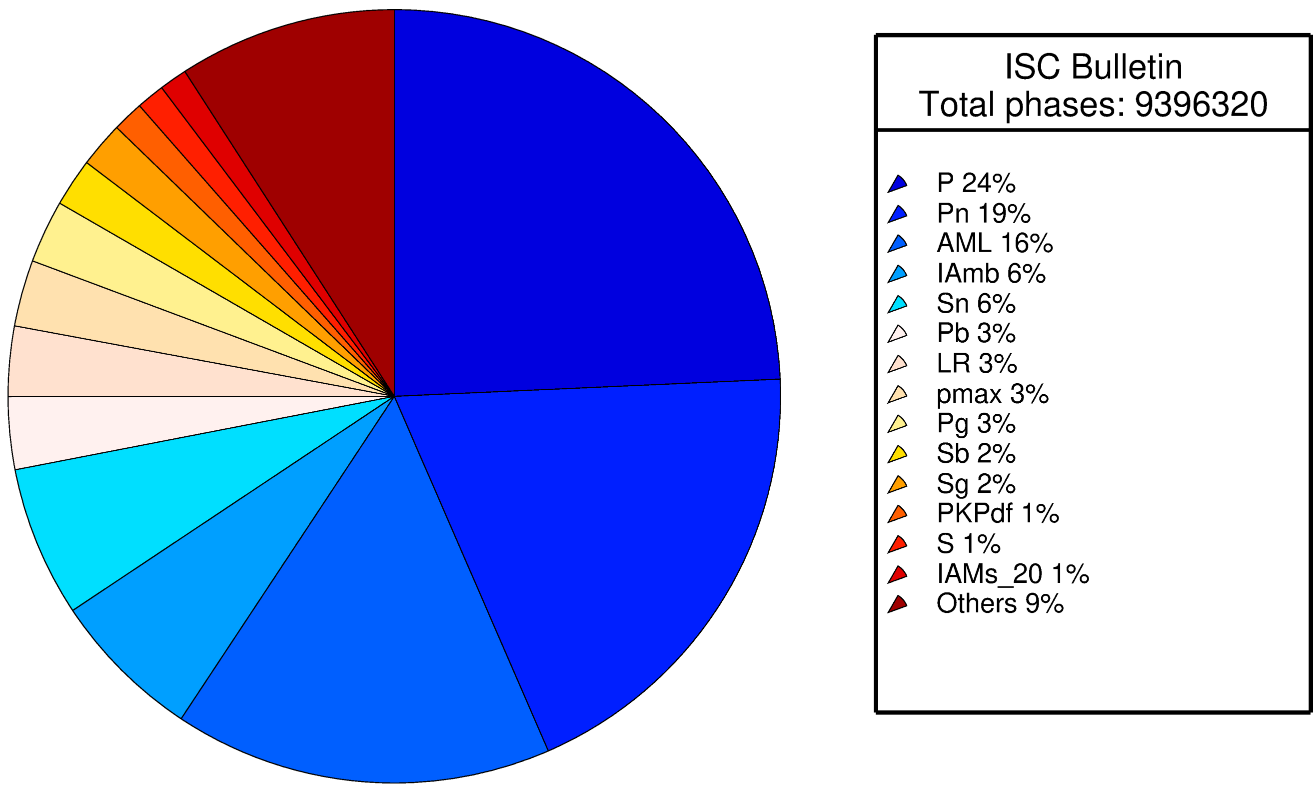

Figure 8.14: *Pie chart showing the fraction of various phase types in the ISC Bulletin for this summary period.*

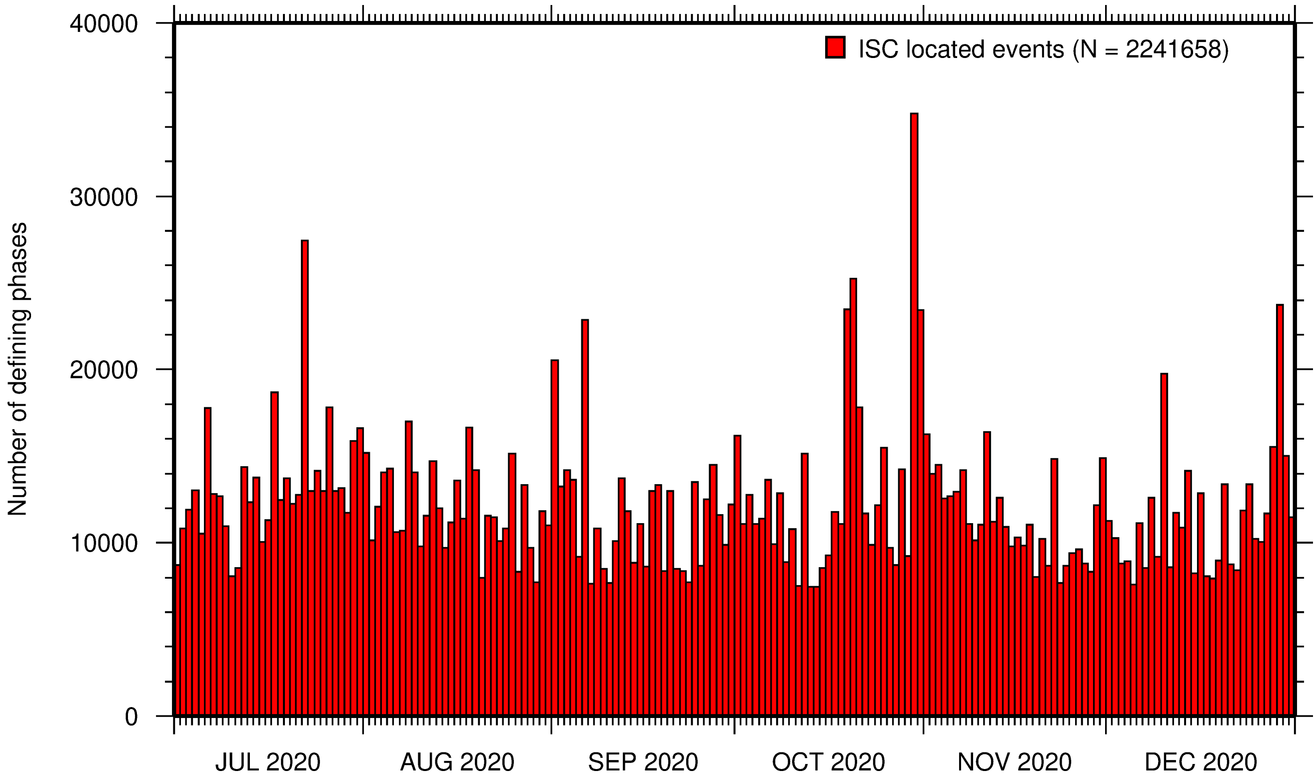

Figure 8.15: *Histogram showing the number of defining phases in the ISC Bulletin, for events located by the ISC.*

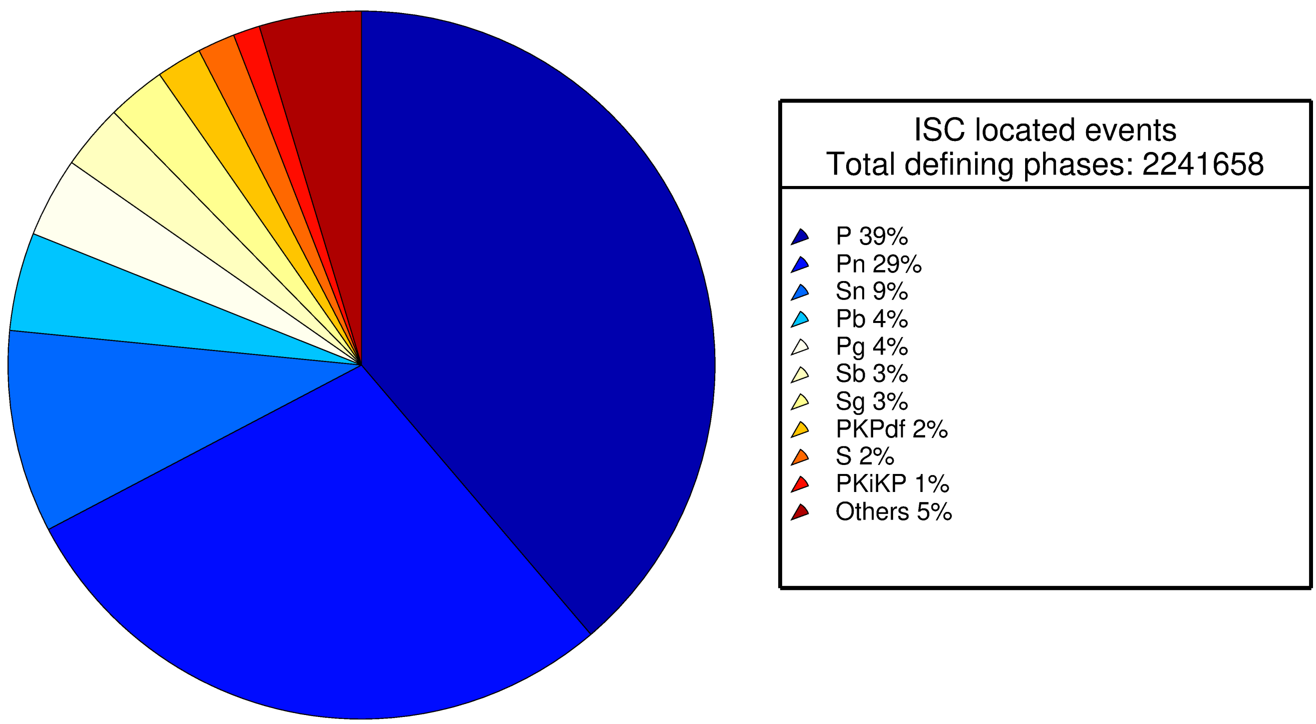

Figure 8.16: *Pie chart showing the defining phases in the ISC Bulletin, for events located by the ISC. A complete list of defining phases is shown in Table 8.1.*

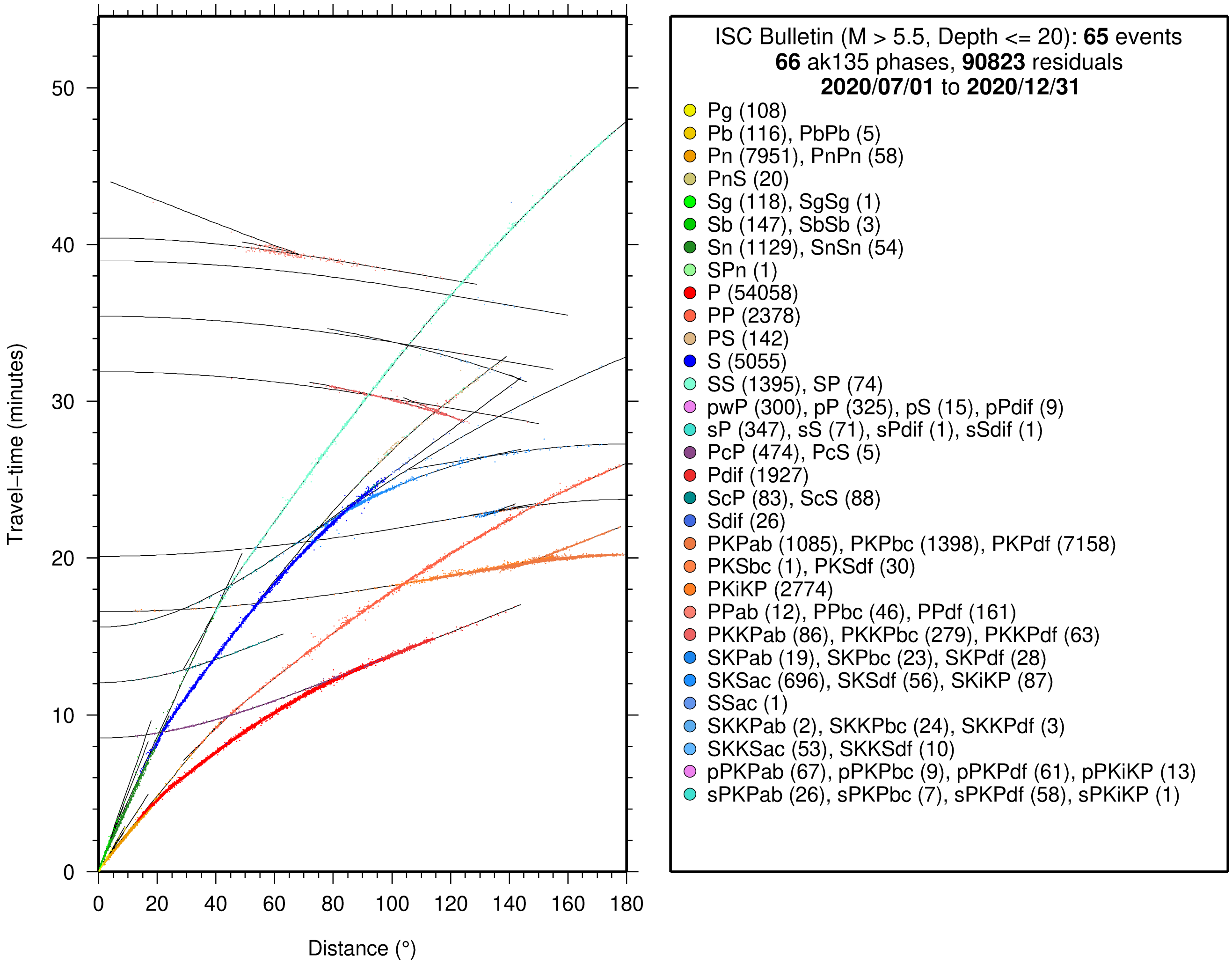

Figure 8.17: *Distribution of travel-time observations in the ISC Bulletin for events with M > 5.5 and depth less than 20 km. The travel-time observations are shown relative to a 0 km source and compared with the theoretical ak135 travel-time curves (solid lines). The legend lists the number of each phase plotted.*

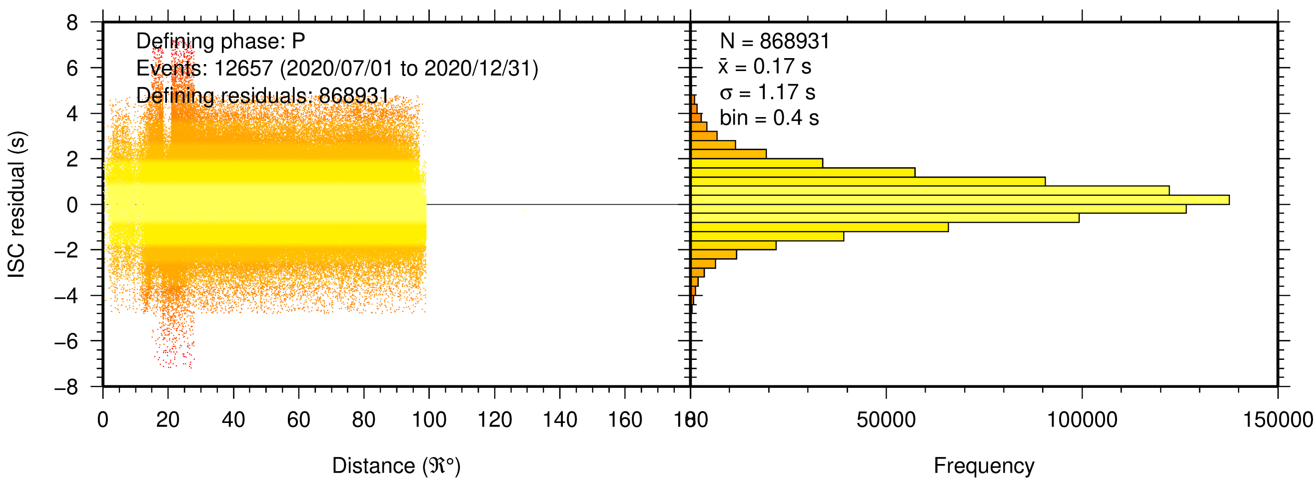

Figure 8.18: *Distribution of travel-time residuals for the defining P phases used in the computation of ISC located events in the Bulletin.*

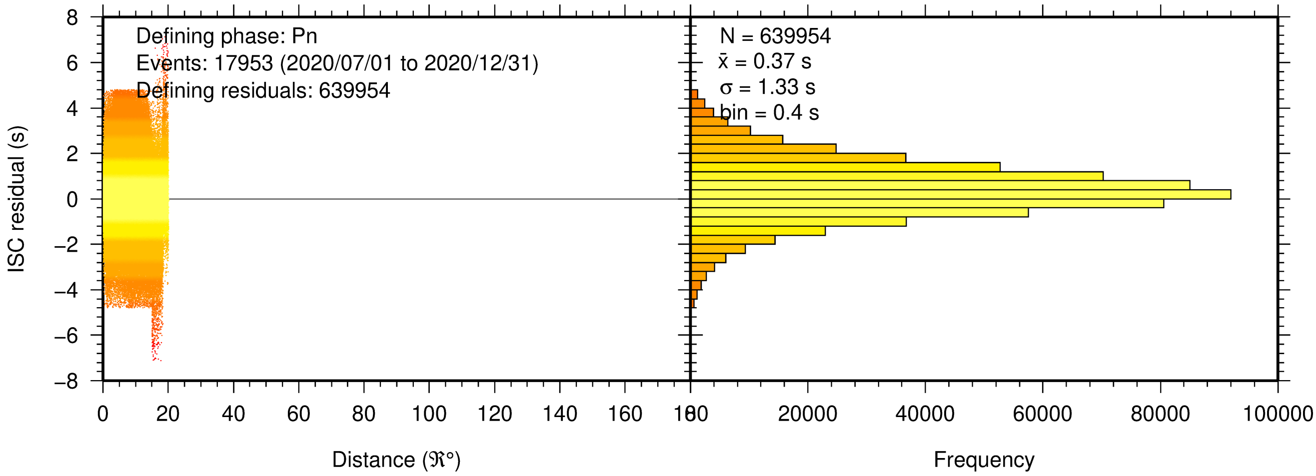

Figure 8.19: *Distribution of travel-time residuals for the defining Pn phases used in the computation of ISC located events in the Bulletin.*

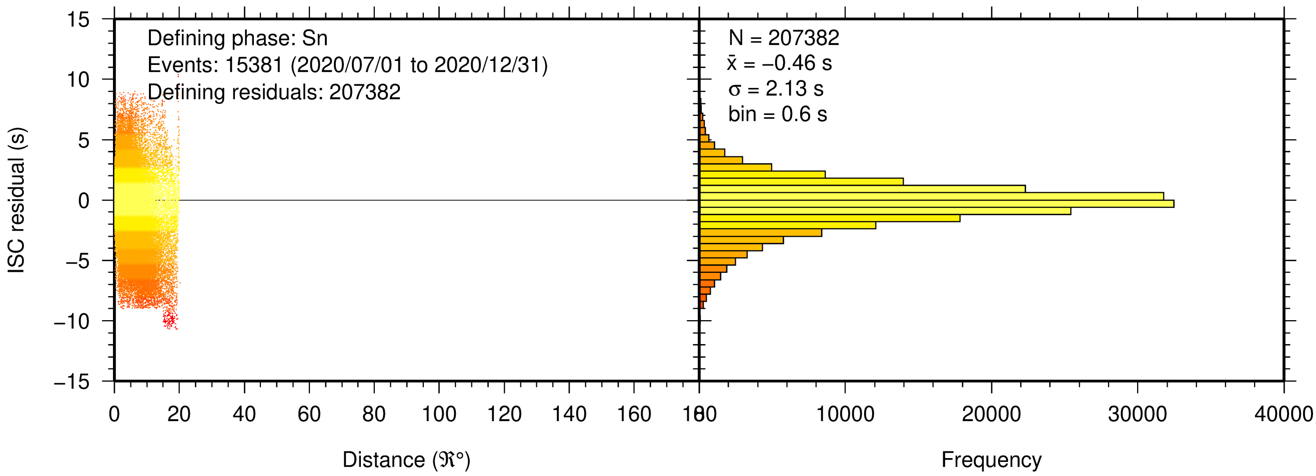

Figure 8.20: *Distribution of travel-time residuals for the defining Sn phases used in the computation of ISC located events in the Bulletin.*

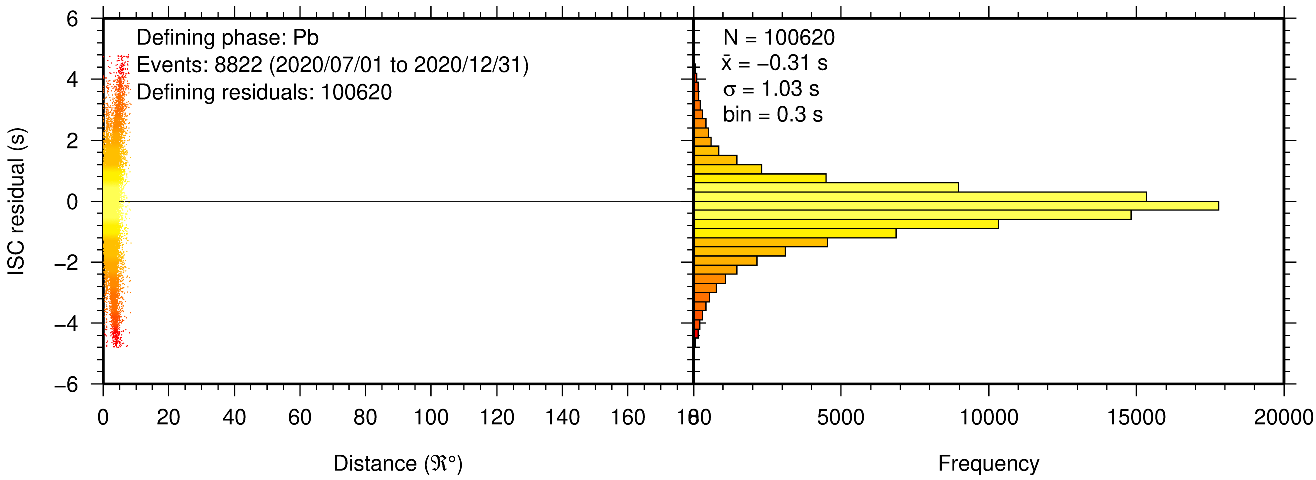

Figure 8.21: *Distribution of travel-time residuals for the defining Pb phases used in the computation of ISC located events in the Bulletin.*

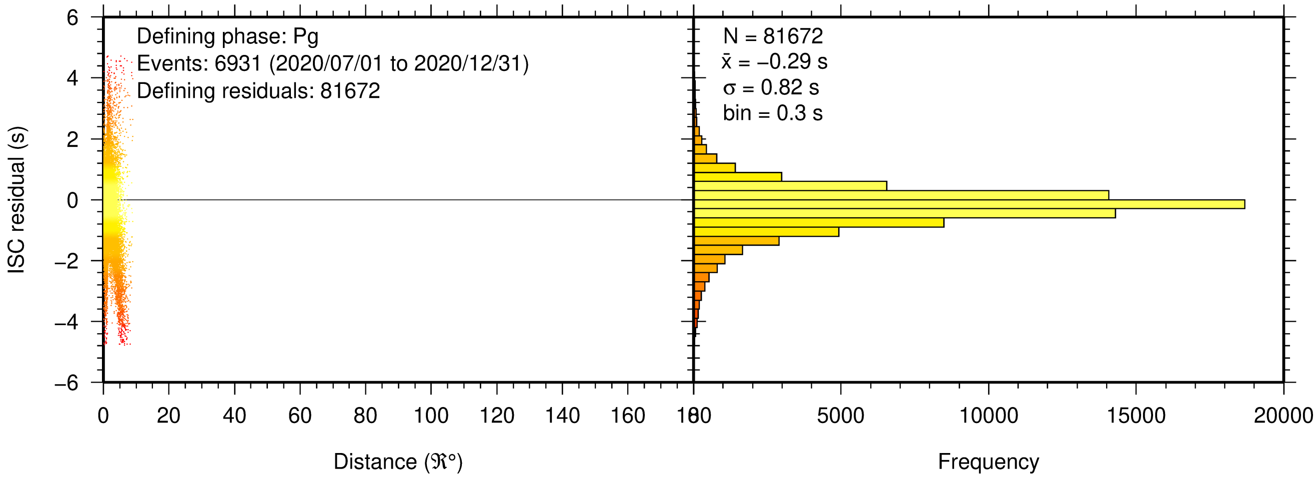

Figure 8.22: *Distribution of travel-time residuals for the defining Pg phases used in the computation of ISC located events in the Bulletin.*

8.3 Seismic Wave Amplitudes and Periods

The ISC Bulletin contains a variety of seismic wave amplitudes and periods measured by reporting agencies. For this Bulletin Summary, the total of collected amplitudes and periods is 682886 (see Section 7.3). For the determination of the ISC magnitudes MS and mb, only a fraction of such data can be used. Indeed, the ISC network magnitudes are computed only for ISC located events. Here we recall the main features of the ISC procedure for MS and mb computation (see detailed description in Section 10.1.4 of Volume 57 Issue I of the ISC Summary). For each amplitude-period pair in a reading the ISC algorithm computes the magnitude (a reading can include several amplitude-period measurements) and the reading magnitude is assigned to the maximum A/T in the reading. If more than one reading magnitude is available for a station, the station magnitude is the median of the reading magnitudes. The network magnitude is computed then as the 20% alpha-trimmed median of the station magnitudes (at least three required). MS is computed for shallow earthquakes (depth $\leq$ 60 km) only and using amplitudes and periods on all three components (when available) if the period is within 10-60 s and the epicentral distance is between 20° and 160°. mb is computed also for deep earthquakes (depth down to 700 km) but only with amplitudes on the vertical component measured at periods $\leq$ 3 s in the distance range 21°-100°.

Table 8.2 is a summary of the amplitude and period data that contributed to the computation of station and ISC MS and mb network magnitudes for this Bulletin Summary.

Table 8.2: *Summary of the amplitude-period data used by the ISC Locator to compute MS and mb.*

	MS	mb
Number of amplitude-period data	154643	528243
Number of readings	137733	524216
Percentage of readings in the ISC located events with qualifying data for magnitude computation	16.7	52.0
Number of station magnitudes	133278	452178
Number of network magnitudes	3560	11350

A small percentage of the readings with qualifying data for MS and mb calculation have more than one amplitude-period pair. Notably, only 17% of the readings for the ISC located (shallow) events included qualifying data for MS computation, whereas for mb the percentage is much higher at 52%. This is due to the seismological practice of reporting agencies. Agencies contributing systematic reports of amplitude and period data are listed in Appendix Table 10.3. Obviously the ISC Bulletin would benefit if more agencies included surface wave amplitude-period data in their reports.

Figure 8.23 shows the distribution of the number of station magnitudes versus distance. For mb there is a significant increase in the distance range 70°-90°, whereas for MS most of the contributing stations are below 100°. The increase in number of station magnitude between 70°-90° for mb is partly due to the very dense distribution of seismic stations in North America and Europe with respect to earthquake occurring in various subduction zones around the Pacific Ocean.

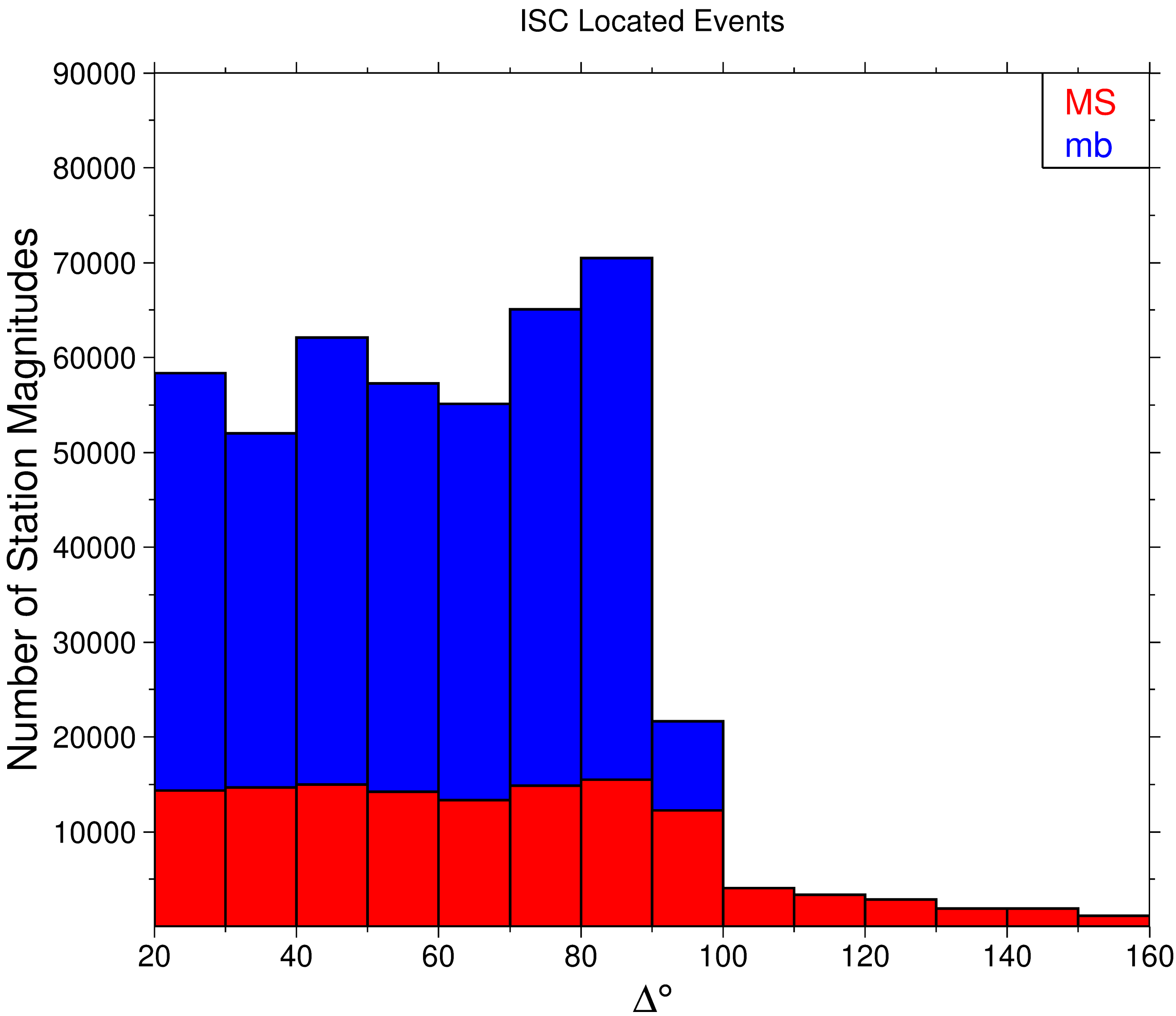

Figure 8.23: *Distribution of the number of station magnitudes computed by the ISC Locator for mb (blue) and MS (red) versus distance.*

Finally, Figure 8.24 shows the distribution of network MS and mb as well as the median number of stations for magnitude bins of 0.2. Clearly with increasing magnitude the number of events is smaller but with a general tendency of having more stations contributing to the network magnitude.

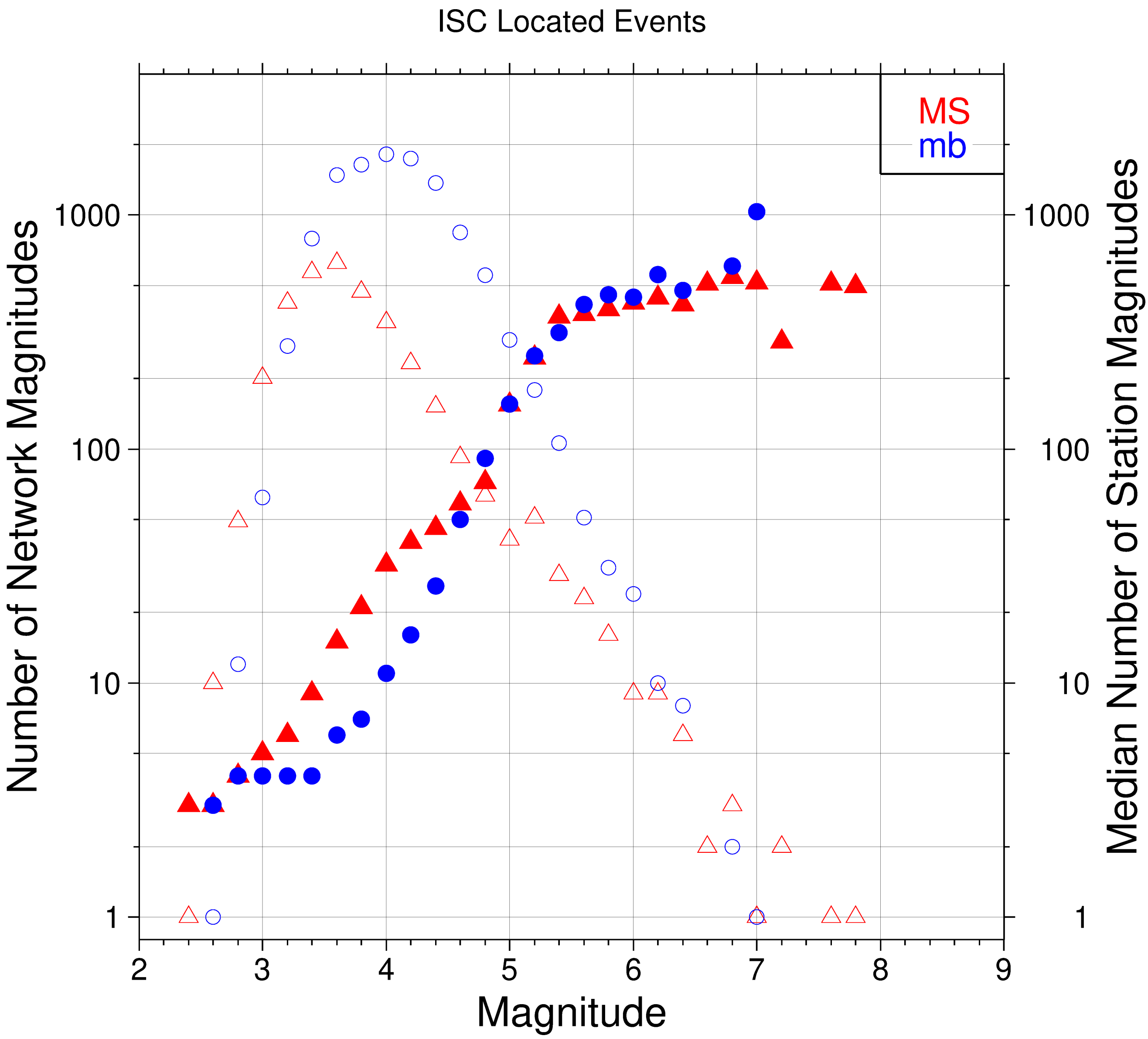

Figure 8.24: *Number of network magnitudes (open symbols) and median number of stations magnitudes (filled symbols). Blue circles refer to mb and red triangles to MS. The width of the magnitude interval δM is 0.2, and each symbol includes data with magnitude in $M \pm \delta M/2$.*

8.4 Completeness of the ISC Bulletin

We define the magnitude of completeness (hereafter M_C) as the lowest magnitude threshold above which all events are believed to be recorded. The Bulletin with events bigger than the defined M_C is assumed to be complete.

Until Issue 53, Volume II (July - December 2016) of the Summary of the ISC an estimation of M_C was computed only with the maximum curvature technique (*Woessner and Wiemer*, 2005). After the completion of the Rebuild Project and relocation of ISC hypocenters from data years 1964 to 2010 (*Storchak et al.*, 2017), the estimate of M_C for the entire ISC Bulletin is re-computed using four catalogue based methodologies (*Adamaki*, 2017, and references therein): the previously used maximum curvature for comparison (maxC), Mc based on the b-value stability (MBS technique), the Goodness of Fit Test with a 90% level of fit (GFT90) and the modified Goodness of Fit Test (mGFT). Further details on each of these methodologies and their statistical behaviour can be found in *Leptokaropoulos et al.* (2018).

The magnitudes of completeness of the ISC Bulletin for this Summary period is shown in Figure 8.25. How M_C varies for the ISC Bulletin over the years is shown in Figure 8.26. The step change in 1996 corresponds with the inclusion of the Prototype IDC (EIDC) Bulletin, followed by the Reviewed Event Bulletin (REB) of the IDC.

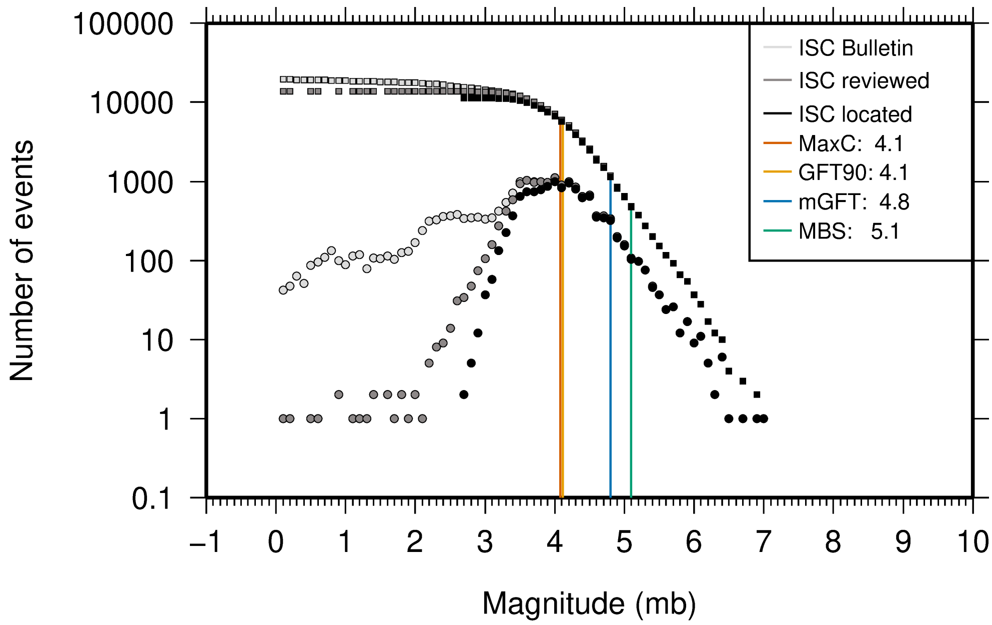

Figure 8.25: *Frequency and cumulative frequency magnitude distribution for all events in the ISC Bulletin, ISC reviewed events and events located by the ISC. The magnitude of completeness (M_C) is shown for the ISC Bulletin. Note: only events with values of mb are represented in the figure.*

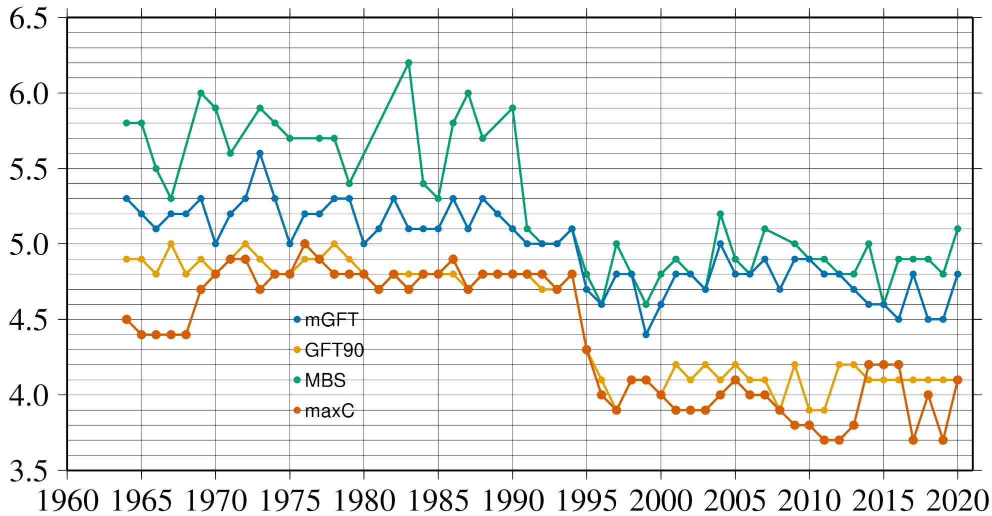

Figure 8.26: *Variation of magnitude of completeness (M_C) for each year in the ISC Bulletin. Note: M_C is calculated only using those events with values of mb.*

8.5 Magnitude Comparisons

The ISC Bulletin publishes network magnitudes reported by multiple agencies to the ISC. For events that have been located by the ISC, where enough amplitude data has been collected, the MS and mb magnitudes are calculated by the ISC (MS is computed only for depths $\leq$ 60 km). In this section, ISC magnitudes and some other reported magnitudes in the ISC Bulletin are compared.

The comparison between MS and mb computed by the ISC locator for events in this summary period is shown in Figure 8.27, where the large number of data pairs allows a colour coding of the data density. The scatter in the data reflects the fundamental differences between these magnitude scales.

Similar plots are shown in Figure 8.28 and 8.29, respectively, for comparisons of ISC mb and ISC MS with M_W from the GCMT catalogue. Since M_W is not often available below magnitude 5, these distributions are mostly for larger, global events. Not surprisingly, the scatter between mb and M_W is larger than the scatter between MS and M_W. Also, the saturation effect of mb is clearly visible for earthquakes with $M_W > 6.5$. In contrast, MS scales well with $M_W > 6$, whereas for smaller magnitudes MS appears to be systematically smaller than M_W.

In Figure 8.30 ISC values of mb are compared with all reported values of mb, values of mb reported by NEIC and values of mb reported by IDC. Similarly in Figure 8.31, ISC values of MS are compared with all reported values of MS, values of MS reported by NEIC and values of MS reported by IDC. There is a large scatter between the ISC magnitudes and the mb and MS reported by all other agencies.

The scatter decreases both for mb and MS when ISC magnitudes are compared just with NEIC and IDC magnitudes. This is not surprising as the latter two agencies provide most of the amplitudes and periods used by the ISC locator to compute MS and mb. However, ISC mb appears to be smaller than NEIC mb for $mb < 4$ and larger than IDC mb for $mb > 4$. Since NEIC does not include IDC amplitudes, it seems these features originate from observations at the high-gain, low-noise sites reported by the IDC. For the MS comparisons between ISC and NEIC a similar but smaller effect is observed for $MS < 4.5$, whereas a good scaling is generally observed for the MS comparisons between ISC and IDC.

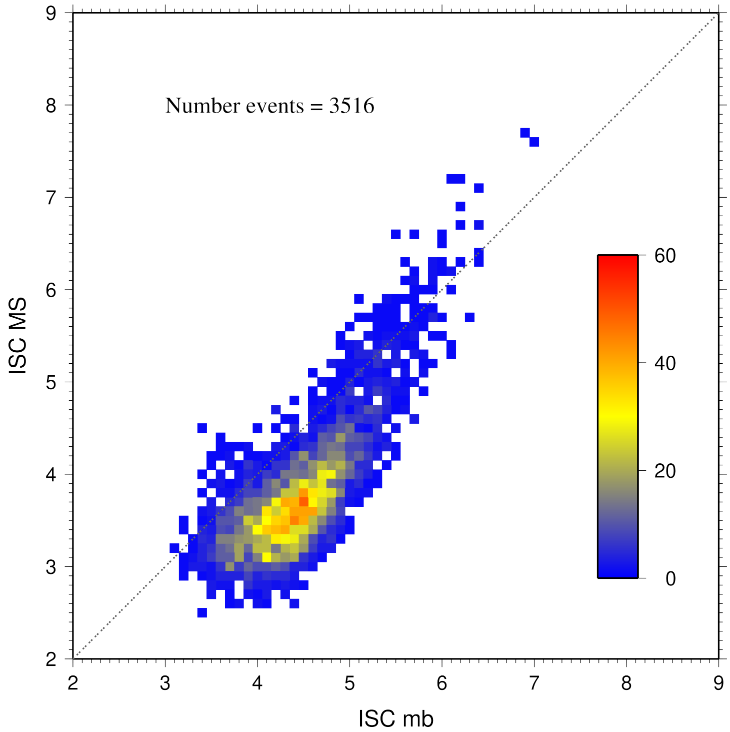

Figure 8.27: *Comparison of ISC values of MS with mb for common event pairs.*

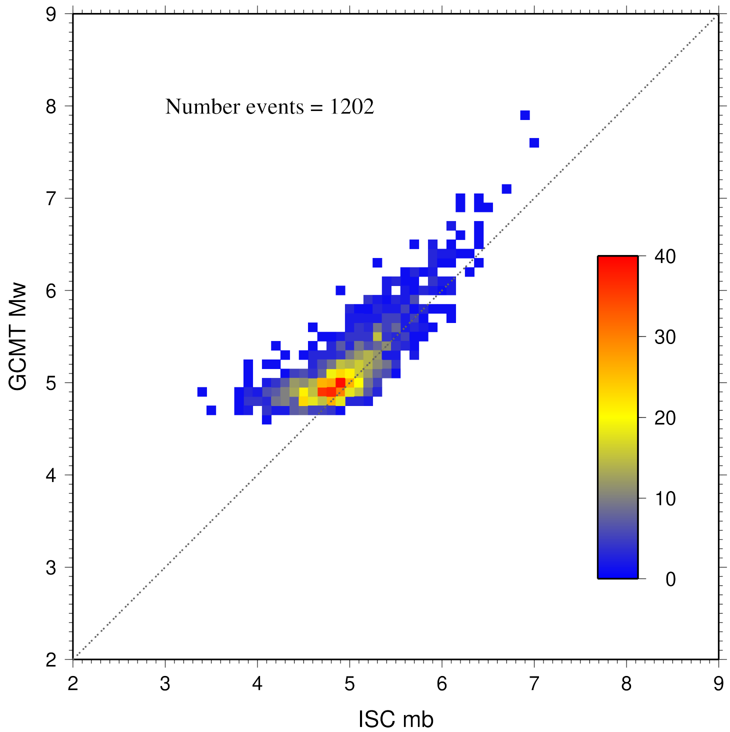

Figure 8.28: *Comparison of ISC values of mb with GCMT M_W for common event pairs.*

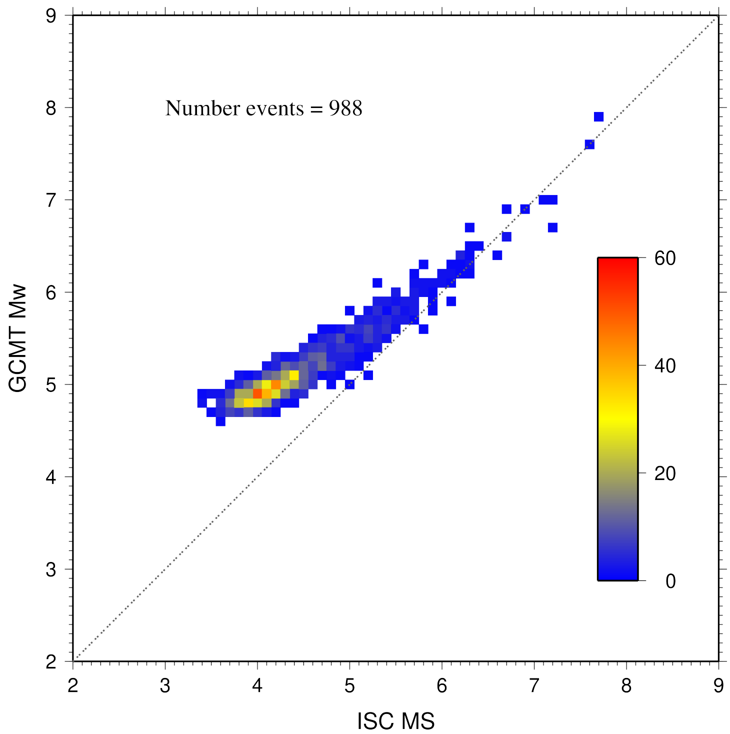

Figure 8.29: *Comparison of ISC values of MS with GCMT M_W for common event pairs.*

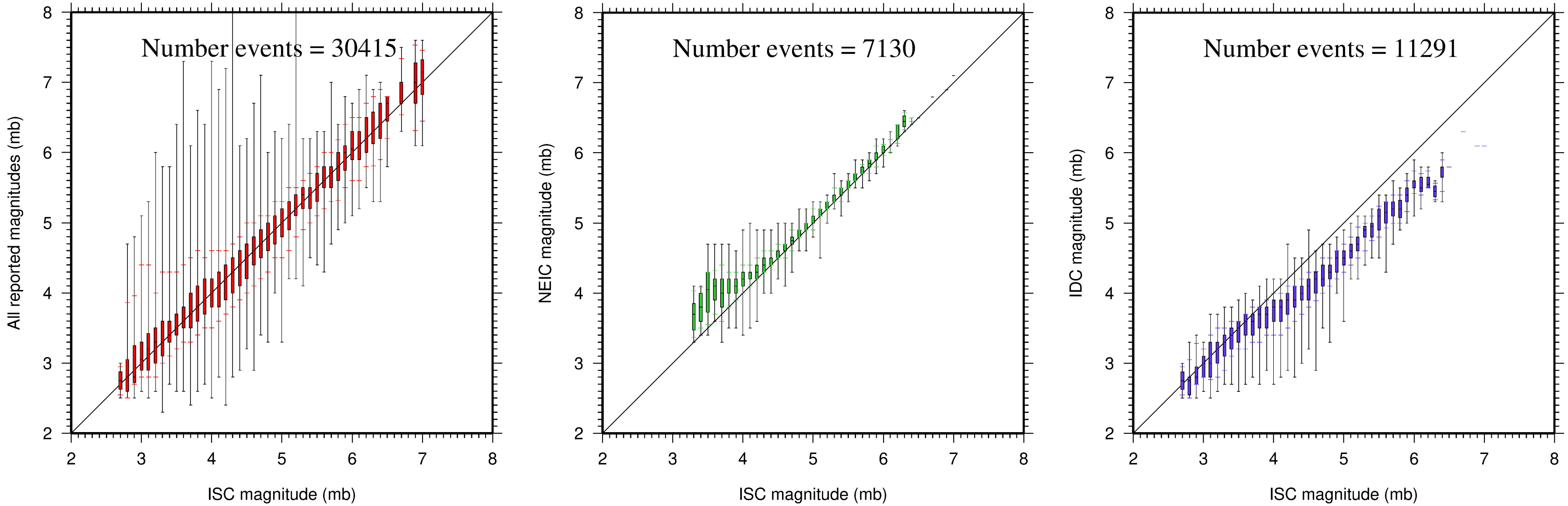

(a) (b) (c)

Figure 8.30: *Comparison of ISC magnitude data (mb) with additional agency magnitudes (mb). The statistical summary is shown in box-and-whisker plots where the 10th and 90th percentiles are shown in addition to the max and min values. (a): All magnitudes reported; (b): NEIC magnitudes; (c): IDC magnitudes.*

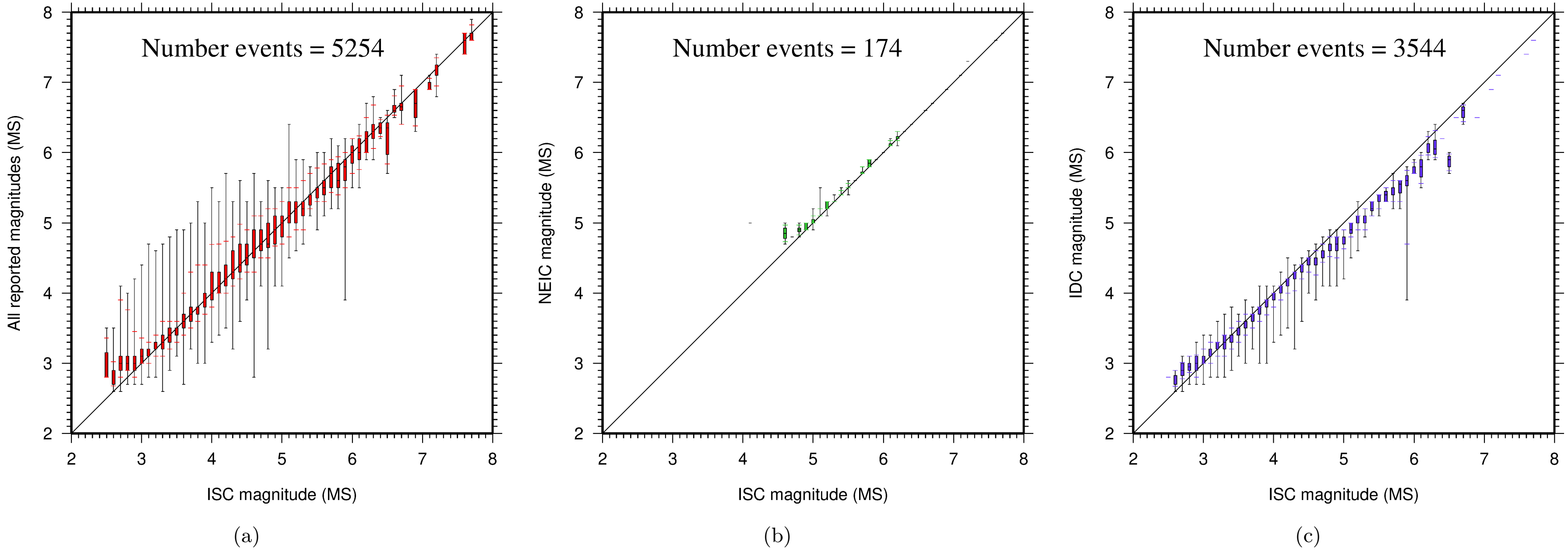

Figure 8.31: *Comparison of ISC magnitude data (MS) with additional agency magnitudes (MS). The statistical summary is shown in the box-and-whisker plots where the 10th and 90th percentiles are shown in addition to the max and min values. (a): All magnitudes reported; (b): NEIC magnitudes; (c): IDC magnitudes.*

9

The Leading Data Contributors

For the current six-month period, 150 agencies reported related bulletin data. Although we are grateful for every report, we nevertheless would like to acknowledge those agencies that made the most useful or distinct contributions to the contents of the ISC Bulletin. Here we note those agencies that:

- provided a comparatively large volume of parametric data (see Section 9.1),
- reported data that helped quite considerably to improve the quality of the ISC locations or magnitude determinations (see Section 9.2),
- helped the ISC by consistently reporting data in one of the standard recognised formats and in-line with the ISC data collection schedule (see Section 9.3).

We do not aim to discourage those numerous small networks who provide comparatively smaller yet still most essential volumes of regional data regularly, consistently and accurately. Without these reports the ISC Bulletin would not be as comprehensive and complete as it is today.

9.1 The Largest Data Contributors

We acknowledge the contribution of IDC, NEIC, BJI, MCSM, GFZ, MOS, CLL and a few others (Figure 9.1) that reported the majority of moderate to large events recorded at teleseismic distances. The contributions of NEIC, IDC, MEX, JMA and several others are also acknowledged with respect to smaller seismic events. The contributions of JMA, AFAD, ISK, RSNC, TAP, WEL and a number of others are also acknowledged with respect to small seismic events. Note that the NEIC bulletin accumulates a contribution of all regional networks in the USA. Several agencies monitoring highly seismic regions routinely report large volumes of small to moderate magnitude events, such as those in Japan, Chinese Taipei, Turkey, Italy, Greece, New Zealand, Mexico and Columbia. Contributions of small magnitude events by agencies in regions of low seismicity, such as Finland are also gratefully received.

We also would like to acknowledge contributions of those agencies that report a large portion of arrival time and amplitude data (Figure 9.2). For small magnitude events, these are local agencies in charge of monitoring local and regional seismicity. For moderate to large events, contributions of NEIC, GFZ, MOS, IDC are especially acknowledged. Notably, four agencies (NEIC, GFZ, MOS and IDC) together reported over 70% of all amplitude measurements made for teleseismically recorded events. We hope that other agencies would also be able to update their monitoring routines in the future to include the amplitude reports for teleseismic events compliant with the IASPEI standards.

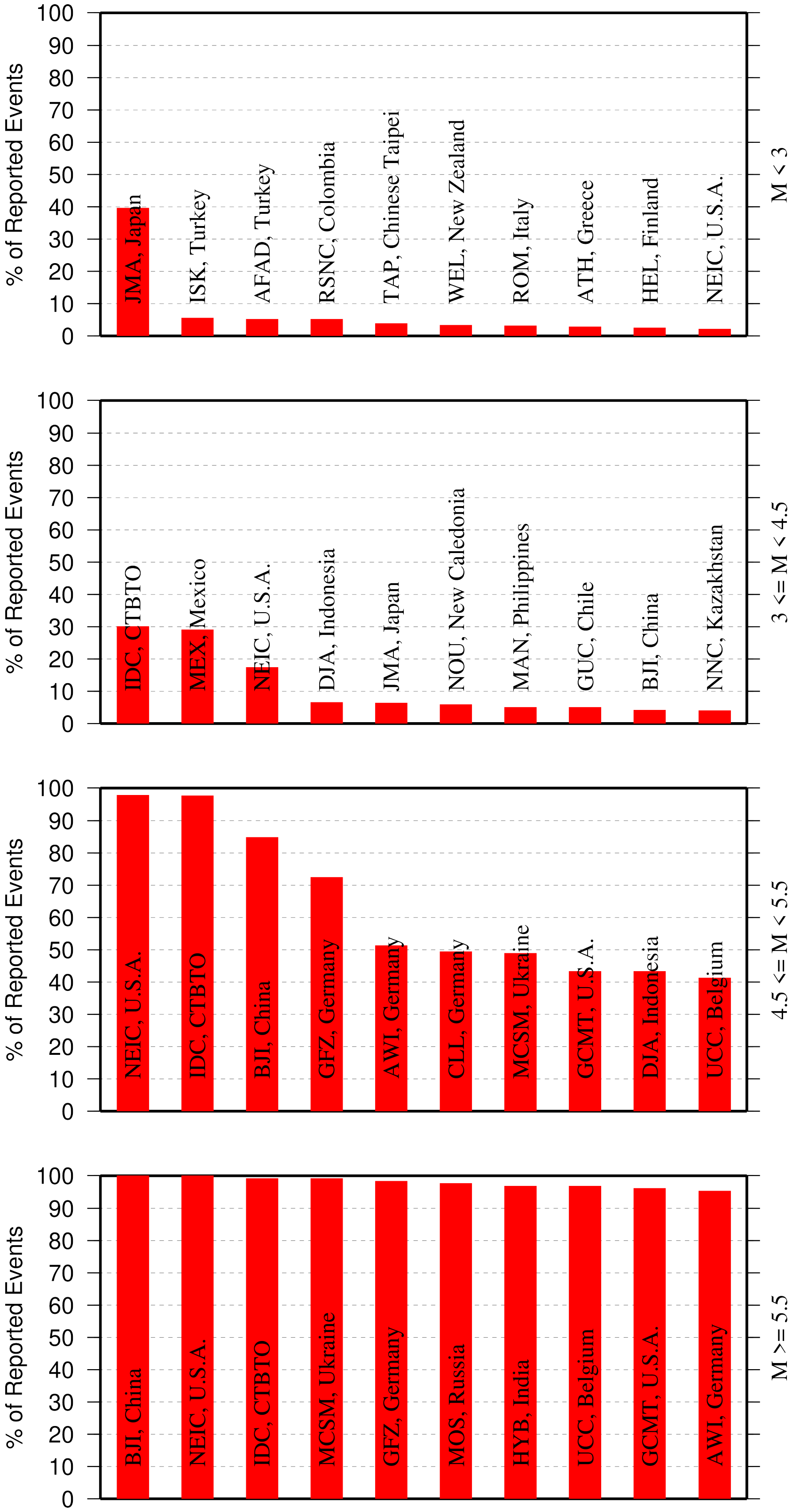

Figure 9.1: *Frequency of events in the ISC Bulletin for which an agency reported at least one item of data: a moment tensor, a hypocentre, a station arrival time or an amplitude. The top ten agencies are shown for four magnitude intervals.*

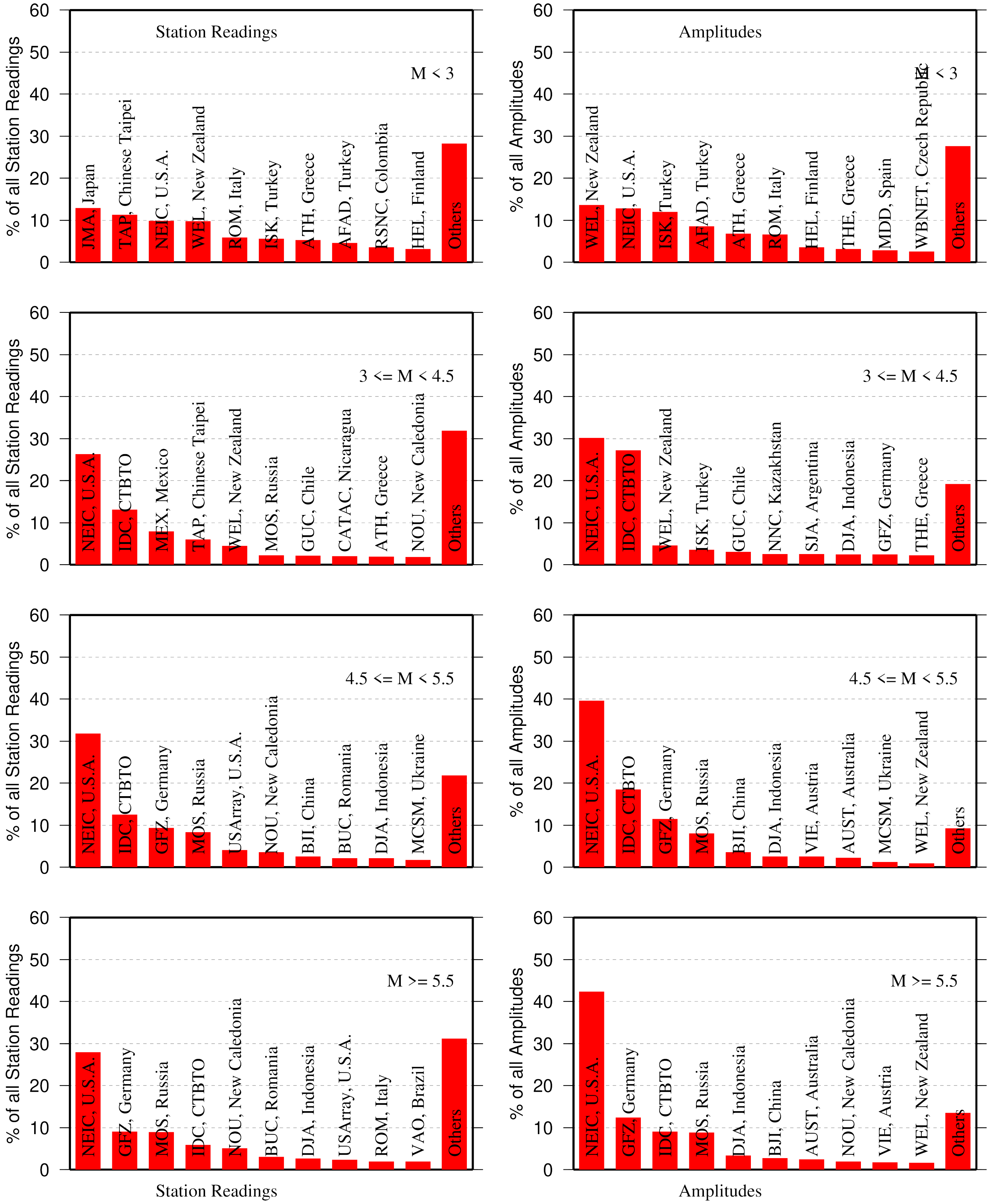

Figure 9.2: *Contributions of station arrival time readings (left) and amplitudes (right) of agencies to the ISC Bulletin. Top ten agencies are shown for four magnitude intervals.*

9.2 Contributors Reporting the Most Valuable Parameters

One of the main ISC duties is to re-calculate hypocentre estimates for those seismic events where a collective wealth of all station reports received from all agencies is likely to improve either the event location or depth compared to the hypocentre solution from each single agency. For areas with a sparse local seismic network or an unfavourable station configuration, readings made by other networks at teleseismic distances are very important. All events near mid-oceanic ridges as well as those in the majority of subduction zones around the world fall into this category. Hence we greatly appreciate the effort made by many agencies that report data for remote earthquakes (Figure 9.3). For some agencies, such as the IDC and the NEIC, it is part of their mission. For instance, the IDC reports almost every seismic event that is large enough to be recorded at teleseismic distance (20 degrees and beyond). This is largely because the International Monitoring System of primary arrays and broadband instruments is distributed at quiet sites around the world in order to be able to detect possible violations of the Comprehensive Nuclear-Test-Ban Treaty. The NEIC reported almost 50% of those events as their mission requires them to report events above magnitude 4.5 outside the United States of America. For other agencies reporting distant events it is an extra effort that they undertake to notify their governments and relief agencies as well as to help the ISC and academic research in general. Hence these agencies usually report on the larger magnitude events. BJI, GFZ, AWI, NAO, CLL, MOS, VIE, UCC each reported individual station arrivals for several percent of all relevant events. We encourage other agencies to report distant events to us.

In addition to the first arriving phase we encourage reporters to contribute observations of secondary seismic phases that help constrain the event location and depth: S, Sn, Sg and pP, sP, PcP (Figure 9.4). We expect though that these observations are actually made from waveforms, rather than just predicted by standard velocity models and modern software programs. It is especially important that these arrivals are manually reviewed by an operator (as we know takes place at the IDC and NEIC), as opposed to some lesser attempts to provide automatic phase readings that are later rejected by the ISC due to a generally poor quality of unreviewed picking.

Another important long-term task that the ISC performs is to compute the most definitive values of

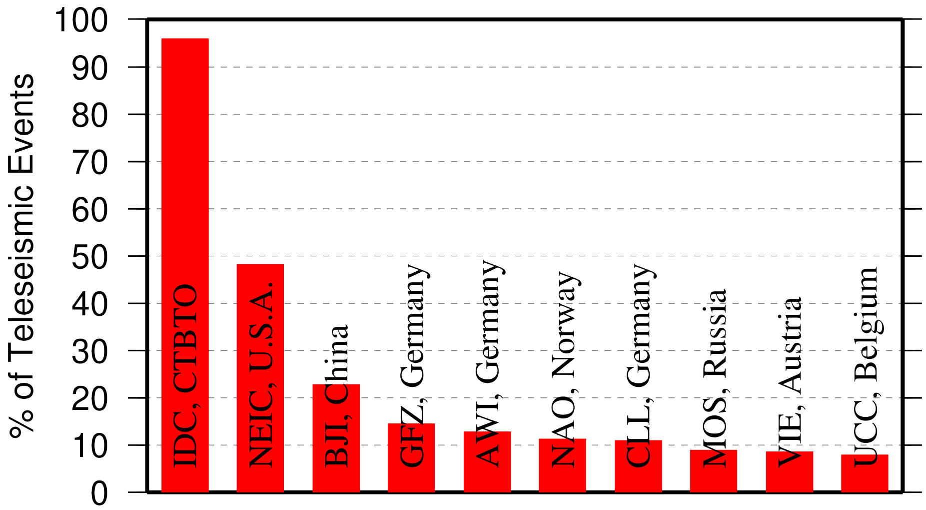

Figure 9.3: *Top ten agencies that reported teleseismic phase arrivals for a large portion of ISC events.*

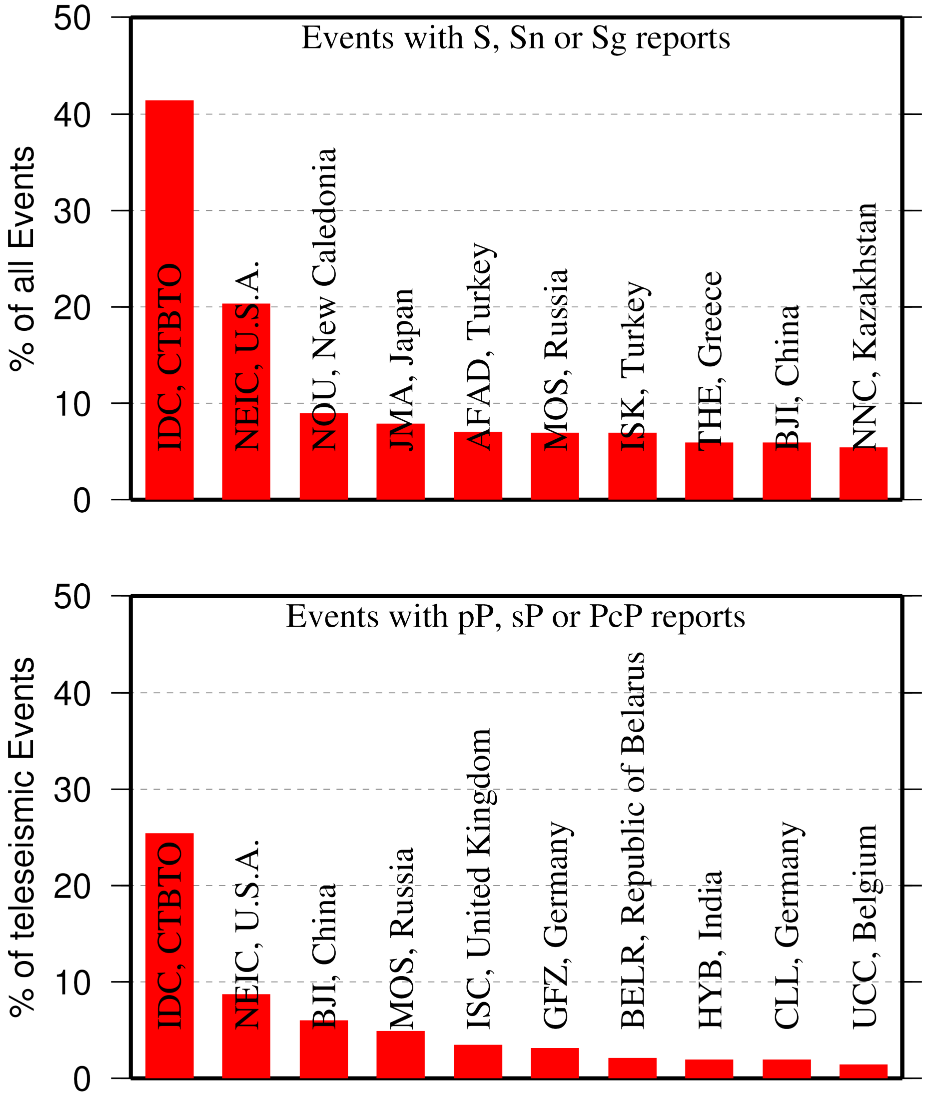

Figure 9.4: *Top ten agencies that reported secondary phases important for an accurate epicentre location (top) and focal depth determination (bottom).*

MS and mb network magnitudes that are considered reliable due to removal of outliers and consequent averaging (using alpha-trimmed median) across the largest network of stations, generally not feasible for a single agency. Despite concern over the bias at the lower end of mb introduced by the body wave amplitude data from the IDC, other agencies are also known to bias the results. This topic is further discussed in Section 8.5.

Notably, the IDC reports almost 100% of all events for which MS and mb are estimated. This is due to the standard routine that requires determination of body and surface wave magnitudes useful for discrimination purposes. NEIC, BJI, MOS, GFZ, CLL and a few other agencies (Figure 9.5) are also responsible for the majority of the amplitude and period reports that contribute towards the ISC magnitudes.

The ISC only recently started to determine source mechanisms in addition to those reported by other agencies. For moment tensor magnitudes we rely on reports from other agencies (Figure 9.6).

Among other event parameters the ISC Bulletin also contains information on event type. We cannot

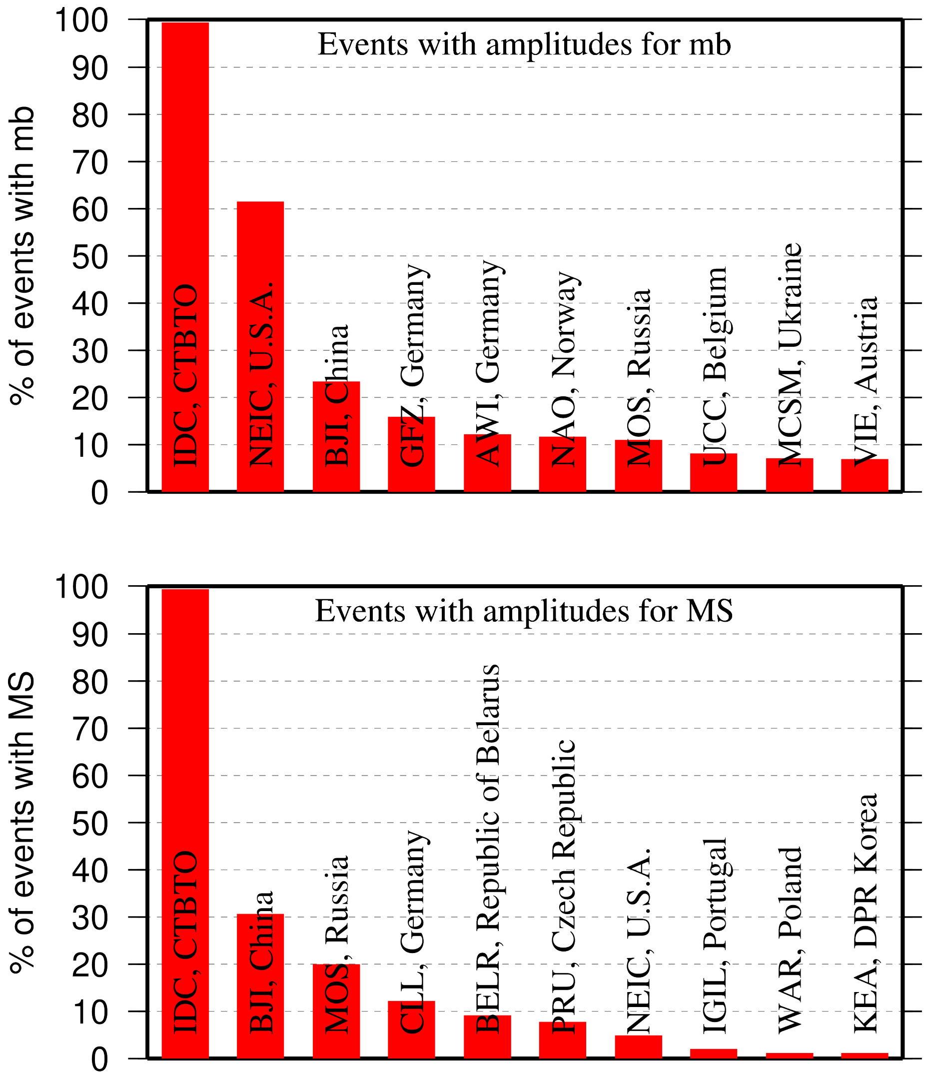

Figure 9.5: *Agencies that report defining body (top) and surface (bottom) wave amplitudes and periods for the largest fraction of those ISC Bulletin events with MS/mb determinations.*

independently verify the type of each event in the Bulletin and thus rely on other agencies to report the event type to us. Practices of reporting non-tectonic events vary greatly from country to country. Many agencies do not include anthropogenic events in their reports. Suppression of such events from reports to the ISC may lead to a situation where a neighbouring agency reports the anthropogenic event as an earthquake for which expected data are missing. This in turn is detrimental to ISC Bulletin users studying natural seismic hazard. Hence we encourage all agencies to join the agencies listed on Figure 9.7 and several others in reporting both natural and anthropogenic events to the ISC.

The ISC Bulletin also contains felt and damaging information when local agencies have reported it to us. Agencies listed on Figure 9.8 provide such information for the majority of all felt or damaging events in the ISC Bulletin.

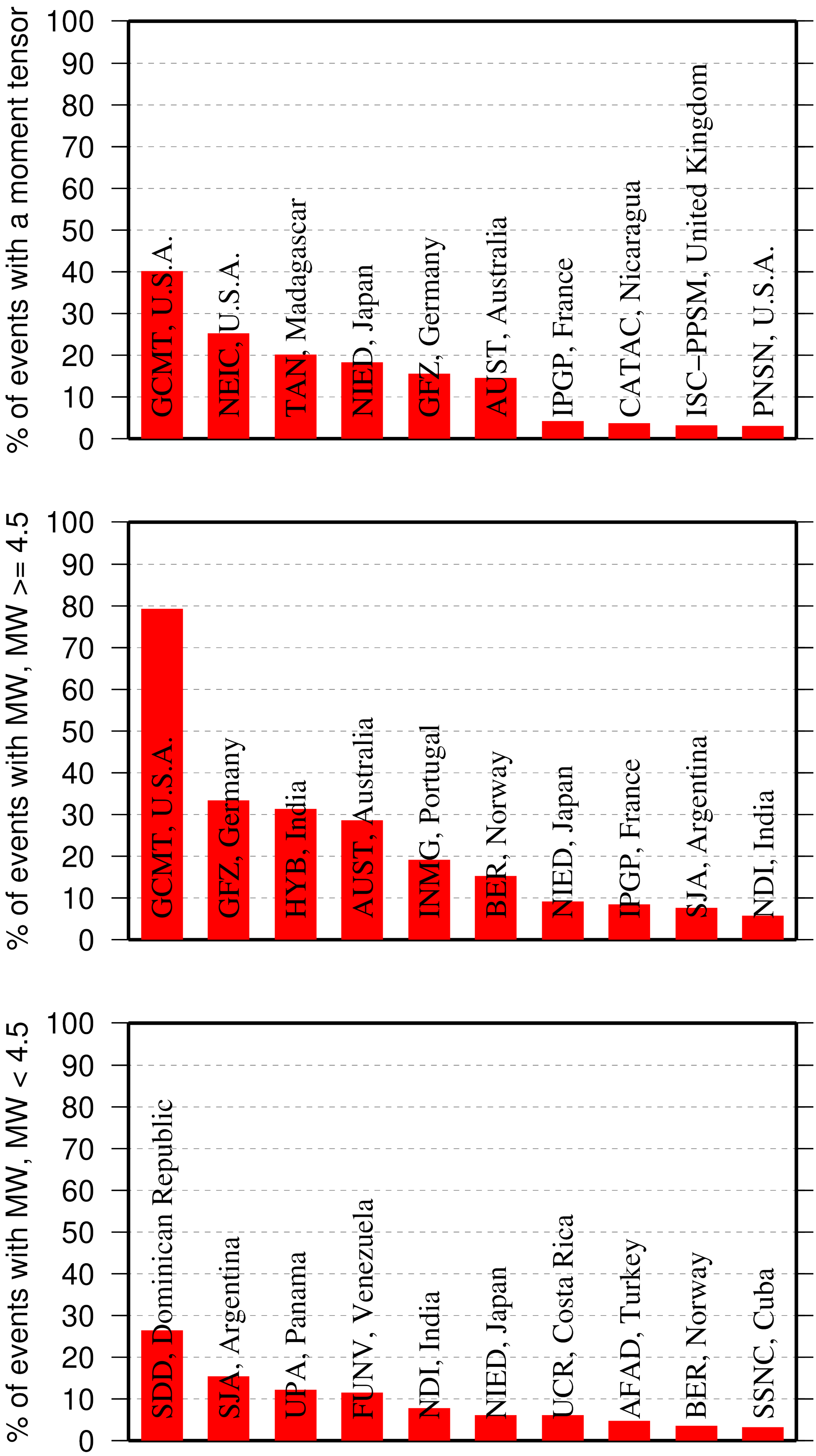

Figure 9.6: *Top ten agencies that most frequently report determinations of seismic moment tensor (top) and moment magnitude (middle/bottom for M greater/smaller than 4.5).*

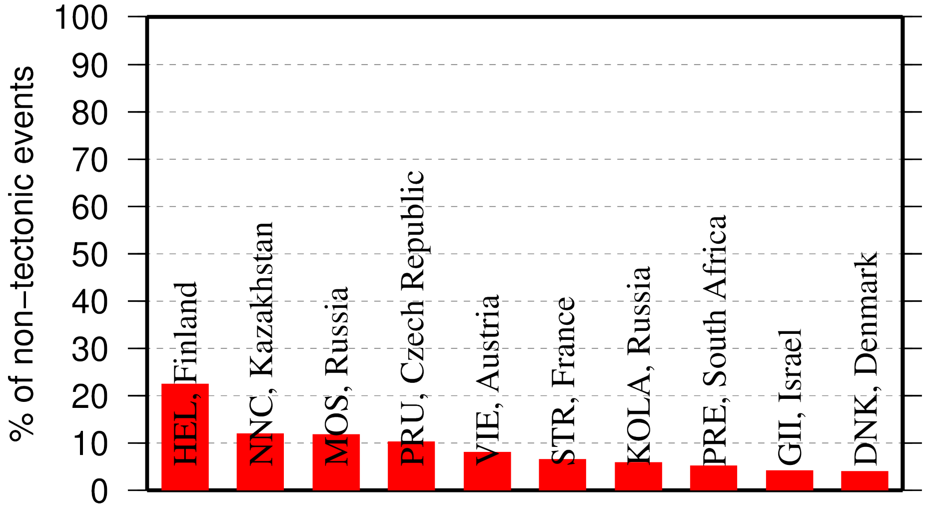

Figure 9.7: *Top ten agencies that most frequently report non-tectonic seismic events to the ISC.*

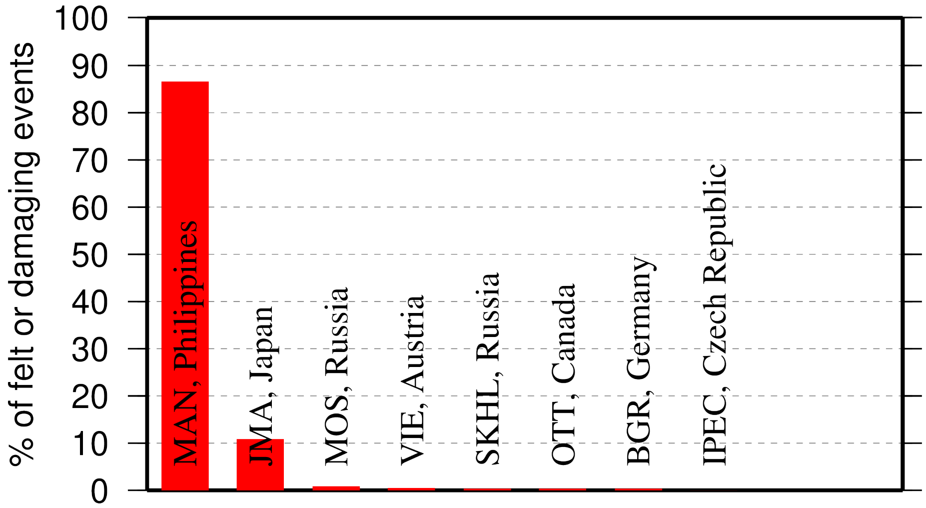

Figure 9.8: *Top ten agencies that most frequently report macroseismic information to the ISC.*

9.3 The Most Consistent and Punctual Contributors

During this six-month period, 27 agencies reported their bulletin data in one of the standard seismic formats (ISF, IMS, GSE, Nordic or QuakeML) and within the current 12-month deadline. Here we must reiterate that the ISC accepts reviewed bulletin data after a final analysis as soon as they are ready. These data, even if they arrive before the deadline, are immediately parsed into the ISC database, grouped with other data and become available to the ISC users on-line as part of the preliminary ISC Bulletin. There is no reason to wait until the deadline to send the data to the ISC. Table 9.1 lists all agencies that have been helpful to the ISC in this respect during the six-month period.

Table 9.1: *Agencies that contributed reviewed bulletin data to the ISC in one of the standard international formats before the submission deadline.*

Agency Code	Country	Average Delay from real time (days)
AUST	Australia	15
ZUR	Switzerland	17
WEL	New Zealand	22
IDC	Austria	26
ATH	Greece	28
IGIL	Portugal	32
NAO	Norway	48
LDG	France	59
KNET	Kyrgyzstan	64
ECX	Mexico	74
PPT	French Polynesia	84
TIR	Albania	120
SVSA	Portugal	123
KEA	Democratic People's Republic of Korea	195
INMG	Portugal	198
BJI	China	212
DSN	United Arab Emirates	228
ISK	Turkey	230
BUC	Romania	255
AFAD	Turkey	261
SJA	Argentina	280
UPP	Sweden	286
OMAN	Oman	289
MRB	Spain	293
IPEC	Czech Republic	300
BYKL	Russia	300
GRAL	Lebanon	306
CATAC	Nicaragua	316
STR	France	317
UCC	Belgium	318
MOS	Russia	340
MIRAS	Russia	363

10

Appendix

10.1 Tables

Table 10.1: *Listing of all 391 agencies that have directly reported to the ISC. The 150 agencies highlighted in bold have reported data to the ISC Bulletin for the period of this Bulletin Summary.*

Agency Code	Agency Name
AAA	Alma-ata, Kazakhstan
AAE	University of Addis Ababa, Ethiopia
AAM	University of Michigan, USA
ADE	Primary Industries and Resources SA, Australia
ADH	Observatorio Afonso Chaves, Portugal
AEIC	Alaska Earthquake Information Center, USA
AFAD	**Disaster and Emergency Management Presidency, Turkey**
AFAR	The Afar Depression: Interpretation of the 1960-2000 Earthquakes, Israel
AFUA	University of Alabama, USA
ALG	Algiers University, Algeria
ANDRE	USSR
ANF	USArray Array Network Facility, USA
ANT	Antofagasta, Chile
ARE	Instituto Geofisico del Peru, Peru
ARO	Observatoire Géophysique d'Arta, Djibouti
ASIES	**Institute of Earth Sciences, Academia Sinica, Chinese Taipei**
ASL	Albuquerque Seismological Laboratory, USA
ASM	University of Asmara, Eritrea
ASRS	**Altai-Sayan Seismological Centre, GS SB RAS, Russia**
ATA	The Earthquake Research Center Ataturk University, Turkey
ATH	**National Observatory of Athens, Greece**
AUST	**Geoscience Australia, Australia**
AVETI	USSR
AWI	**Alfred Wegener Institute for Polar and Marine Research, Germany**
AZER	**Republican Seismic Survey Center of Azerbaijan National Academy of Sciences, Azerbaijan**
BCIS	Bureau Central International de Sismologie, France
BDF	Observatório Sismológico da Universidade de Brasília, Brazil
BELR	**Centre of Geophysical Monitoring of the National Academy of Sciences of Belarus, Republic of Belarus**
BEO	**Republicki seizmoloski zavod, Serbia**
BER	**University of Bergen, Norway**
BERK	Berkheimer H, Germany
BGR	**Bundesanstalt für Geowissenschaften und Rohstoffe, Germany**
BGS	**British Geological Survey, United Kingdom**
BGSI	**Botswana Geoscience Institute, Botswana**

Table 10.1: *Continued.*

Agency Code	Agency Name
BHUJ2	Study of Aftershocks of the Bhuj Earthquake by Japanese Research Team, Japan
BIAK	Biak earthquake aftershocks (17-Feb-1996), USA
BJI	**China Earthquake Networks Center**, **China**
BKK	**Thai Meteorological Department**, **Thailand**
BNS	Erdbebenstation, Geologisches Institut der Universität, Köl, Germany
BOG	Universidad Javeriana, Colombia
BRA	**Geophysical Institute, Slovak Academy of Sciences**, **Slovakia**
BRG	**Seismological Observatory Berggießhübel, TU Bergakademie Freiberg**, **Germany**
BRK	Berkeley Seismological Laboratory, USA
BRS	Brisbane Seismograph Station, Australia
BUC	**National Institute for Earth Physics**, **Romania**
BUD	Geodetic and Geophysical Research Institute, Hungary
BUEE	Earth & Environment, USA
BUG	Institute of Geology, Mineralogy & Geophysics, Germany
BUL	**Goetz Observatory**, **Zimbabwe**
BUT	Montana Bureau of Mines and Geology, USA
BYKL	**Baykal Regional Seismological Centre, GS SB RAS**, **Russia**
CADCG	Central America Data Centre, Costa Rica
CAN	Australian National University, Australia
CANSK	Canadian and Scandinavian Networks, Sweden
CAR	Instituto Sismologico de Caracas, Venezuela
CASC	Central American Seismic Center, Costa Rica
CATAC	**Central American Tsunami Advisory Center**, **Nicaragua**
CENT	Centennial Earthquake Catalog, USA
CERI	Center for Earthquake Research and Information, USA
CFUSG	**Inst. of Seismology and Geodynamics, V.I. Vernadsky Crimean Federal University**, **Republic of Crimea**
CLL	**Geophysikalisches Observatorium Collm**, **Germany**
CMWS	Laboratory of Seismic Monitoring of Caucasus Mineral Water Region, GSRAS, Russia
CNG	Seismographic Station Changalane, Mozambique
CNRM	**Centre National de Recherche**, **Morocco**
COSMOS	Consortium of Organizations for Strong Motion Observations, USA
CRAAG	**Centre de Recherche en Astronomie, Astrophysique et Géophysique**, **Algeria**
CSC	University of South Carolina, USA
CSEM	Centre Sismologique Euro-Méditerranéen (CSEM/EMSC), France
CUPWA	**Curtin University**, **Australia**
DASA	Defense Atomic Support Agency, USA
DBN	Koninklijk Nederlands Meteorologisch Instituut, Netherlands
DDA	General Directorate of Disaster Affairs, Turkey
DHMR	Yemen National Seismological Center, Yemen
DIAS	**Dublin Institute for Advanced Studies**, **Ireland**
DJA	**Badan Meteorologi, Klimatologi dan Geofisika**, **Indonesia**
DMN	**National Seismological Centre, Nepal**, **Nepal**
DNAG	USA
DNK	**Geological Survey of Denmark and Greenland**, **Denmark**

Table 10.1: *Continued.*

Agency Code	Agency Name
DRS	Dagestan Branch, Geophysical Survey, Russian Academy of Sciences, Russia
DSN	**Dubai Seismic Network, United Arab Emirates**
DUSS	Damascus University, Syria, Syria
EAF	East African Network, Unknown
EAGLE	Ethiopia-Afar Geoscientific Lithospheric Experiment, Unknown
EBR	Observatori de l'Ebre, Spain
EBSE	Ethiopian Broadband Seismic Experiment, Unknown
ECGS	European Center for Geodynamics and Seismology, Luxembourg
ECX	**Centro de Investigación Científica y de Educación Superior de Ensenada, Mexico**
EFATE	OBS Experiment near Efate, Vanuatu, USA
EHB	Engdahl, van der Hilst and Buland, USA
EIDC	Experimental (GSETT3) International Data Center, USA
EKA	Eskdalemuir Array Station, United Kingdom
ENT	Geological Survey and Mines Department, Uganda
EPSI	Reference events computed by the ISC for EPSI project, United Kingdom
ERDA	Energy Research and Development Administration, USA
EST	Geological Survey of Estonia, Estonia
EUROP	Unknown
EVBIB	Data from publications listed in the ISC Event Bibliography, Unknown
FBR	Fabra Observatory, Spain
FCIAR	**Federal Center for Integrated Arctic Research, Russia**
FDF	Fort de France, Martinique
FIA0	Finessa Array, Finland
FOR	Unknown Historical Agency, Unknown - historical agency
FUBES	Earth Science Dept., Geophysics Section, Germany
FUNV	**Fundación Venezolana de Investigaciones Sismológicas, Venezuela**
FUR	Geophysikalisches Observatorium der Universität München, Germany
GBZT	Marmara Research Center, Turkey
GCG	**INSIVUMEH, Guatemala**
GCMT	**The Global CMT Project, USA**
GDNRW	Geologischer Dienst Nordrhein-Westfalen, Germany
GEN	**Dipartimento per lo Studio del Territorio e delle sue Risorse (RSNI), Italy**
GEOAZ	UMR Géoazur, France
GEOMR	GEOMAR, Germany
GFZ	**Helmholtz Centre Potsdam GFZ German Research Centre For Geosciences, Germany**
GII	**The Geophysical Institute of Israel, Israel**
GOM	Observatoire Volcanologique de Goma, Democratic Republic of the Congo
GRAL	**National Council for Scientific Research, Lebanon**
GSDM	Geological Survey Department Malawi, Malawi
GSET2	Group of Scientific Experts Second Technical Test 1991, April 22 - June 2, Unknown
GTFE	German Task Force for Earthquakes, Germany
GUC	**Centro Sismológico Nacional, Universidad de Chile, Chile**

Table 10.1: *Continued.*

Agency Code	Agency Name
HAN	Hannover, Germany
HDC	Observatorio Vulcanológico y Sismológico de Costa Rica, Costa Rica
HEL	**Institute of Seismology, University of Helsinki**, **Finland**
HFS	Hagfors Observatory, Sweden
HFS1	Hagfors Observatory, Sweden
HFS2	Hagfors Observatory, Sweden
HIMNT	Himalayan Nepal Tibet Experiment, USA
HKC	**Hong Kong Observatory**, **Hong Kong**
HLUG	Hessisches Landesamt für Umwelt und Geologie, Germany
HLW	**National Research Institute of Astronomy and Geophysics**, **Egypt**
HNR	Ministry of Mines, Energy and Rural Electrification, Solomon Islands
HON	Pacific Tsunami Warning Center - NOAA, USA
HRVD	Harvard University, USA
HRVD_LR	Department of Geological Sciences, Harvard University, USA
HVO	Hawaiian Volcano Observatory, USA
HYB	**National Geophysical Research Institute**, **India**
HYD	National Geophysical Research Institute, India
IAG	Instituto Andaluz de Geofisica, Spain
IASBS	Institute for Advanced Studies in Basic Sciences, Iran
IASPEI	IASPEI Working Group on Reference Events, USA
ICE	Instituto Costarricense de Electricidad, Costa Rica
IDC	**International Data Centre, CTBTO**, **Austria**
IDG	Institute of Dynamics of Geosphere, Russian Academy of Sciences, Russia
IEC	Institute of the Earth Crust, SB RAS, Russia
IEPN	Institute of Environmental Problems of the North, Russian Academy of Sciences, Russia
IFREE	Institute For Research on Earth Evolution, Japan
IGGSL	Seismology Lab, Institute of Geology & Geophysics, Chinese Academy of Sciences, China
IGIL	**Instituto Dom Luiz, University of Lisbon**, **Portugal**
IGKR	Institute of Geology,Komi Science Centre,Ural Branch,Russian Academy of Sciences, Russia
IGQ	**Servicio Nacional de Sismología y Vulcanología**, **Ecuador**
IGS	Institute of Geological Sciences, United Kingdom
INAM	Instituto Nacional de Meteorologia e Geofisica - INAMET, Angola
INDEPTH3	International Deep Profiling of Tibet and the Himalayas, USA
INET	Instituto Nicaraguense de Estudios Territoriales - INETER, Nicaragua
INMG	**Instituto Português do Mar e da Atmosfera, I.P.**, **Portugal**
INMGC	Instituto Nacional de Meteorologia e Geofísica, Cape Verde
IPEC	**The Institute of Physics of the Earth (IPEC)**, **Czech Republic**
IPER	Institute of Physics of the Earth, Academy of Sciences, Moscow, Russia
IPGP	**Institut de Physique du Globe de Paris**, **France**
IPRG	Institute for Petroleum Research and Geophysics, Israel
IRIS	**IRIS Data Management Center**, **USA**
IRSM	Institute of Rock Structure and Mechanics, Czech Republic
ISC	**International Seismological Centre**, **United Kingdom**

***Table 10.1:** Continued.*

Agency Code	Agency Name
ISC-PPSM	**International Seismological Centre Probabilistic Point Source Model**, **United Kingdom**
ISK	**Kandilli Observatory and Earthquake Research Institute**, **Turkey**
ISN	**Iraqi Meteorological and Seismology Organisation**, **Iraq**
ISS	International Seismological Summary, United Kingdom
IST	Institute of Physics of the Earth, Technical University of Istanbul, Turkey
ISU	**Institute of Seismology, Academy of Sciences, Republic of Uzbekistan**, **Uzbekistan**
ITU	Faculty of Mines, Department of Geophysical Engineering, Turkey
JEN	Geodynamisches Observatorium Moxa, Germany
JMA	**Japan Meteorological Agency**, **Japan**
JOH	Bernard Price Institute of Geophysics, South Africa
JSN	**Jamaica Seismic Network**, **Jamaica**
JSO	**Jordan Seismological Observatory**, **Jordan**
KBC	Institut de Recherches Géologiques et Minières, Cameroon
KEA	**Korea Earthquake Administration**, **Democratic People's Republic of Korea**
KEW	Kew Observatory, United Kingdom
KHC	Institute of Geophysics, Czech Academy of Sciences, Czech Republic
KISR	Kuwait Institute for Scientific Research, Kuwait
KLM	Malaysian Meteorological Service, Malaysia
KMA	**Korea Meteorological Administration**, **Republic of Korea**
KNET	**Kyrgyz Seismic Network**, **Kyrgyzstan**
KOLA	**Kola Regional Seismic Centre, GS RAS**, **Russia**
KRAR	Krasnoyarsk Scientific Research Inst. of Geology and Mineral Resources, Russia, Russia
KRL	Geodätisches Institut der Universität Karlsruhe, Germany
KRNET	**Institute of Seismology, Academy of Sciences of Kyrgyz Republic**, **Kyrgyzstan**
KRSC	**Kamchatka Branch of the Geophyiscal Survey of the RAS**, **Russia**
KRSZO	**Geodetic and Geophysical Reasearch Institute, Hungarian Academy of Sciences**, **Hungary**
KSA	Observatoire de Ksara, Lebanon
KUK	Geological Survey Department of Ghana, Ghana
LAO	Large Aperture Seismic Array, USA
LDG	**Laboratoire de Détection et de Géophysique/CEA**, **France**
LDN	University of Western Ontario, Canada
LDO	Lamont-Doherty Earth Observatory, USA
LED	Landeserdbebendienst Baden-Württemberg, Germany
LEDBW	Landeserdbebendienst Baden-Württemberg, Germany
LER	Besucherbergwerk Binweide Station, Germany
LIB	Tripoli, Libya
LIC	Station Géophysique de Lamto, Ivory Coast
LIM	Lima, Peru
LIS	Instituto de Meteorologia, Portugal
LIT	**Geological Survey of Lithuania**, **Lithuania**
LJU	**Slovenian Environment Agency**, **Slovenia**

Table 10.1: Continued.

Agency Code	Agency Name
LPA	**Universidad Nacional de La Plata, Argentina**
LPZ	Observatorio San Calixto, Bolivia
LRSM	Long Range Seismic Measurements Project, Unknown
LSZ	Geological Survey Department of Zambia, Zambia
LVSN	**Latvian Seismic Network, Latvia**
MAN	**Philippine Institute of Volcanology and Seismology, Philippines**
MAT	The Matsushiro Seismological Observatory, Japan
MATSS	USSR
MCO	**Macao Meteorological and Geophysical Bureau, Macao, China**
MCSM	**Main Centre for Special Monitoring, Ukraine**
MDD	**Instituto Geográfico Nacional, Spain**
MED_RCMT	**MedNet Regional Centroid - Moment Tensors, Italy**
MERI	Maharashta Engineering Research Institute, India
MES	Messina Seismological Observatory, Italy
MEX	**Instituto de Geofísica de la UNAM, Mexico**
MIRAS	**Mining Institute of the Ural Branch of the Russian Academy of Sciences, Russia**
MNH	Institut für Angewandte Geophysik der Universitat Munchen, Germany
MOLD	Institute of Geophysics and Geology, Moldova
MOS	**Geophysical Survey of Russian Academy of Sciences, Russia**
MOZ	Direccao Nacional de Geologia, Mozambique
MOZAR	Mozambique
MRB	**Institut Cartogràfic i Geològic de Catalunya, Spain**
MSI	Messina Seismological Observatory, Italy
MSSP	Micro Seismic Studies Programme, PINSTECH, Pakistan
MSUGS	Michigan State University, Department of Geological Sciences, USA
MUN	Mundaring Observatory, Australia
NAI	University of Nairobi, Kenya
NAM	**The Geological Survey of Namibia, Namibia**
NAO	**Stiftelsen NORSAR, Norway**
NCEDC	Northern California Earthquake Data Center, USA
NDI	**National Centre for Seismology of the Ministry of Earth Sciences of India, India**
NEIC	**National Earthquake Information Center, USA**
NEIS	National Earthquake Information Service, USA
NERS	**North Eastern Regional Seismological Centre, Magadan, GS RAS, Russia**
NIC	**Cyprus Geological Survey Department, Cyprus**
NIED	**National Research Institute for Earth Science and Disaster Resilience, Japan**
NKSZ	USSR
NNC	**National Nuclear Center, Kazakhstan**
NORS	North Ossetia (Alania) Branch, Geophysical Survey, Russian Academy of Sciences, Russia
NOU	**IRD Centre de Nouméa, New Caledonia**
NSSC	National Syrian Seismological Center, Syria
NSSP	**National Survey of Seismic Protection, Armenia**
OBM	Institute of Astronomy and Geophysics, Mongolian Academy of Sciences, Mongolia

Table 10.1: *Continued.*

Agency Code	Agency Name
OGAUC	Centro de Investigação da Terra e do Espaço da Universidade de Coimbra, Portugal
OGSO	Ohio Geological Survey, USA
OMAN	**Sultan Qaboos University**, **Oman**
ORF	Orfeus Data Center, Netherlands
OSPL	**Observatorio Sismologico Politecnico Loyola**, **Dominican Republic**
OSUB	Osservatorio Sismologico Universita di Bari, Italy
OSUNB	**Observatory Seismological of the University of Brasilia**, **Brazil**
OTT	**Canadian Hazards Information Service, Natural Resources Canada**, **Canada**
PAL	Palisades, USA
PAS	California Institute of Technology, USA
PDA	Universidade dos Açores, Portugal
PDG	**Institute of Hydrometeorology and Seismology of Montenegro**, **Montenegro**
PEK	Peking, China
PGC	Pacific Geoscience Centre, Canada
PJWWP	**Private Observatory of Pawel Jacek Wiejacz, D.Sc.**, **Poland**
PLV	**Institute of Geophysics, Viet Nam Academy of Science and Technology**, **Viet Nam**
PMEL	Pacific seismicity from hydrophones, USA
PMR	Alaska Tsunami Warning Center,, USA
PNNL	Pacific Northwest National Laboratory, USA
PNSN	**Pacific Northwest Seismic Network**, **USA**
PPT	**Laboratoire de Géophysique/CEA**, **French Polynesia**
PRE	**Council for Geoscience**, **South Africa**
PRU	**Institute of Geophysics, Czech Academy of Sciences**, **Czech Republic**
PTO	Instituto Geofísico da Universidade do Porto, Portugal
PTWC	**Pacific Tsunami Warning Center**, **USA**
QCP	**Manila Observatory**, **Philippines**
QUE	Pakistan Meteorological Department, Pakistan
QUI	Escuela Politécnica Nacional, Ecuador
RAB	Rabaul Volcanological Observatory, Papua New Guinea
RBA	Université Mohammed V, Morocco
REN	MacKay School of Mines, USA
REY	**Icelandic Meteorological Office**, **Iceland**
RHSSO	**Republic Hydrometeorological Service, Seismological Observatory, Banja Luka**, **Bosnia and Herzegovina**
RISSC	**Laboratory of Research on Experimental and Computational Seimology**, **Italy**
RMIT	Royal Melbourne Institute of Technology, Australia
ROC	Odenbach Seismic Observatory, USA
ROM	**Istituto Nazionale di Geofisica e Vulcanologia**, **Italy**
RRLJ	Regional Research Laboratory Jorhat, India
RSMAC	Red Sísmica Mexicana de Apertura Continental, Mexico
RSNC	**Red Sismológica Nacional de Colombia**, **Colombia**
RSPR	**Red Sísmica de Puerto Rico**, **USA**

Table 10.1: Continued.

Agency Code	Agency Name
RYD	King Saud University, Saudi Arabia
SAPSE	Southern Alps Passive Seismic Experiment, New Zealand
SAR	Sarajevo Seismological Station, Bosnia and Herzegovina
SARA	**SARA Electronic Instrument s.r.l., Italy**
SBDV	USSR
SCB	**Observatorio San Calixto, Bolivia**
SCEDC	Southern California Earthquake Data Center, USA
SCSIO	Key Laboratory of Ocean and Marginal Sea Geology, South China Sea, China
SDD	**Universidad Autonoma de Santo Domingo, Dominican Republic**
SEA	Geophysics Program AK-50, USA
SET	Setif Observatory, Algeria
SFS	**Real Instituto y Observatorio de la Armada, Spain**
SGS	**Saudi Geological Survey, Saudi Arabia**
SHL	Central Seismological Observatory, India
SIGU	**Subbotin Institute of Geophysics, National Academy of Sciences, Ukraine**
SIK	Seismic Institute of Kosovo, Unknown
SIO	Scripps Institution of Oceanography, USA
SJA	**Instituto Nacional de Prevención Sísmica, Argentina**
SJS	Instituto Costarricense de Electricidad, Costa Rica
SKHL	**Sakhalin Experimental and Methodological Seismological Expedition, GS RAS, Russia**
SKL	Sakhalin Complex Scientific Research Institute, Russia
SKO	**Seismological Observatory Skopje, North Macedonia**
SLC	Salt Lake City, USA
SLM	Saint Louis University, USA
SNET	**Servicio Nacional de Estudios Territoriales, El Salvador**
SNM	New Mexico Institute of Mining and Technology, USA
SNSN	Saudi National Seismic Network, Saudi Arabia
SOF	**National Institute of Geophysics, Geology and Geography, Bulgaria**
SOMC	Seismological Observatory of Mount Cameroon, Cameroon
SOME	**Seismological Experimental Methodological Expedition, Kazakhstan**
SPA	USGS - South Pole, Antarctica
SPGM	Service de Physique du Globe, Morocco
SPITAK	Armenia
SRI	Stanford Research Institute, USA
SSN	Sudan Seismic Network, Sudan
SSNC	**Servicio Sismológico Nacional Cubano, Cuba**
SSS	Centro de Estudios y Investigaciones Geotecnicas del San Salvador, El Salvador
STK	Stockholm Seismological Station, Sweden
STR	**EOST / RéNaSS, France**
STU	Stuttgart Seismological Station, Germany
SVSA	**Sistema de Vigilância Sismológica dos Açores, Portugal**
SYO	**National Institute of Polar Research, Japan**

Table 10.1: Continued.

Agency Code	Agency Name
SZGRF	Seismologisches Zentralobservatorium Gräfenberg, Germany
TAC	Estación Central de Tacubaya, Mexico
TAN	**Antananarivo, Madagascar**
TANZANIA	Tanzania Broadband Seismic Experiment, USA
TAP	**Central Weather Bureau (CWB), Chinese Taipei**
TAU	University of Tasmania, Australia
TEH	**Tehran University, Iran**
TEIC	Center for Earthquake Research and Information, USA
THE	**Department of Geophysics, Aristotle University of Thessaloniki, Greece**
THR	**International Institute of Earthquake Engineering and Seismology (IIEES), Iran**
TIF	**Institute of Earth Sciences/ National Seismic Monitoring Center, Georgia**
TIR	**Institute of Geosciences, Polytechnic University of Tirana, Albania**
TRI	**Istituto Nazionale di Oceanografia e di Geofisica Sperimentale (OGS), Italy**
TRN	**The Seismic Research Centre, Trinidad and Tobago**
TTG	Titograd Seismological Station, Montenegro
TUL	Oklahoma Geological Survey, USA
TUN	**Institut National de la Météorologie, Tunisia**
TVA	Tennessee Valley Authority, USA
TXNET	**Texas Seismological Network, University of Texas at Austin, USA**
TZN	University of Dar Es Salaam, Tanzania
UAF	Department of Geosciences, USA
UATDG	The University of Arizona, Department of Geosciences, USA
UAV	Red Sismológica de Los Andes Venezolanos, Venezuela
UCB	University of Colorado, Boulder, USA
UCC	**Royal Observatory of Belgium, Belgium**
UCDES	Department of Earth Sciences, United Kingdom
UCR	**Sección de Sismología, Vulcanología y Exploración Geofísica, Costa Rica**
UCSC	Earth & Planetary Sciences, USA
UESG	School of Geosciences, United Kingdom
UGN	Institute of Geonics AS CR, Czech Republic
ULE	University of Leeds, United Kingdom
UNAH	Universidad Nacional Autonoma de Honduras, Honduras
UPA	**Universidad de Panama, Panama**
UPIES	Institute of Earth- and Environmental Science, Germany
UPP	**University of Uppsala, Sweden**
UPSL	**University of Patras, Department of Geology, Greece**
UREES	Department of Earth and Environmental Science, USA
USAEC	United States Atomic Energy Commission, USA
USCGS	United States Coast and Geodetic Survey, USA
USGS	United States Geological Survey, USA
UTEP	Department of Geological Sciences, USA
UUSS	The University of Utah Seismograph Stations, USA

Table 10.1: Continued.

Agency Code	Agency Name
UVC	Universidad del Valle, Colombia
UWMDG	University of Wisconsin-Madison, Department of Geoscience, USA
VAO	**Instituto Astronomico e Geofísico, Brazil**
VIE	**Zentralanstalt für Meteorologie und Geodynamik (ZAMG), Austria**
VKMS	Lab. of Seismic Monitoring, Voronezh region, GSRAS & Voronezh State University, Russia
VLA	Vladivostok Seismological Station, Russia
VSI	University of Athens, Greece
VUW	Victoria University of Wellington, New Zealand
WAR	**Institute of Geophysics, Polish Academy of Sciences, Poland**
WASN	USA
WBNET	**Institute of Geophysics, Czech Academy of Sciences, Czech Republic**
WEL	**Institute of Geological and Nuclear Sciences, New Zealand**
WES	Weston Observatory, USA
WUSTL	Washington University Earth and Planentary Sciences, USA
YARS	**Yakutiya Regional Seismological Center, GS SB RAS, Russia**
ZAG	**Seismological Survey of the Republic of Croatia, Croatia**
ZEMSU	USSR
ZUR	**Swiss Seismological Service (SED), Switzerland**
ZUR_RMT	Zurich Moment Tensors, Switzerland

Table 10.2: *Phases reported to the ISC. These include phases that could not be matched to an appropriate* ak135 *phases. Those agencies that reported at least 10% of a particular phase are also shown.*

Reported Phase	Total	Agencies reporting
P	3929972	
S	1955514	TAP (17%), JMA (14%)
AML	1044712	ROM (46%), WEL (19%), ISK (11%)
NULL	713975	NEIC (35%), IDC (24%), AEIC (19%)
IAML	692828	NEIC (52%), AFAD (21%)
IAmb	463933	NEIC (97%)
Pg	331317	ISK (31%), STR (12%)
Pn	291614	NEIC (37%), ISK (23%)
Sg	252681	ISK (19%), STR (13%), ZAG (12%)
LR	108664	IDC (91%)
pmax	103157	MOS (68%), BJI (31%)
Sn	84883	IDC (12%), NEIC (12%)
IAMs_20	84181	NEIC (97%)
SG	68393	HEL (52%), PRU (26%), IPEC (11%)
PG	63876	HEL (54%), PRU (19%), IPEC (13%)
PKP	36343	IDC (39%), VIE (17%)
Lg	34145	NNC (63%), IDC (19%), KRSZO (13%)
smax	33348	HEL (81%), MOS (13%)
L	32892	BJI (96%)
PN	28711	MOS (36%), HEL (32%), IPEC (12%)
T	27410	IDC (98%)
IVmb_Lg	27331	MDD (100%)
SN	21210	HEL (73%), OTT (13%)
IAmb_Lg	19234	NEIC (100%)
pP	18379	BJI (26%), ISC1 (16%), IDC (11%), VIE (11%)
PKPbc	14725	IDC (65%), NEIC (12%)
MLR	13218	MOS (100%)
PcP	13186	IDC (58%), ISC1 (11%)
PKIKP	12598	MOS (97%)
PP	11703	IDC (19%), BJI (18%), BELR (17%)
SB	11607	HEL (100%)
A	10116	JMA (50%), SKHL (50%)
PB	9457	HEL (100%)
PKPdf	9101	NEIC (47%), AWI (13%), INMG (12%)
SS	8573	MOS (34%), BELR (25%), BJI (18%)
x	8550	NDI (34%), BRG (24%), TRN (14%), CLL (14%)
SPECP	6352	AFAD (100%)
sP	5814	BJI (64%), ISC1 (16%)
MSG	5159	HEL (100%)
Trac	5117	OTT (100%)
PKPab	4967	IDC (50%), INMG (13%)
AMS	4720	PRU (68%), CLL (28%)
PKiKP	4251	VIE (37%), IDC (32%)
PPP	3749	MOS (50%), BELR (44%)
ScP	3708	IDC (73%)
SSS	3248	BELR (56%), MOS (34%)
Amp	3171	BRG (100%)
LRM	2779	BELR (100%)
AMB	2646	SKHL (98%)
*PP	2366	MOS (100%)
LG	2331	BRA (75%), OTT (25%)
PKKPbc	2258	IDC (87%), AWI (12%)
LQ	2107	BELR (67%), PPT (21%)
IVmb_VC	2027	MDD (100%)
PKP2	1967	MOS (99%)
Sb	1727	IRIS (78%), NAO (12%)
Pdiff	1717	VIE (30%), IDC (24%), BGR (14%), AWI (13%)
PKhKP	1701	IDC (100%)
I	1610	IDC (100%)
sS	1488	BJI (68%), BELR (21%)
pPKP	1440	VIE (40%), IDC (22%), BJI (17%)
Smax	1415	BYKL (100%)
Pmax	1278	BYKL (93%)
SKS	1229	BELR (38%), BJI (32%), PRU (12%), VIE (11%)
SKPbc	1093	IDC (85%)
SKSac	1017	BER (40%), AWI (26%), HYB (13%)
Pb	840	IRIS (58%), NAO (25%)
IVmB_BB	839	BER (79%), SSNC (15%)
PS	832	MOS (40%), BELR (25%), CLL (16%)
IVMs_BB	819	BER (78%)

Table 10.2: (continued)

Reported Phase	Total	Agencies reporting
PKPPKP	776	IDC (94%)
ScS	767	BJI (56%), HYB (13%), BELR (11%)
Pdif	738	NEIC (23%), INMG (18%), UCC (12%)
SKP	674	IDC (35%), VIE (32%), BELR (13%)
PKKP	665	VIE (48%), IDC (33%)
END	638	ROM (96%)
PPMZ	561	BJI (100%)
PKHKP	540	MOS (100%)
tx	530	INMG (99%)
Sgmax	524	NERS (100%)
PKPDF	506	PRU (100%)
SP	478	BER (42%), MOS (17%)
PKPAB	421	PRU (100%)
*SP	420	MOS (100%)
max	403	BYKL (100%)
*SS	395	MOS (100%)
pPKiKP	377	VIE (63%), BELR (21%)
pPKPbc	375	IDC (68%), BGR (23%)
PDIFF	374	PRU (37%), BRA (32%), IPEC (27%)
X	343	JMA (71%), SYO (29%)
sPKP	316	BJI (65%), BELR (23%)
SKKS	310	BELR (51%), BJI (45%)
AmB	302	KEA (100%)
PKP2bc	254	IDC (100%)
PKKPab	235	IDC (86%), AWI (11%)
SKKPbc	234	IDC (94%)
SmS	231	BGR (55%), ZUR (45%)
Pgmax	227	NERS (100%)
AMP	226	BER (48%), UPA (44%)
p	224	ROM (54%), MAN (46%)
LV	223	CLL (100%)
LH	222	CLL (100%)
PmP	221	ZUR (50%), BGR (50%)
PPS	205	CLL (54%), LPA (20%), BELR (14%), MOS (12%)
SKPdf	178	BER (34%), CLL (23%), AWI (17%), INMG (14%)
SME	170	BJI (100%)
SMN	168	BJI (100%)
s	161	MAN (100%)
IAMLHF	154	BER (100%)
P3KPbc	153	IDC (100%)
SKKP	146	BELR (51%), VIE (29%), IDC (17%)
pPKPab	141	IDC (33%), CLL (29%), AWI (22%)
AMd	141	TIR (100%)
P'P'	141	VIE (95%)
SSSS	133	CLL (99%)
pPKPdf	132	AWI (34%), CLL (18%), BER (17%)
PKS	131	BELR (57%), BJI (35%)
PKPpre	129	NEIC (52%), PRU (36%), CLL (12%)
IVmB	126	BER (100%)
pPP	126	LPA (50%), CLL (25%), BGR (21%)
SKKSac	121	HYB (56%), CLL (36%)
Lm	116	CLL (100%)
PcS	112	BJI (90%)
pPdiff	112	VIE (75%), BGR (13%)
PKPf	111	BRG (100%)
PKPb	103	BRG (100%)
H	101	IDC (100%)
PCP	99	LPA (67%), MOS (16%), PRU (15%)
SKIKP	86	LPA (100%)
SKIKS	86	LPA (100%)
P4KPbc	85	IDC (100%)
PKIKS	85	LPA (100%)
sPKiKP	84	BELR (56%), VIE (31%)
LmH	75	CLL (100%)
Sdif	75	CLL (64%), BELR (27%)
sPP	72	CLL (64%), BGR (32%)
SCS	67	LPA (94%)
SKSdf	64	HYB (47%), BER (31%), AWI (12%)
LmV	62	CLL (100%)
PKP2ab	59	IDC (100%)
Px	51	CLL (100%)

Table 10.2: (continued)

Reported Phase	Total	Agencies reporting
PgPg	48	BYKL (100%)
Pif	44	BRG (100%)
SgSg	43	BYKL (98%)
Rg	43	IDC (53%), NDI (40%)
PSP	43	LPA (98%)
PKKPdf	42	AWI (76%), CLL (14%)
IAML_BB	41	THR (100%)
SKSa	41	BRG (100%)
(sP)	39	CLL (100%)
sSKS	39	BELR (95%)
sPKPdf	38	AWI (68%), CLL (32%)
SKPab	38	IDC (76%), AWI (16%)
pPcP	36	IDC (94%)
rx	35	INMG (60%), SKHL (40%)
m	35	SIGU (100%)
SKPa	33	NAO (94%)
PPPP	33	CLL (97%)
ATSG	32	OSPL (100%)
ASSG	32	OSPL (100%)
P'P'df	32	AWI (100%)
PKSdf	31	BER (71%), CLL (26%)
Sdiff	29	VIE (83%), LJU (14%)
PSKS	28	CLL (100%)
ASPG	26	OSPL (100%)
P3KP	25	IDC (100%)
ATPG	25	OSPL (100%)
PKP1	25	PPT (84%), LDG (16%)
SDIFF	24	LPA (79%), IPEC (17%)
E	24	YARS (79%), ZAG (12%)
PKKS	24	BELR (100%)
SKKPdf	24	AWI (75%), CLL (21%)
(Pg)	24	CLL (100%)
sSS	23	CLL (83%), BRG (17%)
R2	22	CLL (100%)
SPP	20	BELR (60%), CLL (25%), MOS (15%)
SKiKP	19	IDC (74%), LJU (11%)
Sif	18	BRG (100%)
r	18	BRG (100%)
Plp	17	CLL (100%)
PPlp	17	CLL (100%)
AP	17	MOS (100%)
R	17	AWI (94%)
PKPmax	16	CLL (100%)
Pg_3	16	ATH (100%)
PKPPKPdf	15	CLL (100%)
Lmax	15	CLL (100%)
sPKPab	15	INMG (53%), AWI (27%), HYB (13%)
pS	15	SVSA (73%), CLL (20%)
(SS)	15	CLL (100%)
(PP)	14	CLL (100%)
sPdif	14	CLL (50%), BELR (36%)
pPdif	14	CLL (57%), BELR (43%)
pScP	12	IDC (100%)
sSdif	12	CLL (83%), BELR (17%)
P*	12	BGR (58%), MOS (25%), BJI (17%)
PKPBC	12	PRU (100%)
SKKSdf	12	CLL (75%), HYB (25%)
SDIF	11	PRU (100%)
sPKPbc	10	AWI (60%), CLL (30%)
IVMs	10	BER (100%)
P'P'bc	10	AWI (100%)
(PKiKP)	9	CLL (100%)
SKPPKPdf	9	CLL (100%)
PKPlp	9	CLL (100%)
pPKPf	9	BRG (100%)
MSN	9	HEL (100%)
(PKPdf)	9	CLL (100%)
PnA	9	THR (100%)
R3	8	CLL (100%)
(Sg)	8	CLL (100%)
SCP	8	IPEC (100%)

Table 10.2: (continued)

Reported Phase	Total	Agencies reporting
(SSS)	8	CLL (100%)
SA	8	SJA (50%), DNK (25%), BER (25%)
PKPdif	8	CLL (62%), NEIC (38%)
pPif	8	BRG (100%)
(PKPab)	7	CLL (100%)
sSSS	7	CLL (100%)
PSPS	7	CLL (100%)
(pP)	7	CLL (100%)
sPPP	7	CLL (100%)
(SSSS)	7	CLL (100%)
PSS	6	CLL (83%), BRG (17%)
(PPS)	6	CLL (100%)
sPPS	6	CLL (100%)
(PKPbc)	6	CLL (100%)
SKSP	6	CLL (83%), BRG (17%)
PCS	5	LPA (100%)
P4KP	5	IDC (100%)
(sPP)	5	CLL (100%)
IVmBBB	5	HYB (80%), NDI (20%)
PKSbc	5	CLL (100%)
Pn_2	5	ATH (100%)
(pPKPab)	5	CLL (100%)
SKKSa	4	BRG (100%)
P(2)	4	CLL (100%)
Pn_0	4	ATH (100%)
Sx	4	CLL (100%)
(PcP)	4	CLL (100%)
sPif	4	BRG (100%)
SKPf	4	BRG (100%)
Pdifflp	4	CLL (100%)
XS	4	PRU (100%)
SKSSKSac	4	CLL (100%)
(SKPdf)	4	CLL (100%)
SSmax	4	CLL (100%)
(pPKiKP)	4	CLL (100%)
Sglp	4	CLL (100%)
SKSp	4	BRA (75%), WAR (25%)
(Sn)	4	CLL (100%)
IAMLA	4	BER (50%), DNK (50%)
pPDIFF	4	IPEC (100%)
pPKKPbc	4	CLL (100%)
sSSSS	4	CLL (100%)
pPS	3	CLL (100%)
sPKKPbc	3	CLL (100%)
sPKSdf	3	CLL (100%)
PSSrev	3	CLL (100%)
Pg_4	3	ATH (100%)
Pg_1	3	ATH (100%)
RG	3	HEL (67%), IPEC (33%)
x2	3	ISC1 (100%)
PX	3	IGIL (100%)
S*	3	BGR (67%), BJI (33%)
PPmax	3	CLL (100%)
SH	3	SYO (100%)
(Sdif)	3	CLL (100%)
sSKSac	3	CLL (100%)
sPn	2	HYB (50%), BJI (50%)
sPS	2	CLL (100%)
pSP	2	CLL (100%)
(Pn)	2	CLL (100%)
Sg_0	2	ATH (100%)
Pn_3	2	ATH (100%)
Pn_1	2	ATH (100%)
sPKPf	2	BRG (100%)
P4	2	UPA (100%)
sSKKSac	2	CLL (100%)
PKPPKPbc	2	CLL (100%)
sPSPS	2	CLL (100%)
Sg_3	2	ATH (100%)
PP(2)	2	LPA (50%), CLL (50%)
SSSmax	2	CLL (100%)

Table 10.2: (continued)

Reported Phase	Total	Agencies reporting
(pPKPdf)	2	CLL (100%)
SKKPf	2	BRG (100%)
sSKPbc	2	CLL (100%)
PPPPrev	2	CLL (100%)
Pg_0	2	ATH (100%)
(sPPP)	2	CLL (100%)
(sS)	2	CLL (100%)
sPdiff	2	AWI (100%)
(Pdif)	2	CLL (100%)
pPPP	2	CLL (100%)
BAZ	2	BER (100%)
M	2	LJU (100%)
sPSKS	2	CLL (100%)
sSif	2	BRG (100%)
(pSKPbc)	1	CLL (100%)
(pPKPbc)	1	CLL (100%)
PDIF	1	PRU (100%)
PKPcb	1	BGR (100%)
pPPPrev	1	CLL (100%)
pPPPP	1	CLL (100%)
pPn	1	INMG (100%)
PKPdff	1	INMG (100%)
pPSKS	1	CLL (100%)
sSKKPbc	1	CLL (100%)
(SKKSac)	1	CLL (100%)
SPk	1	CLL (100%)
(P)	1	PJWWP (100%)
(PKPdif)	1	CLL (100%)
pSKKPdf	1	CLL (100%)
PKPPP	1	BRG (100%)
SSPrev	1	CLL (100%)
sPKPPKPd	1	CLL (100%)
(pPdif)	1	CLL (100%)
sPPS(2)	1	CLL (100%)
PKPdfc	1	PJWWP (100%)
PKPdfd	1	PJWWP (100%)
PPPrev	1	CLL (100%)
sPSS	1	CLL (100%)
PnPn	1	INMG (100%)
(PPP)	1	CLL (100%)
sPKKPdf	1	CLL (100%)
PSPSrev	1	CLL (100%)
pSKKPbc	1	CLL (100%)
pSKPbc	1	CLL (100%)
sPKSbc	1	CLL (100%)
Pdifmax	1	CLL (100%)
g	1	BER (100%)
LQ5	1	CLL (100%)
Sk	1	CLL (100%)
PKPbcmax	1	CLL (100%)
PKiKP(2)	1	CLL (100%)
PKKPb	1	BRG (100%)
LQ3	1	CLL (100%)
pPKKPdf	1	CLL (100%)
pSKS	1	HYB (100%)
(PKSdf)	1	CLL (100%)
Sg_2	1	ATH (100%)
sPP(2)	1	CLL (100%)
SSS(2)	1	LPA (100%)
PgA	1	THR (100%)
PKKPbc2	1	CLL (100%)
pPSKSrev	1	CLL (100%)
(PS)	1	CLL (100%)
(sPSPS)	1	CLL (100%)
(sSKSac)	1	CLL (100%)
pPKKPab	1	CLL (100%)
SKSmax	1	CLL (100%)
Lq	1	NNC (100%)
pp	1	NDI (100%)
3PKPbc	1	CLL (100%)
(PKSbc)	1	CLL (100%)

Table 10.2: *(continued)*

Reported Phase	Total	Agencies reporting
(pSKSdf)	1	CLL (100%)
SR	1	NDI (100%)
(SP)	1	CLL (100%)
PKKSbc	1	HYB (100%)
pPPS	1	CLL (100%)
iPKPab	1	INMG (100%)
SKKSacre	1	CLL (100%)
pPdiff2	1	CLL (100%)
Pf	1	BELR (100%)
(S)	1	PJWWP (100%)
(SKPab)	1	CLL (100%)
(PSPS)	1	CLL (100%)
(PPPP)	1	CLL (100%)
pPP(2)	1	CLL (100%)
sSKPab	1	CLL (100%)
AMSG	1	GUC (100%)
(SKSP)	1	CLL (100%)
pwP	1	ISC1 (100%)
LQ2	1	CLL (100%)
(SKSac)	1	CLL (100%)
(SKKPdf)	1	CLL (100%)
PKKPdf2	1	CLL (100%)
EN	1	INMG (100%)
pPKi	1	HYB (100%)
IAmb4	1	DNK (100%)
(PKSab)	1	CLL (100%)
AMPG	1	PLV (100%)
sPdiff2	1	CLL (100%)
sSdiff2	1	CLL (100%)
pPKSdf	1	CLL (100%)
SKKPb	1	BRG (100%)
PSKSrev	1	CLL (100%)
LQ4	1	CLL (100%)
AMb	1	LVSN (100%)
P5KP	1	IDC (100%)
Sm	1	CFUSG (100%)
0SPNP	1	MOS (100%)
sSP	1	BRG (100%)
IVMsBB	1	DNK (100%)
SSS(S)	1	LPA (100%)
PKKPf	1	BRG (100%)
PKPpB	1	WAR (100%)
SKPbcmax	1	CLL (100%)
PKKSdf	1	CLL (100%)
pP1	1	BER (100%)
S4	1	UPA (100%)
pSKSdf	1	CLL (100%)
sPS(2)	1	CLL (100%)
(PSKS)	1	CLL (100%)
PPSmax	1	CLL (100%)

Table 10.3: *Reporters of amplitude data*

Agency	Number of reported amplitudes	Number of amplitudes in ISC located events	Number used for ISC mb	Number used for ISC MS
NEIC	906472	290483	191753	39084
IDC	505509	483226	119561	74636
ROM	479829	14703	0	0
WEL	243894	32065	0	0
AUST	162417	18621	10714	0
AFAD	144579	18461	0	0
ISK	131448	27641	0	0
GFZ	123168	115475	59822	0
MOS	91324	87243	41281	9460
ATH	76148	12101	0	0
NNC	73142	24783	58	0
THE	69950	20266	0	0
BJI	69647	67748	20098	22654
VIE	68552	32380	11202	0
DJA	59710	45776	8822	0
SOME	53748	17813	3412	0
WBNET	45020	0	0	0
INMG	40146	15940	3370	0
TXNET	38407	395	0	0
GUC	36353	9196	0	0
RSNC	33973	14817	2086	0
HEL	32298	1786	0	0
MDD	29383	5242	0	0
SVSA	18151	1218	504	0
SJA	16516	15603	0	0
ZUR	15978	1110	0	0
MAN	14735	3400	0	0
SSNC	14567	1890	92	0
PRE	14541	541	0	0
LDG	14248	2137	0	0
MCSM	13682	13468	6140	0
SDD	13561	4638	0	0
PRU	12792	4622	136	2484
AWI	12750	8251	3162	0
MRB	11016	558	0	0
BER	10436	5287	2054	419
JMA	10076	9921	0	0
NDI	9206	7465	2201	162
BUC	8079	2110	0	0
DNK	7707	4714	3744	21
SKHL	7622	3378	0	0
BELR	7086	3594	622	773
LJU	6805	1030	2	1
PPT	6713	5614	480	0
OSPL	6367	2502	0	0
JSO	6292	4820	268	0

Table 10.3: *Continued.*

Agency	Number of reported amplitudes	Number of amplitudes in ISC located events	Number used for ISC mb	Number used for ISC MS
BGR	5771	5368	3815	0
KRSZO	5202	1253	27	0
OTT	5116	337	0	0
NOU	4880	4772	2720	0
PDG	4541	2771	0	0
BGS	4315	2536	1856	400
ECX	4223	315	0	0
NIC	3899	1544	0	0
CLL	3679	3164	305	912
IPEC	3201	626	0	0
BRG	3171	1133	0	0
YARS	3171	160	2	0
BYKL	3072	1808	0	0
KNET	2963	1153	0	0
BKK	2770	1500	10	0
TIR	2560	816	6	7
UCC	2518	2348	1971	0
NAO	1875	1845	1332	0
SKO	1550	358	0	0
CFUSG	1376	1223	0	0
ASRS	1281	618	0	0
SCB	1263	192	0	0
KEA	1261	592	0	103
LVSN	1215	216	0	0
IGIL	1062	538	124	166
THR	999	949	0	0
BGSI	891	338	0	0
NERS	769	356	0	0
DMN	631	539	0	0
UPA	600	37	0	0
MIRAS	579	77	0	0
GCG	459	446	0	0
NAM	423	57	0	0
SNET	348	73	0	0
SIGU	339	187	0	0
FCIAR	323	128	15	0
WAR	293	283	0	223
PLV	224	82	0	0
ISN	203	193	0	0
HYB	84	84	0	23
PJWWP	18	18	0	0
LIT	4	0	0	0
BEO	1	1	0	0
MEX	1	1	0	0

11

Glossary of ISC Terminology

- Agency/ISC data contributor

  An academic or government institute, seismological organisation or company, geological/meteorological survey, station operator or author that reports or contributed data in the past to the ISC or one of its predecessors. Agencies may contribute data to the ISC directly, or indirectly through other ISC data contributors.

- Agency code

  A unique, maximum eight-character code for a data reporting agency (e.g. NEIC, GFZ, BUD) or author (e.g. ISC, ISC-EHB, IASPEI). Often the agency code is the commonly used acronym of the reporting institute.

- Arrival

  A phase pick at a station is characterised by a phase name and an arrival time.

- Associated phase

  Associated phase arrival or amplitude measurements represent a collection of observations belonging to (i.e. generated by) an event. The complete set of observations are associated to the prime hypocentre.

- Azimuthal gap/Secondary azimuthal gap

  The azimuthal gap for an event is defined as the largest angle between two stations with defining phases when the stations are ordered by their event-to-station azimuths. The secondary azimuthal gap is the largest azimuthal gap a single station closes.

- BAAS

  Seismological bulletins published by the British Association for the Advancement of Science (1913-1917) under the leadership of H.H. Turner. These bulletins are the predecessors of the ISS Bulletins and include reports from stations distributed worldwide.

- Bulletin

  An ordered list of event hypocentres, uncertainties, focal mechanisms, network magnitudes, as well as phase arrival and amplitude observations associated to each event. An event bulletin may list all the reported hypocentres for an event. The convention in the ISC Bulletin is that the preferred (prime) hypocentre appears last in the list of reported hypocentres for an event.

- Catalogue

  An ordered list of event hypocentres, uncertainties and magnitudes. An event catalogue typically lists only the preferred (prime) hypocentres and network magnitudes.

- CoSOI/IASPEI

  Commission on Seismological Observation and Interpretation, a commission of IASPEI that prepares and discusses international standards and procedures in seismological observation and interpretation.

- Defining/Non-defining phase

  A defining phase is used in the location of the event (time-defining) or in the calculation of the network magnitude (magnitude-defining). Non-defining phases are not used in the calculations because they suffer from large residuals or could not be identified.

- Direct/Indirect report

  A data report sent (e-mailed) directly to the ISC, or indirectly through another ISC data contributor.

- Duplicates

  Nearly identical phase arrival time data reported by one or more agencies for the same station. Duplicates may be created by agencies reporting observations from other agencies, or several agencies independently analysing the waveforms from the same station.

- Event

  A natural (e.g. earthquake, landslide, asteroid impact) or anthropogenic (e.g. explosion) phenomenon that generates seismic waves and its source can be identified by an event location algorithm.

- Grouping

  The ISC algorithm that organises reported hypocentres into groups of events. Phases associated to any of the reported hypocentres will also be associated to the preferred (prime) hypocentre. The grouping algorithm also attempts to associate phases that were reported without an accompanying hypocentre to events.

- Ground Truth

  An event with a hypocentre known to certain accuracy at a high confidence level. For instance, GT0 stands for events with exactly known location, depth and origin time (typically explosions); GT5 stands for events with their epicentre known to 5 km accuracy at the 95% confidence level, while their depth and origin time may be known with less accuracy.

- Ground Truth database

  On behalf of IASPEI, the ISC hosts and maintains the IASPEI Reference Event List, a bulletin of ground truth events.

- IASPEI

  International Association of Seismology and Physics of the Earth Interior, www.iaspei.org.

- International Registry of Seismograph Stations (IR)

  Registry of seismographic stations, jointly run by the ISC and the World Data Center for Seismology, Denver (NEIC). The registry provides and maintains unique five-letter codes for stations participating in the international parametric and waveform data exchange.

- ISC Bulletin

  The comprehensive bulletin of the seismicity of the Earth stored in the ISC database and accessible through the ISC website. The bulletin contains both natural and anthropogenic events. Currently the ISC Bulletin spans more than 50 years (1960-to date) and it is constantly extended by adding both recent and past data. Eventually the ISC Bulletin will contain all instrumentally recorded events since 1900.

- ISC Governing Council

  According to the ISC Working Statutes the Governing Council is the governing body of the ISC, comprising one representative for each ISC Member.

- ISC-located events

  A subset of the events selected for ISC review are located by the ISC. The rules for selecting an event for location are described in Section 10.1.3 of Volume 57 Issue I of the ISC Summary; ISC-located events are denoted by the author ISC.

- ISC Member

  An academic or government institute, seismological organisation or company, geological/meteorological survey, station operator, national/international scientific organisation that contribute to the ISC budget by paying membership fees. ISC members have voting rights in the ISC Governing Council.

- ISC-reviewed events

  A subset of the events reported to the ISC are selected for ISC analyst review. These events may or may not be located by the ISC. The rules for selecting an event for review are described in Section 10.1.3 of Volume 57 Issue I of the ISC Summary. Non-reviewed events are explicitly marked in the ISC Bulletin by the comment following the prime hypocentre "Event not reviewed by the ISC".

- ISF

  International Seismic Format (www.isc.ac.uk/standards/isf). A standard bulletin format approved by IASPEI. The ISC Bulletin is presented in this format at the ISC website.

- ISS

  International Seismological Summary (1918-1963). These bulletins are the predecessors of the ISC Bulletin and represent the major source of instrumental seismological data before the digital era. The ISS contains regionally and teleseismically recorded events from several hundreds of globally distributed stations.

- Network magnitude

The event magnitude reported by an agency or computed by the ISC locator. An agency can report several network magnitudes for the same event and also several values for the same magnitude type. The network magnitude obtained with the ISC locator is defined as the median of station magnitudes of the same magnitude type.

- Phase

  A maximum eight-character code for a seismic, infrasonic, or hydroacoustic phase. During the ISC processing, reported phases are mapped to standard IASPEI phase names. Amplitude measurements are identified by specific phase names to facilitate the computation of body-wave and surface-wave magnitudes.

- Prime hypocentre

  The preferred hypocentre solution for an event from a list of hypocentres reported by various agencies or calculated by the ISC.

- Reading

  Parametric data that are associated to a single event and reported by a single agency from a single station. A reading typically includes one or more phase names, arrival time and/or amplitude/period measurements.

- Report/Data report

  All data that are reported to the ISC are parsed and stored in the ISC database. These may include event bulletins, focal mechanisms, moment tensor solutions, macroseismic descriptions and other event comments, as well as phase arrival data that are not associated to events. Every single report sent to the ISC can be traced back in the ISC database via its unique report identifier.

- Shide Circulars

  Collections of station reports for large earthquakes occurring in the period 1899-1912. These reports were compiled through the efforts of J. Milne. The reports are mainly for stations of the British Empire equipped with Milne seismographs. After Milne's death, the Shide Circulars were replaced by the Seismological Bulletins of the BAAS.

- Station code

  A unique, maximum five-character code for a station. The ISC Bulletin contains data exclusively from stations registered in the International Registry of Seismograph Stations.

12

Acknowledgements

We thank Horst Rademacher (formerly of Seismological Observatory Gräfenberg and Berkeley Seismological Laboratory) for kindly accepting our invitation and preparing an article on the history of broadband seismometry included in this issue. This article is based on his lectures given for several years to the students at the University of California, Berkeley.

We are also grateful to the developers of the Generic Mapping Tools (GMT) suite of software (Wessel et al., 2019) that was used extensively for producing the figures.

Finally, we thank the ISC Member Institutions, Data Contributors, Funding Agencies (including NSF Award EAR-1811737 and Royal Society Award INT004) and Sponsors for supporting the long-term operation of the ISC.

References

Adamaki, A. (2017), Seismicity Analysis Using Dense Network Data : Catalogue Statistics and Possible Foreshocks Investigated Using Empirical and Synthetic Data, Ph.D. thesis, Uppsala University, `urn:nbn:se:uu:diva-328057`.

Balfour, N., R. Baldwin, and A. Bird (2008), Magnitude calculations in Antelope 4.10, *Analysis Group Note of Geological Survey of Canada*, pp. 1–13.

Bisztricsany, E. A. (1958), A new method for the determination of the magnitude of earthquakes, *Geofiz. Kozl*, pp. 69–76.

Bondár, I., and D. Storchak (2011), Improved location procedures at the International Seismological Centre, *Geophysical Journal International*, *186*, 1220–1244.

Bormann, P., and J. W. Dewey (2012), The new IASPEI standards for determining magnitudes from digital data and their relation to classical magnitudes, IS 3.3, *New Manual of Seismological Observatory Practice 2 (NMSOP-2), P. Bormann (Ed.)*, pp. 1–44, `https://doi.org/10.2312/GFZ.NMSOP-2_IS_3.3,10.2312/GFZ.NMSOP-2`.

Bormann, P., and J. Saul (2008), The new IASPEI standard broadband magnitude mB, *Seism. Res. Lett*, *79*(5), 698–705.

Bormann, P., R. Liu, X. Ren, R. Gutdeutsch, D. Kaiser, and S. Castellaro (2007), Chinese national network magnitudes, their Relation to NEIC magnitudes and recommendations for new IASPEI magnitude standards, *Bulletin of the Seismological Society of America*, *97*(1B), 114–127, `https://doi.org/10.1785/012006007835`.

Bormann, P., R. Liu, Z. Xu, R. Ren, and S. Wendt (2009), First application of the new IASPEI teleseismic magnitude standards to data of the China National Seismographic Network, *Bulletin of the Seismological Society of America*, *99*, 1868–1891, `https://doi.org/10.1785/0120080010`.

Choy, G. L., and J. L. Boatwright (1995), Global patterns of readiated seismic energy and apparent stress, *J. Geophys. Res.*, *100*(B9), 18,205–18,228.

Dziewonski, A. M., T.-A. Chou, and J. H. Woodhouse (1981), Determination of earthquake source parameters from waveform data for studies of global and regional seismicity, *J. Geophys. Res.*, *86*, 2825–2852.

Engdahl, E. R., and A. Villaseñor (2002), Global seismicity: 1900-1999, *International Handbook of Earthquake Engineering and Seismology, International Geophysics series*, *81A*, 665–690.

Engdahl, E. R., R. van der Hilst, and R. Buland (1998), Global teleseismic earthquake relocation with improved travel times and procedures for depth determination, *Bulletin of the Seismological Society of America*, *88*, 722–743.

Gutenberg, B. (1945a), Amplitudes of P, PP and S and magnitude of shallow earthquakes, *Bulletin of the Seismological Society of America*, *35*, 57–69.

Gutenberg, B. (1945b), Magnitude determination of deep-focus earthquakes, *Bulletin of the Seismological Society of America*, *35*, 117–130.

Gutenberg, B. (1945c), Amplitudes of surface waves and magnitudes of shallow earthquakes, *Bulletin of the Seismological Society of America*, *35*, 3–12.

Hutton, L. K., and D. M. Boore (1987), The ML scale in southern California, *Bulletin of the Seismological Society of America*, *77*, 2074–2094.

IASPEI (2005), Summary of Magnitude Working group recommendations on standard procedures for determining earthquake magnitudes from digital data, http://www.iaspei.org/commissions/CSOI.html#wgmm,http://www.iaspei.org/commissions/CSOI/summary_of_WG_recommendations_2005.pdf.

IASPEI (2013), Summary of magnitude working group recommendations on standard procedures for determining earthquake magnitudes from digital data, http://www.iaspei.org/commissions/CSOI/Summary_of_WG_recommendations_20130327.pdf.

IDC (1999), IDC processing of seismic, hydroacoustic and infrasonic data, *IDC Documentation*.

Kanamori, H. (1977), The energy release in great earthquakes, *J. Geophys. Res.*, *82*, 2981–2987.

Lee, W. H. K., R. Bennet, and K. Meagher (1972), A method of estimating magnitude of local earthquakes from signal duration, *U.S. Geol. Surv.*, Open-File Rep.

Leptokaropoulos, K. M., A. K. Adamaki, R. G. Roberts, C. G. Gkarlaouni, and P. M. Paradisopoulou (2018), Impact of magnitude uncertainties on seismic catalogue properties, *Geophysical Journal International*, *213*(2), 940–951, https://doi.org/10.1093/gji/ggy023.

Nuttli, O. W. (1973), Seismic wave attenuation and magnitude relations for eastern North America, *J. Geophys. Res.*, *78*, 876–885.

Richter, C. F. (1935), An instrumental earthquake magnitude scale, *Bulletin of the Seismological Society of America*, *25*, 1–32.

Ringdal, F. (1976), Maximum-likelihood estimation of seismic magnitude, *Bulletin of the Seismological Society of America*, *66*(3), 789–802.

Storchak, D. A., J. Harris, L. Brown, K. Lieser, B. Shumba, R. Verney, D. Di Giacomo, and E. I. M. Korger (2017), Rebuild of the Bulletin of the International Seismological Centre (ISC), part 1: 1964–1979, *Geoscience Letters*, *4*(32), https://doi.org/10.1186/s40562-017-0098-z.

Tsuboi, C. (1954), Determination of the Gutenberg-Richter's magnitude of earthquakes occurring in and near Japan, *Zisin (J. Seism. Soc. Japan), Ser. II*(7), 185–193.

Tsuboi, S., K. Abe, K. Takano, and Y. Yamanaka (1995), Rapid determination of Mw from broadband P waveforms, *Bulletin of the Seismological Society of America*, *85*(2), 606–613.

Vaněk, J., A. Zapotek, V. Karnik, N. V. Kondorskaya, Y. V. Riznichenko, E. F. Savarensky, S. L. Solov'yov, and N. V. Shebalin (1962), Standardization of magnitude scales, *Izvestiya Akad. SSSR., Ser. Geofiz.*(2), 153–158, Pages 108–111 in the English translation.

Woessner, J., and S. Wiemer (2005), Assessing the quality of earthquake catalogues: estimating the magnitude of completeness and its uncertainty, *Bulletin of the Seismological Society of America*, *95*(2), https://doi.org/10/1785/012040007.

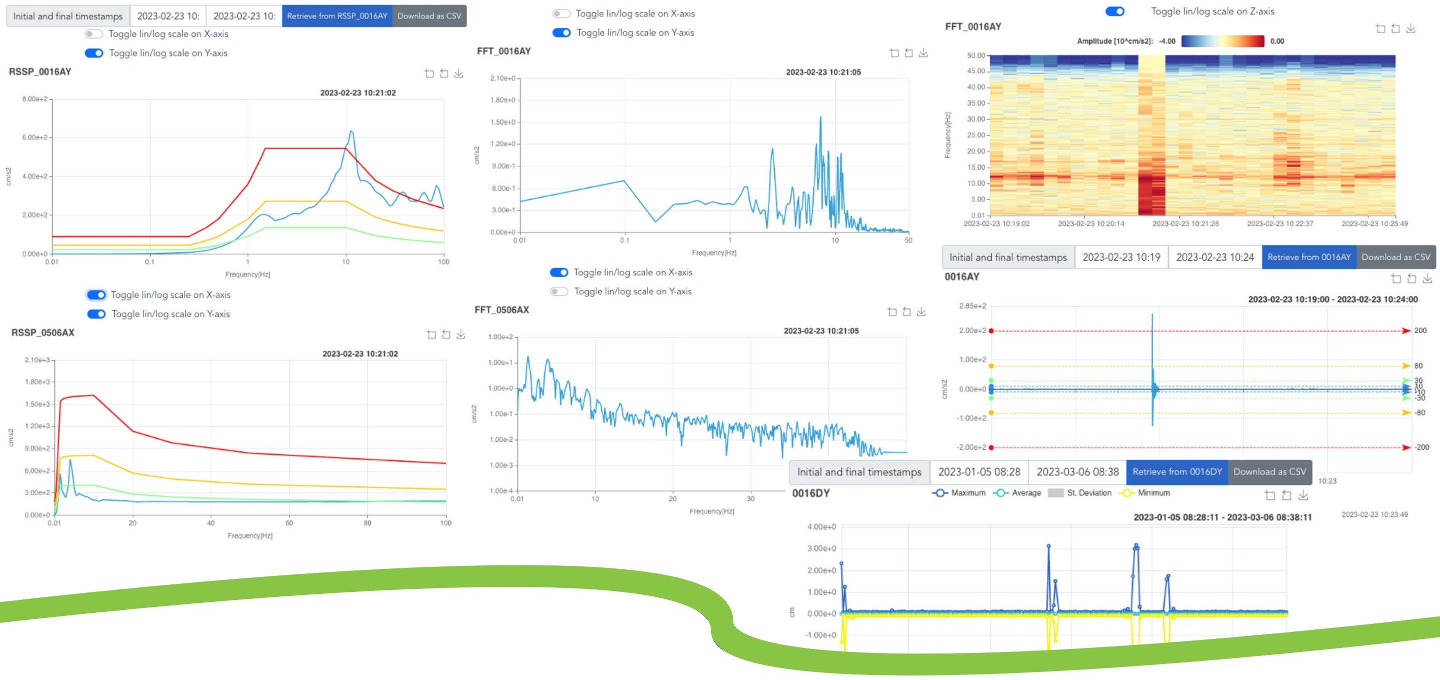

GeoSIG
swiss made to measure

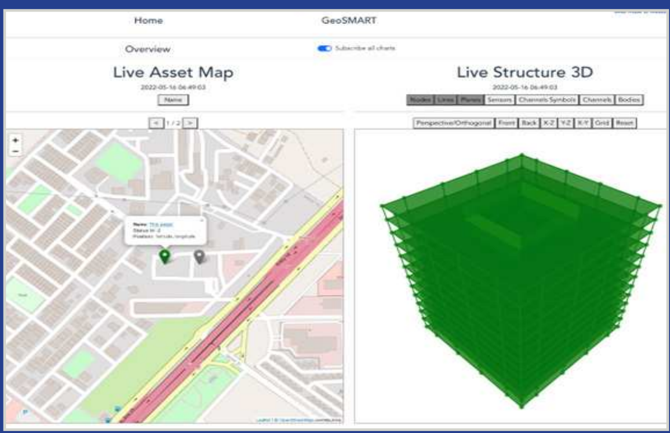

GeoSMART Offers Peak Performance

GeoSMART is an innovative graphical application that provides **tools** for realtime structural health monitoring for civil engineering structures. GeoSMART, with its “smart” features, can **monitor** and display the status of a structure that is equipped with GeoSIG measuring instruments. GeoSMART is S2HM in a Box; it has been designed to meet fundamental engineering requirements with respect to **structural health** monitoring applications.

Main Features of GeoSMART

- Support for any type of sensor such as acceleration, velocity, displacement, tilt, wind, temperature, strain, and many more.
- User-friendly web-interface for an intuitive experience.
- 3D representation of any structure with live status.
- Interactive zoom, rotate, pan, visibility and projection.
- Multiple structures on live interactive map.
- Real-time continuous data acquisition and processing.
- Storage and direct download of all data and graphics.
- Data export for long-term storage.
- Sliding window-based continuous frequency analyses: Amplitude, Spectrogram and Response Spectra.
- Rigid body motions in translations and rotations.
- Interpolations for non-instrumented areas.
- Interstory drift ratios and torsion.
- Exceedance of predefined threshold levels or curves.
- Plot of archive data and statistical information.
- Live screen indicators and HTML formatted emails.
- Individualised notifications to users / user groups.
- Customisable messages such as action plans.
- Reports including actual images of plotted graphics.
- Hardware relays to start or shutdown any process.
- Advanced user accessible powerful database.
- API to fetch and externally manipulate the stored data.

GeoSIG Ltd | Wiesenstrasse 39
8952 Schlieren, Switzerland
T: +41 44 810 2150 | F: + 41 44 810 2350
www.geosig.com

For more information, contact us at info@geosig.com

GaiaCode

www.gaiacode.com

40 years of Research, Design, Production and Installation experience of SEISMIC Instrumentation

OUR INSTRUMENTS

Multidisciplinary Product Range:

Very BroadBand Sensors

α **ALPHA Series sensors** are very low noise broad band sensors with 360 seconds to 150Hz response. Different response options are available. 15Hz to 200 seconds sensor self-noise below the NLNM. Serial interface allows sensor parameters to be accessed through TAU Digitizer.

Very BroadBand Sensors

α **ALPHA Series Posthole** sensor systems**.** Very low noise robust broad band sensor system suitable to be buried under most severe conditions. Stainless steel construction can be installed down to 100 meters depth.

Very BroadBand Sensors

α **ALPHA Series Borehole sensor systems**

The downhole instruments contain three component Alpha broadband and three component Sigma accelerometer sensors and a newly designed single jaw hole-lock to anchor the instrument into the cased borehole. The sensor tilt and orientation and internal humidity of the sensor is part of detailed SOH parameters.

Strong Motion Accelerometer

ε **SIGMA Analogue sensor has** rectilinear dc to 400Hz feedback suspension system. 4 different remotely configurable sensitivity settings and 173dB of dynamic range at 10Hz**.**

Strong Motion Accelerometer

ε **Digital SIGMA Sensor**

ideally suited for EEWS with LOW latency and with multiple sample rate outputs. 8 Channel 24 bit digitiser exploits 173dB dynamic range of SIGMA sensor.

Ω **OMEGA Murray McGowan** is the author of a comprehensive software suite to be used with our **TAU** family of digitizers**. Omega** software gives network administrators a plethora of functions and options. Amongst others, it allows remote control of the parameters of Gaiacode's digitizers and seismic sensors. Station SOH parameters are presented to the user for quality control of the stations.

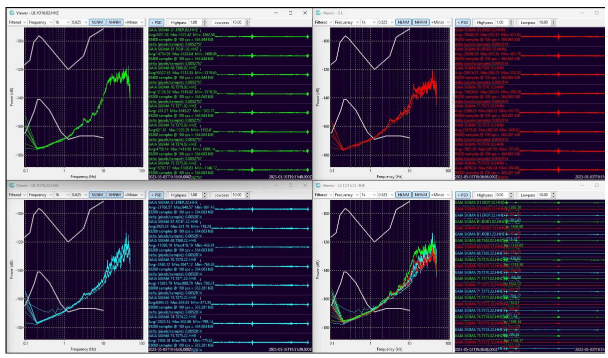

GaiaCode

www.gaiacode.com

Broad Band Sensors

Θ THETA Analogue broad band sensor with user selectable frequency response and velocity gain. Serial interface provides sensor control and sensor characteristics to be accessed through TAU digitiser. Cost effective network sensor.

Broad Band Sensors

Θ Digital THETA broad band sensor 8 channel 24 bit digitiser allows users to record very large dynamic range of the sensor system. Waterproof and robust sensor. Optional MEMS sensor is used for EEWS applications.

Broad Band Sensors

Θ THETA Borehole, Posthole slim-line 50mm diameter system

Three component broad band 120 seconds velocity sensor with programmable frequency response. Can operate up to 25 degrees of tilt. Additionally internal MEMS and humidity sensor provide SOH information.
Single arm hole-lock can be integrated with stackable sensors for VSP type applications. Suitable for cased or uncased boreholes.
Extremely low noise sensor at high frequency, crosses the NLNM at 8Hz and long period at 14 seconds.
Can be installed to a depth of 300 meters.

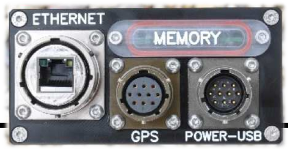

24 Bit 8 channel digitiser MK1

τ TAU high resolution acquisition system. With causal and acausal filters including 4 concurrent sample rates, multiple data format output, low latency data output is suitable for EEWS applications. Internal 24 bit calibration feature is used to calibrate broad band sensors.

τ 24 Bit 8 channel digitiser MK2

In addition to all the features of MK1, Mk2 TAU has more environmental channels including Infrasound sensor, digital inputs and outputs and two 32Gbyte hot swappable SD cards are available. Waterproof casing.

PICO Broad band sensor PICO-TP120-VEL is a completely newly designed mid-range portable feedback broad band seismometer housed inside a waterproof enclosure. Very easy to install remotely. Response configurable broad band sensor with 9 different velocity responses. Waterproof posthole with installable and adjustable connector allows the sensor to be installed in any position conveniently.
Comprehensive sensor SOH parameters are available through a serial interface. Can be installed in ±20 degrees tilted postholes. Internal MEMS sensor reports sensor's tilt levels. Dichromate, anodized and stainless steel. Casing options are available.

Detailed data sheets are available on all products from GaiaCode Ltd

www.gaiacode.com contact@gaiacode.com . GaiaCode Ltd Dickers Farm, Bramley Road, Silchester RG7 2LU, UK